Order Number 9009753

Nonsteady state gas chromatography

Landau, Isaac, Ph.D.

City University of New York, 1989

U·M·I
300 N. Zeeb Rd.
Ann Arbor, MI 48106

NONSTEADY STATE GAS CHROMATOGRAPHY

by

ISAAC LANDAU

A dissertation submitted to the Graduate Faculty in Chemistry in partial fulfillment of the requirements for the degree of Doctor of Philosophy, The City University of New York.

1989

This manuscript has been read and accepted for the Graduate Faculty in Chemistry in satisfaction of the dissertation requirement for the degree of Doctor of Philosophy.

9 September 89
Date

David C. Locke
Chair of Examining Committee

9/12/89
Date

A. M.
Executive Officer

Supervisory Committee

The City University of New York

Abstract

NONSTEADY STATE GAS CHROMATOGRAPHY

by

Isaac Landau

Adviser: Professor David C. Locke

Nonsteady state gas chromatography is a novel GC technique in which a solvent relatively volatile at the column temperature is injected into a column packed only with solid support, and allowed to equilibrate and be slowly eluted out of the column. During elution of the solvent, small samples of solutes of volatility greater than the solvent (volatility is the product of vapor pressure and activity coefficient) are injected repetitively. Because the weight of the solvent decreases with time as it elutes, the retention time of a solute injected repetitively will decrease over the lifetime of the column. It is possible to show that the limiting (infinite dilution) activity coefficient of the solute, γ_2^∞, is simply related to the solvent and solute vapor pressures, p_1^0 and p_2^0, respectively, the average flow rate, $\bar{F}$, and to the change in retention volume, ΔV_R^0, over a time interval Δt, by

$$\gamma_2^\infty = (p_1^0/p_2^0) \,/\, [-1/\bar{F}\,(\Delta V_R^0/\Delta t)].$$

The technique has been shown to give reliable limiting coefficients for a diversity of binary systems. Two different solid supports have been compared and the results are presented. The column dynamics and mechanism of solvent elution have been explored.

The process proves to be a fast, efficient method of determining limiting activity coefficients which are necessary for thermodynamic relations

and are useful in water pollution control, toxicological studies, process engineering, and other diverse areas.

Acknowledgement

I would like to thank Dr. David C. Locke for his guidance, support, and encouragement. In addition, I would like to express my appreciation for the time we spent discussing everything but chemistry, including music, literature, and politics. It was the combination of all of these that got me through this work.

I would also like to thank Dr. Johna Leddy for her help and humor, and Mr. Robert B. Wurman for his technical expertise with a human touch. They made the past four years, not just bearable, but enjoyable.

Finally, I would like to express my appreciation to the staff of the Chemistry Department at Queens College and at the CUNY Graduate Center for helping me deal with all the bureaucracy, and to Dr. Neil Jesperson for some experimental ideas that helped prove the model.

To my devoted parents and loving wife,

who made it possible,

and my wonderful son,

who made it necessary.

Table of Contents

List of Tables

List of Figures

I. Introduction

Nonsteady State Gas Chromatography (NSGC) (1–4) is a novel gas chromatographic technique in which a solvent relatively volatile at the column temperature is injected into a column packed only with solid support, and allowed to equilibrate and be slowly eluted out of the column. During elution of the solvent, small samples of solutes of volatility greater than the solvent (volatility is the product of vapor pressure and activity coefficient) are injected repetitively. Because the weight of the solvent decreases with time as it elutes, the retention time of a solute injected repetitively will decrease over the lifetime of the column. This nonsteady state in the column makes it possible to measure physiochemical properties of solutions, such as the limiting (infinite dilution) activity coefficient.

NSGC follows a long line of chromatographic methods. The classical technique of chromatography involves filtering a solution through a powder column on which a mixture of solutes are separated into distinct zones and are thus resolved (5). Two pioneers in the development of chromatography were David Talbot Day and Mikhail Tswett. In 1897, Day published a paper on what he called "fractional diffusion" (6). Other papers followed (7,8), inspired by his work on geological surveys and mineral resources. Day became interested in the different colored samples of Pennsylvania oils. He suggested that the differences in the oils were due to some large scale fractional filtration process that could be reproducible in the laboratory. He, and later, Gilpen and others (9–11) experimented by passing crude oil and various hydrocarbon mixtures through pulverized Fuller's earth. They found that the mixtures were fractionated and eluted in the order of lightest to heaviest. They also observed

the top–to–bottom sequence in large scale columns of saturated aliphatic hydrocarbons, aromatic and unsaturated substances, and finally, nitrogen and sulfur compounds whose amounts increased towards the bottom. They attributed this to "selective adsorption."

In a lecture in 1903 (12), and then in two papers in 1906 (13,14), Mikhail Tswett described what he called a *chromatogram* and his *chromatographic method.* Interested in chloroplast pigments, and the green chlorophylls and yellow carotenoids of which they are composed, he discovered that there are two types of chlorophyll in leaves. Filtering a petroleum ether solution of plant extract through a narrow glass tube of firmly packed calcium carbonate, Tswett found that the pigments were resolved according to an adsorption sequence from top to bottom into various colored zones. If one subsequently passed pure solvent through the column, the different components of the mixture separated on the calcium carbonate "like light rays in the spectrum." He explained that this occurred because the more strongly adsorbed pigments displaced the more weakly adsorbed ones and forced them farther downward. He established the law that "there exists a certain adsorption sequence according to which substances are able to displace one another. ...It is self–evident that the adsorption phenomena described are not restricted to the chlorophyll pigments, and one must assume that all kinds of colored and colorless chemical compounds are subject to the same laws." Tswett published over 50 papers proving this method and brought it all together in a book in 1910 entitled "Chromophylls in the Plant and Animal Kingdom" (15) which dealt with a multitude of colored and colorless substances.

There is no evidence that either Day or Tswett was aware of the work

of the other (16). Day's work remained unnoticed until 1948 (17). Tswett was cited in a paper in the U.S. by Palmer (18) in 1922, but not by any Europeans until 1931. Following two papers by Kuhn, Lederer, and Winterstein (19,20) "an avalanche of papers followed throughout the world under Tswett's revived and powerful influence" (16). Tswett enjoys more of the glory than Day because he recognized and correctly interpreted chromatographic processes.

Since Tswett's work chromatography has grown and expanded in many different directions. Though paper chromatography can be dated as far back as Pliny the Elder (21), it was not until the mid–1930's that chromatography began mushrooming into the wide class of analytical methods it is today. Strain (22) summarizes the developments and modifications made, as follows. Chromatography has been utilized in various geometric modifications; with *one–way* or *linear flow* of solvent in columns, strips, sheets, or thin layers of the sorbent (23–25); with *two–way* or *transverse flow* with two different solvents in succession in sheets or thin layers of the sorbent; and with *radial flow* from a central zone or point in a sheet or layer of the sorbent (26,27). It has been used with all kinds of liquids as the chromatographic solvent – *solution chromatography* (28–48). It has been modified through the use of many different sorptive materials such as surface–active liquids (32) as well as solids – *adsorption chromatography* (14,23–37,49–52), ion–exchange zeolites and cationic and anionic resins – *ion–exchange chromatography* (29–31,33–39,47,48,53), fixed polar liquids – *liquid–liquid* or *partition chromatography*, fixed nonpolar liquids – *reversed phase partition chromatography*, paper alone – *paper adsorption chromatography*, paper plus fixed liquids – *paper partition chromatography* (23–36,40–44,49,51,52,54), and polymeric gels – *gel filtration chromatography* and *gel permeation*

chromatography (45).

Variations of the sorptive phase have been accompanied by great variation of the solvents, which range from nonpolar hydrocarbons – *sorption solvents*, to polar acids, bases, and aqueous solutions – *elution solvents* (49,30). It has also been adapted to determination of the migration of various solutes relative to the migration of the solvents or wash liquid – *frontal analysis* (24,28,33–36).

Chromatography has been refined by the use of inert gases to carry mixtures of gases or vapors through sorption columns – *gas chromatography.* In these modifications, the sorbents are usually surface–active solids – *gas–adsorption chromatography*, or fixed, nonvolatile liquids – *gas partition* or *gas–liquid chromatography.* James and Martin (63) introduced gas–liquid chromatography (GLC) in 1952. It became firmly established as a powerful and versatile method of analysis, and, later, its separating powers were exploited for laboratory preparative separations and production–scale industrial separations (64). Gas chromatography has been found to be useful with all kinds of gaseous and volatile compounds (55–62).

Since it was necessary to rationalize the properties of solutes and stationary phases so as to improve column performance, gas chromatography developed into a method of studying physical processes. In 1941, Martin and Synge (65) introduced liquid–liquid chromatography and developed a chromatographic plate theory which they used to measure liquid–liquid partition coefficients. They were the first to use chromatography for physiochemical measurements. In 1947, Glueckauf (66) found that adsorption isotherms could be determined from the breakthrough curves of gas–solid chromatography (GSC). This was the first mention of any form of

physiohemical measurements by gas chromatography (GC). At the same time, however, Cremer and Prior (67,68) developed a method of using elution GSC to measure free energies. Since Glueckauf's experiments were primarily concerned with liquid–solid chromatography, it was not until 1954 that James and Phillips (69) used the chromatographic method to obtain gas–solid isotherms. Five years after the development of GSC as a tool for physiochemical measurements, in 1952, James and Martin (63) published a paper introducing a second form of GC, namely gas–liquid chromatography (GLC). Since that time, there has been a rapid development of GC, included in which are the various physiochemical measurements that could be determined by it. Figure I.1 illustrates the uses of GC and the physical properties which can be measured by it.

Conder and Young (70) write that the earliest physical measurements by GLC date back to 1955 and 1956, shortly after the James and Martin paper (63). Several authors (71–75) described how to measure boiling points, partition coefficients, and heats of entropies of solution for a volatile solute dissolved in a non–volatile solvent. Porter, Deal, and Stross (73) extended the method to activity coefficients. Martin (74) wrote in 1956 that "the method of gas chromatography provides, perhaps, the easiest of all means of studying the thermodynamics of the interaction of a volatile solute with a non–volatile solvent, and its potential value for providing this type of data should be very great." History has proven Martin a wise prophet. NSGC helped expand the GC technique to include volatile solvents as well.

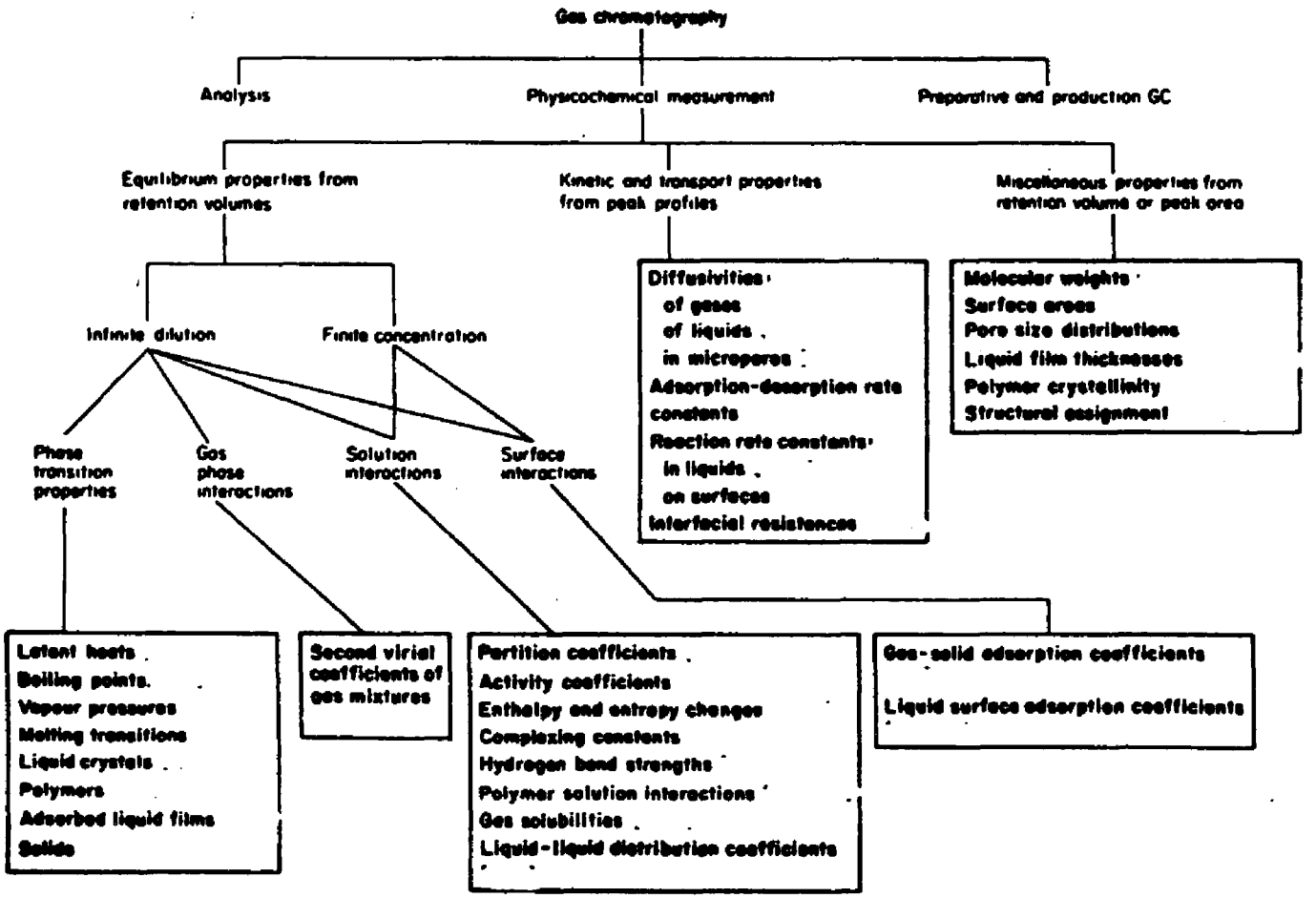

Figure I.1. Physiochemical Applications of Gas Chromatography (70).

References

(1) Belfer, A.J. Neftekhim. 1972, 12, 435; CA 1973, 78, 20591.

(2) Belfer, A.J.; Locke, D.C. Anal. Chem. 1985, 56, 2485.

(3) Landau, I.; Locke, D.C.; Belfer, A.J. Paper Presented at the Eastern Analytical Symposium, Oct. 1986, New York.

(4) Landau, I.; Locke, D.C.; Belfer, A.J. Paper Presented at the Eastern Analytical Symposium, Oct. 1988, New York.

(5) Zechmeister, L. "Chromatography," 2nd. Edn., Heftmann, E. Ed., 1967, Reinhold Publishing Corp., New York, p. 3.

(6) Day, D.T. Proc. Am. Phil. Soc. 1897, 36, 112.

(7) Day, D.T. Congr. Intern. Petrole Paris 1900, 1, 53; CA 1910, 4, 1803.

(8) Day, D.T. Science 1903, 17, 1007.

(9) Gilpen, J.E.; Cram, M.P. Am. Chem. J. 1908, 40, 495.

(10) Gilpen, J.E.; Bransky, O.E. Am. Chem. J. 1910, 44, 251.

(11) Gilpen, J.E.; Schneeberger, P. Am. Chem. J. 1913, 50, 59.

(12) Tswett, M. Proc. Warsaw Soc. Nat. Sci., Biol. Sec. 1903, 14, No. 6; CA 1907, 1, 2905.

(13) Tswett, M. Ber. Deut. Botan. Ges. 1906, 24, 316.

(14) Tswett, M. Ber. Deut. Botan. Ges. 1906, 24, 384.

(15) Tswett, M. "Chromofilli v rastitelnon i zhivotnom mire," 1910, Warsaw.

(16) Zechmeister, L. *ibid.*, p. 7.

(17) Zechmeister, L. Ann. N.Y. Acad. Sci. 1948, 49, 145.

(18) Palmer, L.S. "Carotinoids and Related Pigments," 1922, Chemical Catalog Co., New York.

(19) Kuhn, R.; Lederer, E. Ber. 1931, 64, 1349.

(20) Kuhn, R.; Winterstein, A.; Lederer, E. Hoppe–Seyler's Z. Physiol. Chem. 1931, 197, 141.

(21) Baily, K.C. "The Elder Pliny's Chapters on Chemical Subjects," 1929, Arnold & Co., London.

(22) Strain H.H. "Chromatography," 2nd. Edn., Heftmann, E. Ed., 1967,

Reinhold Publishing Corp., New York, p. 13.

(23) Bobbit, J.M. "Thin–Layer Chromatography," 1963, Reinhold, New York.

(24) Randerath, K. "Thin–Layer Chromatography," 1963, Academic Press, New York.

(25) Stahl, E. (Ed.) "Duennschicht–chromatographie; ein Laboratorium–shandbuch," 1962, Springer, Berlin. (English translation by Cambridge Consultants, 1965, Academic Press, New York.)

(26) Brown, W.G. Nature 1939, 143, 377.

(27) Strain, H.H.; Sato, T.R.; Engelke, J. Anal. Chem. 1954, 26, 90.

(28) Strain, H.H. Anal. Chem. 1960, 32, 3R.

(29) Cassidy, H.G. "Fundamentals of Chromatography," 1957, Interscience, New York.

(30) Lederer, E.; Lederer, M. "Chromatography, a Review of Principles and Applications," 2nd. Edn., 1957, Elsevier, New York.

(31) Lederer, E. (Ed.) "Chromatographie en Chimie Organique et Biologique," 1959, Masson et Cie, Paris. (English translation of selected parts by James, A.T. "Chromatography; a Review of Principles and Applications" 1958, Elsevier, Amsterdam.)

(32) Strain H.H. J. Phys. Chem. 1953, 57, 638.

(33) Strain, H.H. Anal. Chem. 1950, 22, 41.

(34) Strain, H.H.; Murphy, G.W. Anal. Chem. 1952, 24, 50.

(35) Strain, H.H.; Sato, T.R. Anal. Chem. 1956, 28, 687.

(36) Strain, H.H. Anal. Chem. 1958, 30, 620.

(37) Blasius, E. "Chromatographische Methoden in der analytischen und praeparativen anorganischen Chemie unter besonderer Beruecksichtigung der Ionenaustauscher," 1958, Enke, Stuttgart.

(38) Kunin, R. "Ion Exchange Resins," 2nd. Edn., 1958, Wiley, New York.

(39) Salmon, J.E.; Hale, D.K. "Ion Exchange: A Laboratory Manual," 1959, Butterworths, London; Academic Press, New York.

(40) Hais, I.M.; Macek, K. "Handbuch der Papierchromatographie," Vol. I and II, 1958 & 1960, (English translation by Kalina, B.; Nemecek, K., 1963, Academic Press, New York and Publishing House of the Czechoslovak Academy of Sciences, Prague.

(41) Linskens, H.F. "Papierchromatographie in der Botanik," 2nd Edn., 1959, Springer, Berlin.

(42) Cramer F. "Papierchromatographie," 4th Edn., 1958, Verlag Chemie, Weinheim.

(43) Block, R.J. Durrum, E.L.; Zweig, G. "A Manual of Paper Chromatography and Paper Electrophoresis," 2nd. Edn., 1958, Academic Press, New York.

(44) Smith, I. (Ed.) "Chromatographic Techniques: Clinical and Biochemical Applications," 1958, Heinemann Medical Books, Ltd., London; Interscience, New York.

(45) Moore, J.C.; Hendrickson, J.G. J. Polymer Sci. 1963, Pt. C, No. 8, 233.

(46) Heftmann, E. Anal. Chem. 1962, 34, 13R; *ibid.* 1964, 36, 14R; *ibid.* 1966, 38, 31R.

(47) Kunin, R.; McGarvey, F.X. Anal. Chem. 1962, 34, 48R, 101R.

(48) Walton, H.F. Anal. Chem. 1964, 36, 51R.

(49) Strain, H.H. "Chromatographic Adsorption Analysis," 1942, Interscience, New York.

(50) Zechmeister, L.; Cholnoky, L.V. " Die chromatographische Adsorptions–methode. Grundlagen, Methodik, Anwendungen," 2nd. Edn., 1938, Springer, Berlin.

(51) Strain, H.H. Anal. Chem. 1951, 23, 25.

(52) Winterstein, A. "Handbuch der Pflanzenanalyse," Vol. IV, Klein, G. Ed., 1933, Springer, Vienna, p. 1403.

(53) Williams, T.I. "The Elements of Chromatography," 1953, Philosophical Library, New York.

(54) Strain, H.H. "Frontiers in Colloid Chemistry," Vol. VIII, Burk, R.E.; Grummitt, O. Eds., 1950, Interscience, New York, p. 29.

(55) Phillips, C. "Gas Chromatography," 1956, Academic Press, New York.

(56) Dal Nogare, S.; Juvet Jr., R.S. "Gas–Liquid Chromatography, Theory and Practice," 1962, Interscience, New York.

(57) Juvet Jr., R.S. Anal. Chem. 1964, 36, 36R.

(58) Burchfield, H.P.; Storrs, E.E. "Biochemical Applications of Gas Chromatography," 1962, Academic Press, New York.

(59) Ettre, L.S. "Open Tubular Columns in Gas Chromatography," 1965,

Plenum Press, New York.

(60) James, A.T.; Morris, L.J. (Eds.) "New Biochemical Separations," 1964, Van Nostrand, New York.

(61) Morris, C.J.O.R. "Separation Methods in Biochemistry," 1964, Pitman, London.

(62) Roeck, H. "Ausgewaehlte moderne Trennverfahren zur Reinigung organischer Stoffe," 1957, Steinkopff, Darmstadt.

(63) James, A.T.; Martin, A.J.P. Biochem. 1952, 50, 679.

(64) Conder, J.R.; Young, C.L. "Physicochemical Measurement by Gas Chromatography," 1979, Wiley, Chichester, p. 1.

(65) Martin, A.J.P.; Synge, R.J.M. Biochem. 1941, 35, 1358.

(66) Glueckauf, E. J. Chem. Soc. 1947, 1302.

(67) Prior, F. Ph.D. Thesis, University of Innsbruck, 1947.

(68) Cremer, E.; Prior, F. Z. Electrochem. 1951, 55, 66.

(69) James, D.H.; Phillips, C.S.G. J. Chem. Soc. 1954, 1066.

(70) Conder, J.R.; Young, C.L. *ibid.*, p. 3.

(71) Littlewood, A.B.; Phillips, C.S.G.; Price, D.T. J. Chem. Soc. 1955, 1480.

(72) Hoare, M.R.; Purnell, J.H. Trans. Faraday Soc. 1956, 52, 222.

(73) Porter, P.E.; Deal, C.H.; Stross, F.H. J. Am. Chem. Soc. 1956, 78, 2999.

(74) Martin, A.J.P. Analyst 1956, 81, 52.

(75) Anderson, J.R. J. Am. Chem. Soc. 1956, 78, 5692.

II. The Activity Coefficient

i. Molecular View of Solutions

A solution is a mixture of two or more species. One species is singled out and is labelled the solvent. All the remaining species are called solutes. Though no rule exists that determines which species should be regarded as the solvent, it is the usual practice, and it will be so in this work, that it's the species in highest proportion (1). For liquid (condensed phase) solutions, mixing behavior is dictated by intermolecular forces. Two species whose mutual attraction is greater than the attraction of either for itself mix completely. Even weak van der Waal's forces are sufficient to cause mixing. If the attraction of the liquid for itself is greater than that for the second liquid, the liquids are relatively immiscible. An example of the former is ethyl alcohol and water, while the latter is water and n–hexane. In general, two polar or two non–polar liquids are miscible. A polar and a non–polar liquid tend to be immiscible. If unlike substances were to mix, this would cause an increase in potential energy of the system which could only come from taking kinetic energy from the thermal motion of the molecules. This implies a decrease in the entropy of the system and is unfavorable. Therefore, the situation where there will be a maximum in entropy would be where there would not be complete miscibility (2).

ii. Ideal Solutions

A solution is said to be ideal if the chemical potential of *every* component is a linear function of the logarithm of its mole fraction according to the relation

$$\mu_i = \mu_i^* + RT \ln x_i \qquad (1)$$

where R is the gas constant, T is the system temperature (K), and x_i is the mole fraction of the ith species. μ_i^* is the standard state chemical potential of pure component i and is a function only of temperature and pressure. It is a reference point taken as the value of μ_i when $x_i = 1$. Thus, as regards component A, μ_a^* is the chemical potential of pure A at the temperature and pressure of the solution under investigation. (3).

Equation 1 is of the same form as the definition of an ideal gaseous solution,

$$\mu_i(g) = \mu_i^o(g) + RT \ln P_i \qquad (2)$$

where $\mu_i^o(g)$ is the chemical potential of pure component i at the same temperature and pressure as the system being studied, and P_i is the numerical value of the partial pressure when expressed in atmospheres. Equations 1 and 2 are related by Raoult's Law. It (Raoult's Law) gives the total vapor pressure of an ideal solution by summing, for all components of the system, the relation

$$P_i = x_i P_i^* \qquad (3)$$

where P_i is the partial pressure of component i in the vapor in equilibrium with the solution and P_i^* is the vapor pressure of pure component i. The standard state chemical potential for a pure liquid in equilibrium with its vapor is defined as

$$\mu_i^*(l) = \mu_i^o(g) + RT \ln P_i^* \qquad (4)$$

hence equation 2 (4). The chemical potential is defined as

$$\mu_i = \left(\frac{\partial G}{\partial n_i}\right)_{T,P,n_j} \qquad (5)$$

From this and the above relations all the thermodynamic functions of ideal solutions can be derived (5). Given the Gibbs free energy (G), entropy (S),

enthalpy (H), and volume (V), the behavior of a system is described completely.

A more physical description of an ideal gaseous solution is a system consisting of freely moving particles of negligible volume and having negligible forces of interaction (6). So too, the molecular basis for ideality in liquids. The forces between the molecules of the components in a solution are identical. All interactions between like and/or unlike molecules are the same (7). Raoult's Law describes this behavior. It states that the pressure of the vapor of a component in equilibrium with its liquid phase is unaffected by any other component. The only influence on the magnitude of the vapor pressure is the mole fraction, x_i. This is illustrated in Figure II.1. Plotting von Zawidzki's data (8) for the vapor pressures of the mixture ethylene bromide and propylene bromide at 85^{o}C against the mole fraction of propylene bromide, we see that the solution is nearly ideal. A straight line is obtained for each component, giving a straight line for the total vapor pressure. This system obeys Raoult's Law.

The ideal solution is the simplest case. It is used as a standard by which to describe real solutions. The term "ideal solution" is used for either a solid, liquid, or gaseous mixture, or any combination of these phases (9). Extensive attention has been devoted to ideal solutions for several reasons: (a) the behavior of ideal solutions is the simplest conceivable, both mathematically or physically; (b) statistical theory predicts that solutions of similar species, in particular isotopes, will behave ideally; (c) it is found experimentally that near ideal solutions exist, for example, benzene and bromobenzene; (d) although real solutions, other than isotopic ones, are not ideal, in many cases the resemblances between a real solution and an ideal one

are more striking than the differences (5).

Few solutions behave ideally, i.e., obey Raoult's Law. Those that do are generally the exception, not the rule. However, in the case where the components are closely similar in molecular structure, as in the afore–mentioned system and for the solution of benzene and bromobenzene at $80^{o}C$ (10) an approximation to ideal behavior is found (11). Another exception to the rule is the behavior of the solvent in a dilute solution (12). In the limit where the mole fraction of the solvent is sufficiently close to unity and the mole fractions of the solutes are very small, $x_s \longrightarrow 1$ and $x_i \longrightarrow 0$ where s denotes the solvent and i the solutes, the molecules of solvent are all surrounded by similar molecules apart from a few exceptions that have the other species as neighbors. As the solution becomes increasingly dilute the limiting condition is for all the solvent molecules to be in an environment of the same species, as occurs in the pure liquid (13). Each solute molecule, however, is completely surrounded by solvent molecules and is not related to the state characteristic of pure liquid solute. The behavior of the solute does not follow Raoult's Law.

Raoult's Law is the result of the special case of a perfect solution, i.e., a solution that is ideal over the whole composition range. A perfect solution in equilibrium with its vapor has the property

$$\mu_i(l) = \mu_i(g) \tag{6}$$

Then,

$$\mu_i^*(l) + RT \ln x_i = \mu_i^o(g) + RT \ln P_i \tag{7}$$

This can be simplified by writing

$$P_i = x_i k_i \tag{8}$$

where k_i is

$$k_i = \exp[(\mu_i^* - \mu_i^o)/RT] \quad (9)$$

In the limit where $x_i = 1$, $k_i = P_i^*$, and equation 8 becomes Raoult's Law (14). Physically, this means that the component i behaves as though it were alone, uninfluenced by anything around it, an ideal solution. In the case of an ideal dilute solution, the solvent follows Raoult's Law, not the solute. However, since the case is one of an ideal solution, the solute must preserve the proportionality

$$P_i = x_i k_i \quad (10)$$

This states that the vapor pressure of the dissolved substance is proportional to its mole fraction in an ideal solution and is called Henry's Law (12).

iii. Real Solutions and the Activity Coefficient

A solution, as stated earlier, is a condensed phase of two or more components. Few real mixtures behave ideally (15). Even in very dilute solutions it is incorrect to compare the state of the dissolved components to that of molecules in the gas state . Each dissolved solute molecule is subject to strong forces exerted on it by solvent molecules (16,17). A convenient correlation between the thermodynamic properties of real and ideal solutions can be made using excess functions. Guggenheim (15) developed this for all the functions of mixing. However, the actual deviations from the laws of perfect solutions may be expressed formally by introducing the activity coefficient γ_i in the expression for the chemical potential of a ideal solution (18). "The method due to G.N. Lewis permits to formally extend the properties of perfect solutions to actual solutions in a most elegant way" (19). Many texts, such as those of Guggenheim (15) and Smith (20), use the concept of activity, a_i. The activity of a substance is related to its mole fraction in solution by the relation

$$a_i = \gamma_i x_i \tag{11}$$

The chemical potential of a solute in a real solution takes the form

$$\mu_i = \mu_i^* + RT \ln a_i = \mu_i^* + RT \ln \gamma_i x_i \tag{12}$$

Activity may be regarded as the effective concentration of a component relative to its standard state. In real solutions, the effective concentration may differ greatly from the true concentration as a result of the interactions between molecules. The extent to which this is so is measured by the activity coefficient (20). Activity is defined only in so far as the standard state to which it refers is also specified. For an ideal solution it is convenient to define activity in such a way that it is equal to the mole fraction, which is to say that the activity coefficient is equal to unity. Activity coefficients can be normalized using one of two possible standard states. The activity coefficients of solutions that use the ideal Raoult's Law solution as their reference state are normalized by the condition

$$\gamma_i \longrightarrow 1 \text{ as } x_i \longrightarrow 1 \tag{13}$$

for each component i in in the solution. Since this holds for both the solvent and the solute this method (equation 13) is called the symmetric convention of normalization. If the reference solution is an ideal dilute Henry's Law solution then γ_i is normalized by

$$\gamma_1 \longrightarrow 1 \text{ as } x_1 \longrightarrow 1 \text{ (solvent)}$$
$$\gamma_2 \longrightarrow 1 \text{ as } x_2 \longrightarrow 0 \text{ (solute)} \tag{14}$$

Since the solute and the solvent are treated differently, this convention is referred to as unsymmetric normalization (21). Solutions containing more than two components can easily be described using the symmetric convention. γ_i of any i approaches unity as its mole fraction does. Extension of the unsymmetric convention to multicomponent systems is more complicated (22).

The establishment of a standard state is essential because, in general, thermodynamic computations can only deal with differences, not absolute quantities. Therefore, any thermodynamic expression must include a reference point. In this discussion of solutions the reference point is the ideal solution. Deviation from ideal behavior is expressed as real solution behavior; the deviations are reflected in the activity coefficient. Using Raoult's and Henry's Laws, a reference line of ideal behavior can be graphed in a plot of vapor pressure versus mole fraction, illustrated in Figure II.1. Real solutions will deviate from this line positively and/or negatively. Figure II.2 illustrates a case where all the activity coefficients are less than unity. Therefore, the total vapor pressure p is less than the perfect pressure represented by the line P_1P_2, the line expected from Raoult's Law. This is an example of a negative deviation from ideality. The system chloroform + ethyl ether exhibits negative deviations from ideality (23). Figure II.3 is a plot of p vs. x_2 for the system methylal + carbon disulfide from the data of von Zawidski (8). In this case, all the activity coefficients are greater than unity so that the total pressure is greater than for an ideal system. The deviations from ideality are positive. If deviations from ideality are large enough, the total vapor pressure passes through a maximum or a minimum. Extreme values of p correspond to the formation of azeotropes. Thus, azeotropes can only occur as a result of non–ideal solution behavior (23). The Raoult's/Henry's Law straight line obeys the relation

$$p = mx_i \tag{15}$$

The activity coefficient can be thought of as the ratio of the value of the real solution behavior line to the reference line for a given value of the mole fraction on one of these plots, and would yield the relation

$$p = \gamma_i m x_i \tag{16}$$

The numerical value of γ_i will be different at each x_i (24).

iv. The Limiting (Infinite Dilution) Activity Coefficient

As a solution of a given solute in a given solvent becomes increasingly dilute, the value γ_i asymptotically approaches a limiting value, γ_i^∞. γ_i^∞ is the correction factor compensating for non–ideal behavior in a solution in the Henry's Law region. The convention used in this work for binary systems is that the solvent is denoted by the subscript 1, and the solute by 2. The symbol for the limiting activity coefficient for the solute in a binary system at infinite dilution is γ_2^∞.

Activity coefficients of organic compounds in nonelectrolyte solutions are necessary for both theoretical and practical applications in thermodynamics of solutions, chemical engineering, and environmental chemistry. Nonelectrolyte solutions can be described by the solute excess partial molar Gibbs free energy of the solute at infinite dilution, $\mu_2^{e,\infty}$, derived from γ_2^∞ by

$$\mu_2^{e,\infty} = RT \ln \gamma_2^\infty \tag{17}$$

As noted earlier, from $\mu_2^{e,\infty}$ all the other excess thermodynamic functions can be derived (15). The excess partial molar enthalpy can be determined directly from the temperature dependence of γ_2^∞ by (25)

$$\bar{h}_2^{e,\infty} = -R[d \ln \gamma_2^\infty / d(1/T)] \tag{18}$$

and since

$$\mu_2^{e,\infty} = \bar{h}_2^{e,\infty} - T\bar{s}_2^{e,\infty} \tag{19}$$

the excess partial molar entropy can be estimated. Finally, the excess partial molar heat capacity can be calculated from $\bar{h}_2^{e,\infty}$ by

$$\overline{c}^{e,\infty}_{p,2} = [\mathrm{d}\,\overline{h}^{e,\infty}_{2}/\mathrm{dT}] \qquad (20)$$

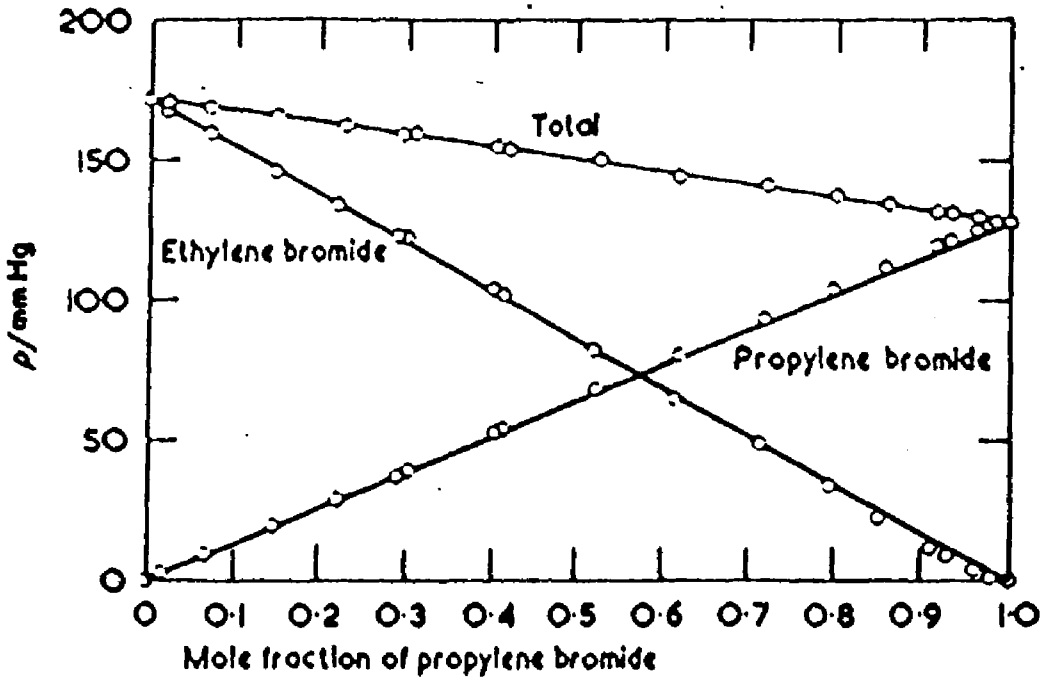

Figure II.1. Partial and total vapor pressures of mixtures of ethylene bromide and propylene bromide at 85°C (26).

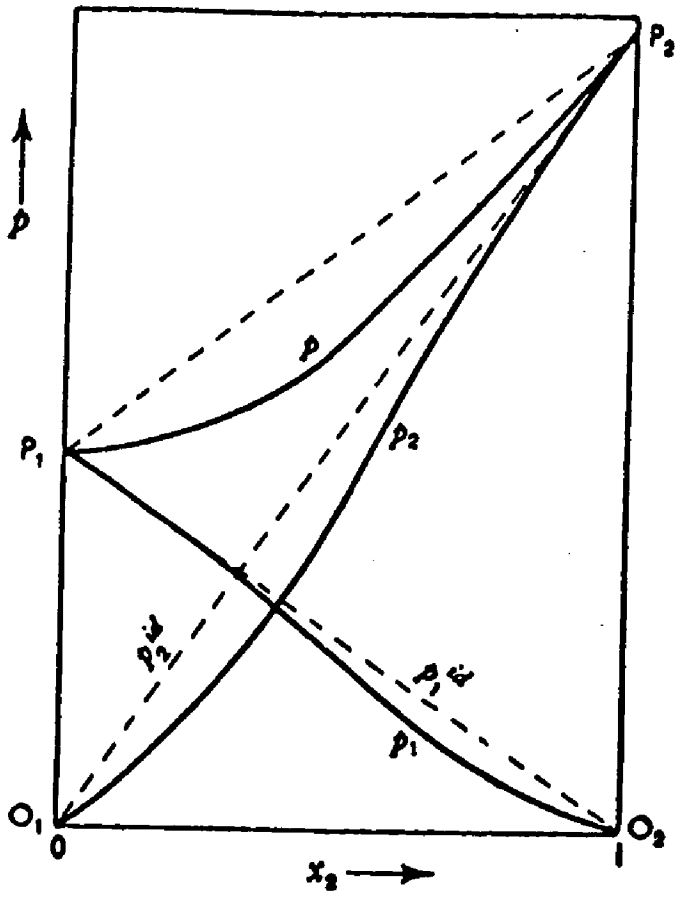

Figure II.2. Negative deviations from ideality (27).

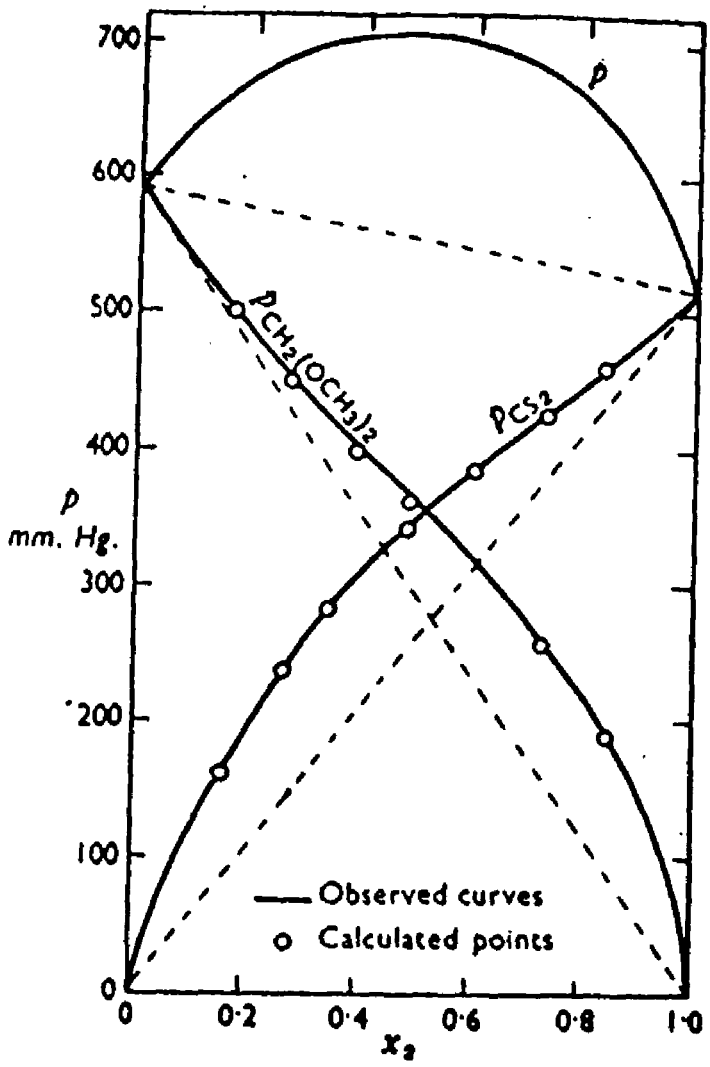

Figure II.3. Positive deviations from ideality for the system methylal + carbon disulfide (23).

References

(1) Guggenheim, M.A. "Thermodynamics," 5th Edn., 1967, North–Holland Publishing Co., Amsterdam, p. 220.

(2) Denbigh, K. "The Principles of Chemical Equilibrium", 4th Ed., 1986, Cambridge University Press, London, p. 244.

(3) Denbigh, K. *ibid.*, p. 249.

(4) Smith, E.B. "Basic Chemical Thermodynamics," 3rd Edn., 1982, Clarendon Press, Oxford, p. 77.

(5) Guggenheim, M.A. *ibid.*, p. 187.

(6) Denbigh, K. *ibid.*, p. 115.

(7) Smith, E.B. *ibid.*, p. 80.

(8) von Zawidzki, J. Z. Physik. Chem. 1900, 36, 129.

(9) Rowlinson, J.S.; Swinton, F.L. "Liquids and Liquid Mixtures," 3rd Edn., 1982, Butterworth Scientific, London, p. 92.

(10) McGlashan M.L.; Wingrove, R.J. Trans. Faraday Soc. 1956, 52, 470.

(11) Denbigh, K. *ibid.*, p. 223

(12) Prigogine, I.; Defay, R. "Chemical Thermodynamics," (trans./rev. D.H. Everett), 1962, John Wiley & Sons Inc., New York, p. 334.

(13) Smith, E.B. *ibid.*, p. 85.

(14) Prigogine, I.; Defay, R. *ibid.*, p. 332.

(15) Guggenheim, M.A. *ibid.*, p. 190–219.

(16) Wolf, K.L. Z. Physik. Chem. 1949, 61, 191.

(17) Trieschmann, H.G. Z. Physik. Chem. 1938, B39, 109.

(18) Lewis G.N.; Randall, M. "Thermodynamics," 1923, McGraw Hill, New York.

(19) Prigogine, I. "The Molecular Theory of Solutions," 1957, North Holland Publishing Co., Amsterdam, p. 11.

(20) Smith, E.B. *ibid.*, p. 97.

(21) Prausnitz, J.M.; Lichtenthaler, R.N.; de Azevedo, E.G. "Molecular Thermodynamics of Fluid–Phase Equilibria," 2nd Edn., 1986, Prentice Hall

Inc., Englewood Cliffs, p. 200.

(22) Van Ness, H.C.; Abbott, M.M. AIChE J. 1979, 25, 645.

(23) Prigogine, I.; Defay, R. *ibid.*, p. 338.

(24) Fanelli, A. J. Chem. Ed. 1986, 63(2), 112.

(25) Belfer, A.J.; Locke D.C. Anal. Chem. 1984, 56(13), 2487.

(26) Guggenheim, M.A. *ibid.*, p. 189.

(27) Prigogine, I.; Defay, R. *ibid.*, p. 337.

III. Experimental Methods of Determining Limiting Activity Coefficients

There has been a lot of work devoted to the development of experimental methods to determine limiting activity coefficients (1). What follows is a brief discussion of some of the methods used.

A. Ebulliometric Method – Differential Ebulliometry

Gautreaux and Coates (2) derived four expressions for γ_i^∞ in terms of pure component properties and the limiting slopes of pressure and temperature with respect to liquid– and vapor–phase composition. They suggested a direct experimental determination of the limiting activity coefficient. Eckert, et al. (3) limited the possible experiments to the simplest and most convenient one by the conditions: "(a) *a priori* gravimetric determination of composition rather than analysis of samples, since several highly dilute compositions are necessary in every run, and (b) dynamic rather than static vapor–liquid equilibrium to assure rapidity of measurement." These conditions limited them to a boiling point elevation experiment since the limiting slope to be measured is that of temperature vs. liquid composition at constant pressure.

In 1924, Swientoslawski and Romer (4) designed the ebulliometer. An ebulliometer, based on the principle of the Cottrell pump, is an instrument capable of measuring boiling points with an accuracy of $\pm 0.0015^{\circ}C$. Figure III.1 is a schematic diagram of an ebulliometer. Ebulliometry has been used to determine boiling points, molecular weights, mutual solubilities, sample purities, and limiting activity coefficients (5). Eckert, et al. (3) improved on the earlier work of Null (6) and Wong and Eckert (7) by designing a system that solved the major problems of pressure fluctuations and loss of volatile

components. They used a differential ebulliometric system containing five ebulliometers in a manifold to avoid the errors inherent in measuring absolute rather than differential quantities and to be able to determine four limiting activity coefficients simultaneously (8). Figure III.2 illustrates the experimental setup and support equipment necessary for differential ebulliometry when using two ebulliometers. Eckert, et al. simply added three more to this type of set–up.

Based on the expressions developed by Gatreaux and Coates (2) and adding terms to account for vapor–phase nonidealities, the equation used by Eckert, et al. (8) to determine limiting activity coefficients from the differential ebulliometric experiment is

$$\gamma_1^{\infty} = \phi^{(P_2^s)}[P_2^s-(1-P_2^sV_2/RT+(P_2^s/\phi_2^s))(\partial\phi_2/\partial P)\times (dP_2^s/dT)(dT/dx_1)_P^{\infty}]/\{P_1^s\phi_1^s\exp[(P_2^s-P_1^s)V_1/RT]\} \qquad (1)$$

where ϕ is the the vapor–phase fugacity coefficient, ϕ^s is the fugacity coefficient at saturation pressure, P is the total pressure, P^s is the saturation pressure, and V is the liquid molar volume. Fugacity coefficients were calculated by the method of Hayden and O'Connell (9). In general, the effects of the fugacity coefficient and Poynting correction are of little significance (8) so that the above equation may be simplified to

$$\gamma_1^{\infty} = [P_2^s-(dP_2^s/dT)(dT/dx_1)_P^{\infty}]/P_1^s \qquad (2)$$

The only term requiring binary data is $(dT/dx_1)_P^{\infty}$, i.e., the limiting composition derivative of the boiling temperature at constant total pressure. This quantity is determined by accurately measuring the boiling point difference between an ebulliometer containing only solvent and one containing the solute/solvent mixture.

The procedure involves first filling the ebulliometers gravimetrically

with the solvent to be studied, heating the system, setting the pressure, and allowing it to equilibrate. After measuring the equilibrium temperature difference using very sensitive temperature probes in each ebulliometer, an exact amount of solute (determined gravimetrically by weighing the syringe before and after the injection) is introduced into the loading one and the system is allowed to equilibriate. The temperature difference is then taken again. The process is repeated with another weighed sample of solute and the temperature difference is recorded. Eckert, et al. (3,8) did 6 injections of solute per system. In their later work (8), where they had five ebulliometers connected in a manifold, they were able to determine γ_1^∞ for four solutes in a given solvent simultaneously. The whole process, however, took 6–8 hours since equilibration time was required after each injection.

The limiting slope, $(dT/dx_1)_P^\infty$, is determined by fitting the data to a two term analytical polynomial equation of the form

$$\Delta T = ax + bx^2 \qquad (3)$$

and to one and three term polynomials of the same form. The value of a gives the limiting slope. The enrichment of the vapor phase or the liquid holdup of the more volatile component must be corrected for. Eckert, et al. (8) cite these corrections as resulting in less then 10% error for relatively ideal systems with as much as a 50°C boiling difference, or for systems of components of similar volatilities and values of γ_i^∞ as high as 40. The data for $(dT/dx_1)_P^\infty$ is then fit into eq. 1 and γ_1^∞ is directly calculated. Where the error in $(dT/dx_1)_P^\infty$ is large, values obtained from equation 1 were averaged with those from a solution to the Gibbs–Duhem (10,11) equation using either the Wilson (12) or Van Laar (13) equations.

Pividal and Sandler (14) conducted an ebulliometric experiment similar

to that of Eckert, et al., but used the expression and method derived by Dohnal and Novotná (15,16). The two equations are, in effect, the same, but Pividal and Sandler correct x_i for the composition differences due to enrichment or liquid holdup by using an evaporation factor, f, defined as

$$f = (N_V + N_V^{VLE})/N_L^{VLE} \tag{4}$$

where N_L^{VLE} and N_V^{VLE} are the moles of liquid and vapor in equilibrium and N_V is the moles of condensed vapor holdup not yet returned to the boiling chamber. They were able to show, from a mass balance around the ebulliometer, that

$$f = (z_i - x_i)/(K_i x_i - z_i) \tag{5}$$

or

$$x_i = z_i\{(1+f)/(1+K_i f_i)\} \tag{6}$$

where z_i is the feed mole fraction of component i and K_i is the volatility of component i, $K_i = y_i/x_i$. Equation 6 gives the true mole fraction to be used in the expressions for γ_i^∞ once f is determined. To determine f, K_i is needed. This is obtained by an iterative process. First, the raw $(dT/dx_1)_P^\infty$ data s fit into equation 1 to yield a rough value of γ_i^∞. Second, the result is used to estimate the parameters in the two–suffix Margules (17), Van Laar (13), Wilson (12), NRTL(18), and UNIQUAC (19) equations. Third, these parameters and vapor pressure data are used to determine the K_i factor for each feed composition, from which f was calculated. Finally, the corrected x_i values are then fit back into the original γ_i^∞ equation to get an accurate result.

Tamir and Wisniak (20,21) used a modified all–glass Dvorak–Boublik recirculation still (22) to determine activity coefficients and boiling points at 760 mmHg for the systems methanol/acetonitrile and acetonitrile/propyl bromide. All analyses were carried out by gas chromatography. Calibrations

were required to convert the peak area ratio to the weight composition of the mixture. Concentration measurements were generally accurate to ±0.5%, and that of the temperature and pressure were $\Delta T = \pm 0.02^{o}C$ and $\Delta P = \pm 2$ mmHg. The activity coefficients were found to be thermodynamically consistent according to the Herington criteria (23), and correlated well with the Redlich–Kister equation (24) and with the Wilson correlation (12).

Eckert, et al. (8) report results for 147 systems which were in good agreement with literature values. However, the literature values are extrapolated from VLE data of higher concentration, and not all the data correspond to the temperatures of the ebulliometric experiment. The same limitation applies to the work of Pividal and Sandler (14). For nearly ideal systems ($0.7 < \gamma_i^{\infty} < 2.0$), the reproducibility and agreement with literature values is excellent, i.e. within 2–3%. For more highly nonideal systems, the values differ by 30% or more. Eckert, et al. (8) state that this can be attributed to "the difficulty in extrapolating finite concentration data to infinite dilution for these highly nonideal systems."

B. Chromatographic Methods

i. Gas–Liquid Chromatography

A gas–liquid chromatographic method of determining limiting activity coefficients was developed by Young (25) in 1968 (1,26). Conder and Young (27) described the experimental procedure in the following way. The necessary instrumentation included a commercial analytical GC with a thermal conductivity detector, a manometer, a pressure gauge to measure the inlet pressure, and a soap–bubble meter to measure the flow rate (Figure III.3).

Using the system suggested by Kenworthy, Miller, and Martire (28) of dinonylphthalate as the stationary phase on 60–80 mesh unsilanized white diatomaceous support, they packed a 1.2 m × 6 mm od copper column with 25% stationary phase. Studying benzene, cyclohexane, cyclohexene, and n–hexane at between 70–90^{o}C they measured retention times of the solutes in the range of 3–12 minutes at a gas flow rate of 50 ml/min. These systems yielded activity coefficients whose values were readily compared with the literature and easily explained in terms of solution interaction (29). The GC was turned on and allowed to equilibrate an hour before the experiment. Solute samples in the range of 0.1–1 μl were injected with some air so as to get an air peak too. The retention time, flow rate, inlet and outlet pressure , and room and column temperature were measured and recorded. Having this information, the infinite dilution activity coefficient were readily determined.

The retention time t_R is the time the average molecule of solute takes to travel the length of the column. A portion of this time, t_M, is the time it takes the solute to pass through the mobile phase space from inlet to outlet. The retention volume V_R is defined as

$$V_R = Ft_R \tag{7}$$

where F is the flow rate of gas (mobile phase) observed at the pressure at the column. The product of t_M and F yields the mobile phase (gas) holdup V_M. The contribution of the retention by the stationary phase alone is the adjusted retention volume $V_R^{'}$:

$$V_R^{'} = V_R - V_M \tag{8}$$

This value is true for outlet pressure and must be corrected for mean column pressure. James and Martin (30) considered the migration of the peak along the column and derived the true retention time at mean column pressure,

taking into account the pressure drop along the column and the resulting acceleration of compressible carrier gas (31), by the relation

$$t_R = V_R^o / J_2^3 F \qquad (9)$$

where V_R^o is the corrected retention volume and J_2^3 is the pressure–gradient correction factor given by

$$J_2^3 = (3/2)\{[(P_i/P_o)^2 - 1]/[(P_i/P_o)^3 - 1]\} \qquad (10)$$

where P_i and P_o are the column inlet and outlet pressures, respectively. Extensive tables of J_2^3 have been prepared (32). The corrected retention volume is

$$V_R^o = J_2^3 V_R \qquad (11)$$

and the same applies for the mobile phase holdup. So, from equations 11 and 8, the net retention volume V_N can be derived:

$$V_N = J_2^3 V_R' = J_2^3 (V_R - V_M) \qquad (12)$$

In addition, the flow rate determined with a soap–film meter refers to ambient (flow meter) conditions, which need to be corrected to column outlet conditions. The vapor pressure of the soap solution is assumed equal to the vapor pressure of pure water at the meter temperature, and a correction for the temperatures in the column and the flow meter not being equal must be made. Therefore, the flow rate that should be used to determine the retention volume is the corrected flow rate, F_{corr}, given by

$$F_{corr} = F_{fm}(T_{col}/T_{fm})(P_{fm}/P_o) \qquad (13)$$

where F_{fm} is the measured flow rate, T_{col} is the column temperature, T_{fm} is the temperature of the flow meter, P_{fm} is the carrier gas pressure in the flow meter which is equal to the difference between atmospheric pressure and the vapor pressure of water P_w at that temperature ($P_{atm} - P_w$), and P_o is the carrier gas pressure at the outlet of the column which is equal to atmospheric

pressure (P_{atm}). Conder and Young (33) combine this all into the retention volume expression by the relation

$$V_N = (z_R/s)J_2^3F_{fm}[1-(P_w/P_{fm})](T_{col}/T_{fm}) \qquad (14)$$

where z_R is chart recorder distance between peaks of non–sorbed solute and of a sorbed one, and s is the chart speed.

The partition coefficient K_L is defined for a linear isotherm by the equation

$$K_L = q/c \qquad (15)$$

where q is the equilibrium concentration of solute in the liquid phase and c is the corresponding concentration of solute in the gas phase. This is a measure of the distribution of the solute between the gas and liquid phases at equilibrium. For ideal gases, the retention volume V_N, the partition coefficient K_L, and the activity coefficient γ_i are related by (25,34–36)

$$V_N = K_L V_L = (RTW_L/p_2^oM_L\gamma_2) = (RTn_L/p_2^o\gamma_2) \qquad (16)$$

where V_L is the volume of the stationary phase, W_L is the mass of the stationary phase in the column and M_L is its molecular weight, p_2^o is the solute partial vapor pressure, and n_L is the number of moles of stationary phase in the column (W_L/M_L). The activity coefficient of a solute is determined under the experimental conditions from

$$\gamma_2 = (RTW_L/V_Np_2^oM_L) \qquad (17)$$

If there is a much higher concentration of stationary phase to solute, i.e. if the solution is in the Henry's Law region, equation 17 corresponds to the infinite dilution activity coefficient γ_2^∞. For greater accuracy, gas–phase imperfection and carrier gas compressibility must be taken into account, using, for example, the relation (37–42)

$$\ln\gamma_2^{\infty}(0) = \ln(RTW_L/V_N p_2^o M_L) - [(B_{22} - v_2^o)p_2^o/RT] + [(2B_{23} - v_2^{\infty})P_o J_3^4/RT] \quad (18)$$

where B_{22} and B_{23} are the second virial coefficients characterizing interactions between two solute molecules, and a solute and a carrier gas molecule, respectively, v_2^o is the molar volume of liquid solute, v_2^{∞} is the partial molar volume of the solute at infinite dilution in the stationary phase, and

$$J_3^4 = (3/4)\{[(P_i/P_o)^4 - 1]/[(P_i/P_o)^3 - 1]\} \quad (19)$$

$\gamma_2^{\infty}(0)$ is the limiting activity coefficient at zero total pressure.

Many researchers (3,43,44,37,38,45–54) have obtained values for activity coefficients using some form of the support–coated GLC method. This method, however, was originally limited to volatile solutes in non–volatile stationary phases, such as squalane (55), octadecane (56), and quinoline (57), since the solvent had to stay on the support. Chao, et al. (50,58–64) did study relatively volatile solvents such as 4–methyl–2–pentanone and phenol. The GLC set–up and procedure were basically the same as those just described; however, they had thermal conductivity cells both in front of and behind the chromatographic column to detect and time the solute vapor in the carrier gas. They fit their data to an equation similar to the one preferred by engineers (equation 20, cited later in this chapter), and obtained results for many different kinds of solutes with root mean square deviations of the duplicates never exceeding 1%, and the uncertainty of the measured γ_i^{∞} values estimated to be below 2%.

There have been some applications of the technique to systems containing even more volatile solvents (3,58,65–68). Eckert, et al. (3,68) modified the GLC system for volatile solvent applications by adding a presaturator and a presaturating column between the carrier gas supply and

the GC gas inlet (Figure III.4). The helium carrier gas is saturated with solvent by passing the helium through the presaturator outside the temperature bath and, then, through the second presaturating column inside the temperature bath. The presaturated carrier gas stream is then split, half of it running through the heated sample injector block and then through the well–thermostated test column, in which the solvent is the "stationary" phase. The half passing through this column then runs through one side of the detector, while the other half from the presaturated feed goes through the other side. In this type of set–up the detector of choice is a thermal conductivity detector (TCD), because the large amounts of solvent present would saturate a flame ionization detector (FID) (3). However, the TCD has its limitations. Because the carrier gas is saturated with solvent, its ability to transfer heat is greatly reduced. This reduces the sensitivity of the detector. Therefore, small quantities of solutes cannot be detected when using volatile solvents. To standardize and correct for the amount of solvent that has been stripped off by gas phase expansion, the same solute is injected at the beginning and end of each run. The overall effect can be minimized by running the experiment at low pressure drops (68). This limits the length of the column to 20–30 cm (3).

Eckert, et al. used the methods of Parcher and Urone (69) and Kruppa, et al. (70) to coat, dry to the desired percentage of solvent, and pack the substrate into the column. They wanted solvent loadings of greater than 10% (their determined percentage for reproducible results of all detectable solutes) but small enough so that the solute could elute from the column in less than 30 min. (68). The column was installed in the GC, He allowed to flow through for about 20 min., the detector filaments turned on, and the system allowed to

equilibrate for 30 min. The flow rate was kept at around 20 ml/min. according to Harris' (71) efficiency study. Injections of the solutes (0.15–0.35 μl) were then made sequentially. As stated earlier, the same solute was injected at the beginning and end of each series to account for and check stripping. To determine percent solvent loading at the end of a series of experiments, the column was removed from the GC, the ends were taped, water bath residue was rapidly dried off the column, and it was weighed. The contents were then emptied, the column reweighed, the substrate washed in acetone, dried, and weighed. The amount of substrate within the column and the weight of the solvent upon the substrate were then calculated (68). Given 3 assumptions, (i) equilibrium is achieved throughout the column, (ii) the solute is sufficiently dilute to be within the Henry's Law region, and (3) the solid support is inert relative to the solvent and solute, the limiting activity coefficient can be determined from the retention data by the form of the GLC equation preferred by chemical engineers (35,72–75):

$$\gamma_2^{\infty} = [RT\phi_2 Z_m \exp(-v_2^{\infty}P/RT)n_1^1]/[\phi_2^s P_2^s(V_R - V_M)] \qquad (20)$$

where ϕ_2 is the vapor–phase fugacity coefficient of solute at P, Z_m is the compressibility of the mixture, v_2^{∞} is molar volume of solute at infinite dilution, n_1^1 is the number of moles of solvent on the column, P_2^s is the saturation vapor pressure of the solute, ϕ_2^s is the fugacity coefficient of the solute at P_2^s, and V_M is the volume of the mobile phase.

In their later paper, Eckert, et al. (68) reported experimental γ_2^{∞} values for various solutes in 34 solvents. Itsuki, et al. (76,77), also using a GLC system with a presaturator, determined partial molar free energies of acetonitrile/benzene systems and of 18 organic solutes in n–hexane. They obtained results consistent with those from vapor pressure data (78). These

systems are industrially–interesting systems covering wide ranges of polarizability, polarity, and hydrogen–bonding ability. Though they report their method as generally being self–consistent to within 5%, the absolute accuracy is difficult to determine. Eckert, et al. (68) estimated that the expected accuracy for this method is 15% or better for most solvents, but not better than 40% for γ_2^∞ values greater than 100. Therefore, water data would be difficult to determine.

This dynamic GC method of γ_2^∞ determination is fast because it does not entail the preparation of solutions of the solute in the solvent of interest. Once a column with an accurately known amount of well–defined stationary phase is available, only the measure of the column dead volume and retention volume of the solutes of interest must be made experimentally. Thus, it is possible to inject mixtures of solutes (if separable) and generate data quite rapidly. However, even though the method has already been expanded to somewhat more volatile solvents (3,65–68), column preparation and determination of the mass of stationary phase liquid is tedious and prone to error. This step is the limitation of the accuracy and precision of the method (79,80). Corrections for the compressibility of the mobile phase and the pressure differential across the column must be made quite accurately and the effect of adsorption at the high surface area gas/solid or gas/liquid interface must be assessed and a correction made when significant (81). The experiment must be run under isothermal conditions; hence, a mixture of solutes must be well separated at the temperature of interest. Conventional integrators cannot be used because when asymmetric peaks are encountered, the first moment is used as t_R. This requires on–line acquisition of the signal and postrun data analysis because conventional integrators do not compute t_R by first moment

of peak. To obtain limiting activity coefficients, the solutes must be injected at quite low concentration to avoid nonlinear isotherms. However, where the method is applicable, precise results, as good as 0.2%, can be obtained (80). Other advantages of the dynamic GLC method include the fact that the detector need not be calibrated, since the elution times and the flow rates are the critically important measurements, and it is possible to obtain the solute–carrier gas virial coefficient B_{23} by varying the inlet pressure to the column thereby changing the flow rate (82).

ii. Headspace Gas Chromatography

Headspace GC (HSGC) is an application of gas chromatography which employs a specialized sampling and sample introduction technique, making use of the equilibrium established between the volatile components of a liquid or solid phase and the gaseous/vapor phase in a closed sample container. Aliquots of the gaseous phase are sampled for analysis (83,84). The method has been used to test alcohol levels in blood and urine as well as for other volatiles which may be present in the blood (85), quality and production control of beer constituents and other brewing products (86,87), aromatic flavors and trace volatiles in foods and soft drinks (88–93), atmospheric monitoring of hazardous trace pollutants (94–96), in the analysis of residual monomers and other process residues in plastics packaging and consumer products (97), and in the analysis of volatile free fatty acids produced by bacteria (98,99). The clean nature of the sample makes HSGC ideal for automatic repetitive quantitative and qualitative analysis, at the same time prolonging the effective lifetime of a column (85).

Hussam and Carr (81), following the pioneering work of Renon (100),

developed an HSGC method to determine limiting activity coefficients. This static method was adopted for several reasons. Volatile solvents, such as mixtures of methanol and water, can be studied without presaturating the mobile phase with the solvent. Also, the headspace method is readily amenable to the measurement of vapor pressure, as well as activity coefficients over a finite concentration range. Thus, the entire phase diagram can be determined. Figure III.5 is a schematic of the device used for HSGC determination of γ_2^∞ values. It includes the following operational features: (1) rapid analysis of samples; (2) accurate temperature control of samples (better than $\pm 0.01^{o}C$); (3) ability to work at low sample concentration (mole fraction <0.01); (4) minimal perturbation of the equilibrium by the sampling process; (5) ability to vary composition of the solvent automatically. Hussam and Carr (81) used a vacuum transfer system to achieve the precision inherent in the sample loop and to minimize the perturbation of the vapor/liquid equilibrium by use of a small sample (~200 μl). The sample cells used were glass vessels (volume ca. 12 ml) connected via glass–metal seals to 1/4 in. then to 1/16 in. zero dead volume Swagelok stainless steel fittings and placed in a controlled–temperature water bath (with a tolerance of $\pm 0.001\ ^{o}C$). The system was designed with only glass and metal components (with one exception) to avoid the problem of a septum being attacked by solvent or imbibing sample. In order to allow high sensitivity and analysis of complex mixtures of gases, a commercial temperature programmed capillary (macrobore) GC was used as the analyzer.

To develop an expression for the activity coefficient from headspace GC data, γ_i must be developed differently than the approach taken in chapter II of this work. Prausnitz et al. (101) explain that at equilibrium, the fugacities of

any solute must be equal in the liquid and gas phases

$$f_i^l = f_i^g \tag{21}$$

At any given temperature, the fugacities in the liquid and gas phase are functions of the composition, concentration, and pressure only, and are expressed by Raoult's Law as

$$f_i^l = \gamma_i x_i f_i^o \tag{22}$$

$$f_i^g = \phi_i y_i P \tag{23}$$

where γ_i is the activity coefficient of species i, x_i is its mole fraction, and f_i^o is the fugacity of pure liquid i. Similarly, in the gas phase, ϕ_i is the fugacity coefficient, y_i is its mole fraction, and P is the total pressure. For pure i,

$$f_i^o = P_i^o \phi_i^o \exp[v_i^l (P - P_i^o)/RT] \tag{24}$$

where ϕ_i^o is the fugacity coefficient of pure i which corrects for the deviation of the saturated vapor pressure, P_i^o, from ideal gas behavior, the exponential term accounts for the effect of applied pressure on the vapor pressure, and v_i^l is the molar volume of pure liquid i. Combining equations 21–24, Prausnitz (101) solved for the activity coefficient

$$\ln\gamma_i = \ln(y_i P/x_i P_i) + \ln(\phi_i/\phi_i^o) - [v_i^l (P - P_i^o)/RT] \tag{25}$$

Gas–phase fugacity coefficients ϕ_i can be approximated at low pressure by the virial equation of state truncated after the second virial coefficient

$$\ln\phi_i = (2/v)\sum_{j=1}^{m} y_i B_{ij} - \ln Z_{mix} \tag{26}$$

where v is the molar volume of the mixture and Z_{mix} is the compressibility of the mixture. Z_{mix} is related to the virial coefficients by the equation

$$Z_{mix} = 1 + PB_{mix}/RT \tag{27}$$

where

$$B_{mix} = \sum_{ij}^{nn} y_i y_j B_{ij} \tag{28}$$

and B_{mix} is the mixture virial coefficient. Equations 25–28 are the basis for

the thermodynamic correction for the nonideality of gases.

Hussam and Carr (81) applied equation 25 to the headspace method as follows. If a gas standard is used and the detector is linear over the measured concentration range, the peak area is related to the molar concentration C_i of sample gas by the equation

$$A_i = kV_{loop}C_i \tag{29}$$

and, for the gas standard (GS),

$$A_{GS} = kV_{loop}C_{GS} \tag{30}$$

where k is a constant response factor and V_{loop} is the volume of the sample loop. The partial pressure of i in the headspace is related to the vapor–phase concentration by the equation

$$P_i = C_iRTZ_{mix} \tag{31}$$

Combining equations 29–31,the partial pressure equals

$$P_i = (A_i/A_{GS})C_{GS}RTZ_{mix} \tag{32}$$

where Z_{mix} refers to the solute i, solvent, and the air present in the headspace. Since C_{GS} (known from the weight of standard and volume of the sample bulb) is the analytical concentration of the solute in the standard gas bulb, no assumption regarding nonideality of gases in the standard is required. By definition, $P_i = y_iP$, so equation 25 can be combined with equation 32 to give for the activity coefficient

$$\ln\gamma_i^{GS} = \ln(A_iC_{GS}/A_{GS}x_i)+\ln(RTZ_{mix}/P_i^o)+ \ln(\phi_i/\phi_i^o)-[v_i^l(P-P_i^o)/RT] \tag{33}$$

Equation 33 relates the activity coefficient of solute i to the peak areas A_i and A_{GS} when a gas standard of known composition is used.

If a pure liquid standard is to be used, then, the peak area for a pure liquid (LS) in the presence of air is

$$A_{LS} = kV_{loop}C_{LS} \tag{34}$$

Combining equations 29 and 34 gives the concentration of the solute as

$$C_i = C_{LS}A_i/A_{LS} \tag{35}$$

The vapor pressure is equal to

$$P_i^* = C_{LS}RTZ_{mix}^* \tag{36}$$

where P_i^* is the vapor pressure of the liquid in the presence of air and Z_{mix}^* is the compressiblity under the same conditions. The compressibilities Z_{mix} and Z_{mix}^* refer to the sample condition and not that in the sampling loop. Combining equations 31, 35, and 36 gives

$$P_i = P_i^*(A_i/A_{LS})(Z_{mix}/Z_{mix}^*) \tag{37}$$

To obtain P_i^*, the vapor/liquid equilibrium of the liquid standard in the presence of air must be considered. Following the assumption that the solubility of air in the pure liquid is negligible, then, for pure liquid

$$f_i^l = f_i^o = P_i^o\phi_i^o \exp[v_i^l(P-P_i^o)/RT] \tag{38}$$

For the vapor phase

$$f_i = \phi_i^* P_i^* \tag{39}$$

where $P_i^* = y_iP$ and ϕ_i^* is the fugacity coefficient of pure vapor in the presence of air. Combining equations 38 and 39 gives

$$P_i^* = P_i^o(\phi_i^o/\phi_i^*) \exp[v_i^l(P-P_i^o)/RT] \tag{40}$$

Equation 40 corrects the true (saturated liquid vapor) pressure (P_2^o) to that which should be observed in the presence of air at total pressure P. Combining equations 25, 37, and 40, the activity coefficient based on a liquid standard can be calculated as

$$\gamma_i^{LS} = (A_i/A_{LS}x_i)(\phi_i/\phi_i^*)(Z_{mix}/Z_{mix}^*) \tag{41}$$

Hussam and Carr (81) state that in many cases it should be possible to assume that when the partial pressures of the solute and solvent pairs are low, the

terms ϕ_i/ϕ_i^* and Z_{mix}/Z_{mix}^* will approach unity. Thus, when virial coefficients are unknown, the use of the pure liquid solute as the analytical standard is advantageous. The first two terms of equation 33 are the uncorrected activity coefficient of the solute; the terms after that are usually small and approach unity, particularly in the case of infinite dilution.

The experimental procedure consists of first ensuring that the detector response is linear and that there is a zero intercept on the calibration plot. This is accomplished by running two different standards in the concentration limits to be studied. Then, a sample mixture to be studied is placed in the headspace vial and allowed to equilibrate by constant stirring. The headspace is sampled into a 20 μl sample loop and immediately injected into the GC. Once the peak areas of the samples and standards are known, the vapor pressures and infinite dilution activity coefficients can be directly assessed from equations 32, 33, 40, and 41. Hussam and Carr (81) studied the γ_i^∞ values of n–hydrocarbons in n–octadecane and the system p–dioxane/acetonitrile. They obtained a relative precision of better than 1%, and their results were in good agreement with literature values (102). Hussam and Carr used solute concentrations 10 times lower than those used to establish the literature values since solute mole fractions below 10^{-3} can be easily measured by headspace capillary GC. Therefore, their γ_i values are essentially in the infinite dilution region. However, accurate preparation of the sample, due to the high volatility of the solutes and, hence, their evaporation, severely limits the accuracy of the technique.

Sagert and Lau (103) used a cell virtually identical to that described by Milanová, Afrashtehfar, and Cave (104–107), to measure limiting activity coefficients for butanols in water, n–octane, and carbon tetrachloride by

determining butanol concentrations in the vapor over dilute solutions using HSGC. The cell was a vertical cylindrical chamber, about 150 mm high by 50 mm in diameter, fitted with a sampling valve at the top. This valve incorporated a rotatable head fitted with three calibrated sampling volumes. The cell was placed in a water bath maintained at 20.00 ± 0.04°C. Analyses were done using a Varian 1860 GC fitted with both an FID and a TCD detector. The GC was calibrated by injecting known, varying amounts of solute so that the peak areas were known as a function of the number of moles of solute. Fifty ml samples were placed in the cell and stirred with a magnetic stirrer. Once equilibrium was achieved, samples were injected into the GC. From the calibration curve, solute concentrations in the vapor and liquid were calculated, correcting the solute concentration in the liquid for solute evaporation into the cell, and correcting for the temperature difference between the cell at 20°C and the sample loops at room temperature. The GC measurements were reliable to within ±2%. Activity coefficients, corrected for gas–phase nonidealities, were calculated by (104,108)

$$\ln\gamma_2 = \ln(C_2/x_2C_{02})+2B_{22}(C_2-C_{02})+2B_{12}C_1 \qquad (42)$$

where C_2 is the molar concentration of solute in the equilibrium vapor, corrected for the temperature difference between the water bath and the sampling loop, C_{02} is the molar concentration of solute vapor over pure solute, x_2 is the mole fraction of solute in the liquid, C_1 is the solvent concentration in the vapor, and B_{12} and B_{22} are the second virial coefficients of the mixture and pure solute, respectively. The B_i values were taken from Dymond and Smith (109). Their results agreed well with earlier data (104,110).

Yin and Hassett (111) determined the fugacity and Henry's Law constant of Mirex ($C_{10}Cl_{12}$) in water using a method similar to HSGC but

made practical the use of large gas volumes. They called their method *gas–phase partitioning.* It is also commonly referred to as *gas stripping.* The cell was a 20 l glass carboy fitted with a metal screw cap. Analysis was done by thermodesorption–capillary GC. Yin and Hassett (111) record that the methods developed to quantitatively distinguish between bound and free hydrophobic organic compounds include solubility methods (112), equilibrium dialysis (113), reverse–phase separation techniques (114), and gas–phase partitioning (115). Solubility methods are inherently unsuitable for analysis of natural samples. Dialysis is not promising as a field technique because of potential biodegradation of cellulose membranes and because the membranes strongly absorb some hydrophobic compounds (114,116). Reverse–phase partitioning, though it might be suitable for field studies, would require pretreatment of samples by filtration or centrifugation to remove particles that otherwise would be trapped in the extraction column. Yin and Hasset (111), therefore, chose gas–phase partitioning. It is the most promising method for field studies because it offers direct measurement of fugacity of a hydrophobic compound in the presence of particles and dissolved organic matter with no pretreatment.

Gas–stripping as an experimental method for the determination of infinite dilution activity coefficients was developed by Renon (100) in 1977. His apparatus consisted of a saturator, a cylindrical cell 1 cm in diameter and 10 cm high, which was filled with 8 ml of an extremely dilute ($\sim 10^{-4}$ solute mole fraction) solution. The gas entered the saturator through a number of narrow holes (10 μm) to form small diameter bubbles. A magnetic stirrer was used to keep the solution homogenous. The saturator was thermostated at a temperature T_1. The escaping gas was sent through a stream line, kept at

temperature T_1+1°C, to a regulating valve which maintained the pressure at a set value. The expanded and now undersaturated gas is sampled by a stream valve kept at temperature T_3, greater than T_1. The low content component was monitored by GC.

Cori and Delogu (1) used Renon's method (100) to determine γ_2^∞ values of ethanol/n–alkane systems and to test the popular calculative model methods. They outlined the aspects of the apparatus that: (i) it can work under pressure (typically 3–4 atm), which would allow for operation at temperatures even higher than the normal boiling point of the solvent, and the evaporation rate of the solvent can be controlled; (ii) only the γ_i^∞ of the more volatile component can be easily measured. However, in minimum azeotropic systems, such as ethanol/n–alkane, the more volatile component is always the one at higher dilution so that both γ_i^∞ values can be obtained by the same technique; (iii) the accuracy offered by the method had a standard deviation of ±0.5 in the experimental range. The measured variables had accuracies (as measured by standard deviations, σ) of σ_P = 1 mmHg, σ_F = 40 ml/h, σ_T = 0.5°C. The reproducibility of the measurements was, at worst, ±5% of the mean value. Though the method, overall, is clean, fast and efficient, it still requires accurate sample preparation and ample equilibration time.

iii. Liquid–Liquid Chromatgraphy

Though GLC is an accurate method for the determination of the infinite dilution activity coefficient of a solute in a solvent (stationary phase), as stated earlier in this chapter, it is somewhat difficult to do when volatile solvents are used as the stationary phase. Liquid–liquid chromatography (LLC) has been in use since 1941 (43) for physiochemical measurements, such

as liquid–liquid partition coefficients. However, LLC has not found extensive application in the determination of thermodynamic data because it only provides relative values, i.e., ratios of the activity coefficients of a solute at infinite dilution in the two phases used, the mobile and stationary phases. Locke and Martire (117) related the specific retention volume to the ratio of solute activity coefficients by

$$\ln(V^{O}_{gi})_{L} = \ln(\gamma_i^{m,\infty}/\gamma_i^{s,\infty})+\ln(M_m/M_s\rho_m)+ [(\bar{P}-1)/RT](\bar{v}_i^{m}-\bar{v}_i^{s}) \quad (43)$$

where $(V^{O}_{gi})_{L}$ is the specific retention volume of component i in liquid–liquid chromatographic measurements, $\gamma_i^{m,\infty}$ and $\gamma_i^{s,\infty}$ are the infinite dilution activity coefficients of i in the mobile and stationary phases, respectively, M_m and M_s are the molecular weights of the mobile and stationary phases, respectively, ρ_m is the density of the mobile phase, $\bar{P}$ is the mean pressure in the column, and $\bar{v}_i^{m}$ and $\bar{v}_i^{s}$ are the solute partial molar volumes of the mobile and stationary phases, respectively. To obtain the solute activity coefficient in the mobile phase it is necessary to determine, by other means, the corresponding quantity in the stationary phase. Locke (118) combined GLC with LLC using the same stationary phase at the same temperature. He studied acetonitrile (mobile phase and solvent of interest) in squalane (stationary phase, solvent). $\gamma_i^{s,\infty}$ is determined by GLC, and $\gamma_i^{m,\infty}$ by the combination of the GLC value for $\gamma_i^{s,\infty}$ data and the LLC retention data, V^{O}_{g}. Locke observed that the $\gamma_i^{m,\infty}$ values were indistinguishable from equilibrium measurements except for large values, which were higher than equilibrium measurements. The discrepancy was attributed to adsorption phenomena which are likely to occur at the liquid–liquid interface.

Alessi and Kikic (119–121) did the GLC/LLC experiment on the

systems aniline in Apiezon–L, squalane, and n–hexadecane, and acetonitrile in Apiezon–L and squalane. They attributed the discrepancy Locke found to the mutual solubilities of the two solvents used as the mobile and stationary phases. Alessi and Kikic consider the γ_2^∞ values as those in the saturated solvents, not as in pure solvents, because that is their condition when used in LLC. Therefore, LLC allows the determination of γ_2^∞ values only when the mutual solubilities between the stationary and mobile phases are negligible (below 2 mole%). Mutual solubilities can be lowered by either lowering the temperature or using high molecular weight and/or polymeric substances as the stationary state. However, when polymers are used, the adsorption phenomena and the risk of swelling by the action of the mobile phase give rise to some difficulties. Futhermore, the molecular weight is not accurately known, and γ_2^s is then ill–defined. The experiments were done using Chromosorb P as the solid support and varying the stationary phases from the above mentioned list. Also, using the same stationary phase, they did the determination at 25°C and at 2°C. They found that decreasing the mutual solubility does allow for the determination of γ_2^∞ values in "pure" solvents directly. The last term of equation 43, $[(\overline{P}-1)/RT](\bar{v}_i^m-\bar{v}_i^s)$ is negligible at the operating pressures of the experiment (below 10 atm). The reproducibility of the specific retention volumes is about 1–2%.

Hammers, Meurs, and De Ligny (122) studied the activity coefficients, interfacial tensions, and retention in reversed–phase liquid chromatography on LiChrosorb RP–18 with methanol/water mixtures. They showed that the affinity of the adsorbent towards solutes is a result of apolar interactions in the RP–18 phase and of polar interactions in the interfacial layer of adsorbed methanol. Hammers, et al. concluded that values of $\ln\gamma_2^\infty$ in water for solutes

of different sizes, shapes, and polarities are linearly related to the product of the interfacial tension and the molecular surface area of the solute when the interfacial tension is equal to or greater than 10 dyne/cm. Solute retention on LiChrosorb RP–18 with methanol/water mixtures and water as eluents is mainly controlled by the solute activity coefficient in the mobile phase. The adsorbent affinity towards solutes is approximately constant in the range of 40–70% (v/v) methanol. This is due to a constant amount of adsorbed methanol in this range. Therefore, Locke's model (123) of displacement adsorption is the preferred way to explain what is going on inside the column.

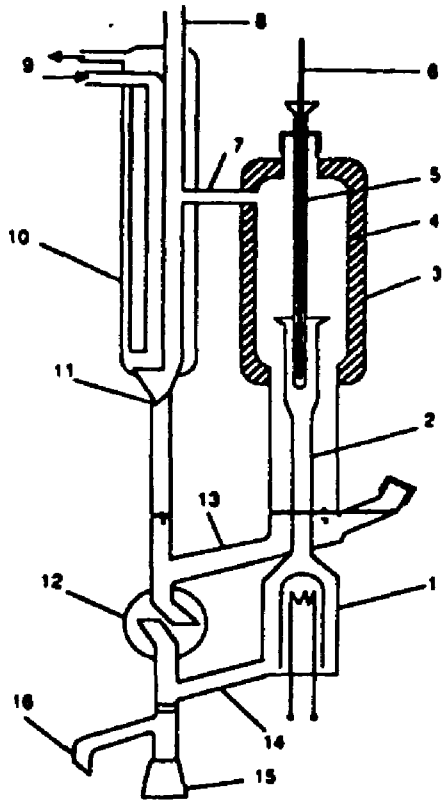

Figure III.1. Schematic diagram of the ebulliometer: (1) still pot, (2) Cottrell pump, (3) insulation, (4) VLE chamber, (5) thermowell, (6) thermocouple, (7) vapor passover, (8) to pressure controller, (9) coolant inlet and outlet, (10) condenser, (11) condenser vapor drop, (12) mixing chamber, (13) and (14) liquid recycle, (15) stopcock, and (16) drain port. From ref. (10).

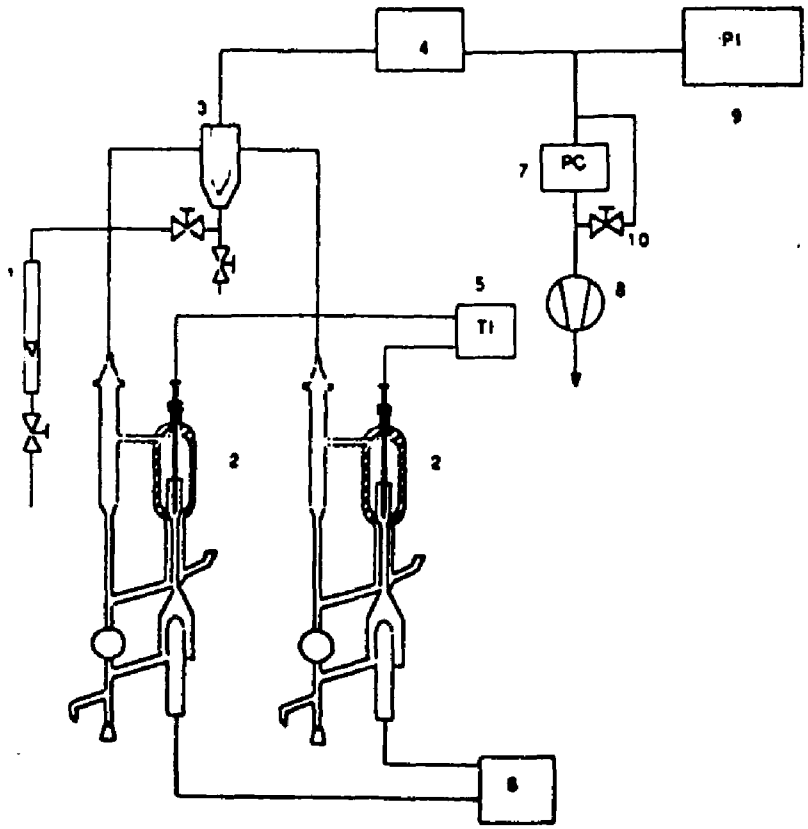

Figure III.2. Experimental setup and support equipment for comparative ebulliometry: (1) flow indicator for the nitrogen purge, (2) twin ebulliometers, (3) cold trap, (4) 50 l buffer volume, (5) thermocouple and digital readout, (6) heating units, (7) pressure indicator and controller, (8) vacuum pump, (9) pressure indicator, and (10) valve. From ref. (10).

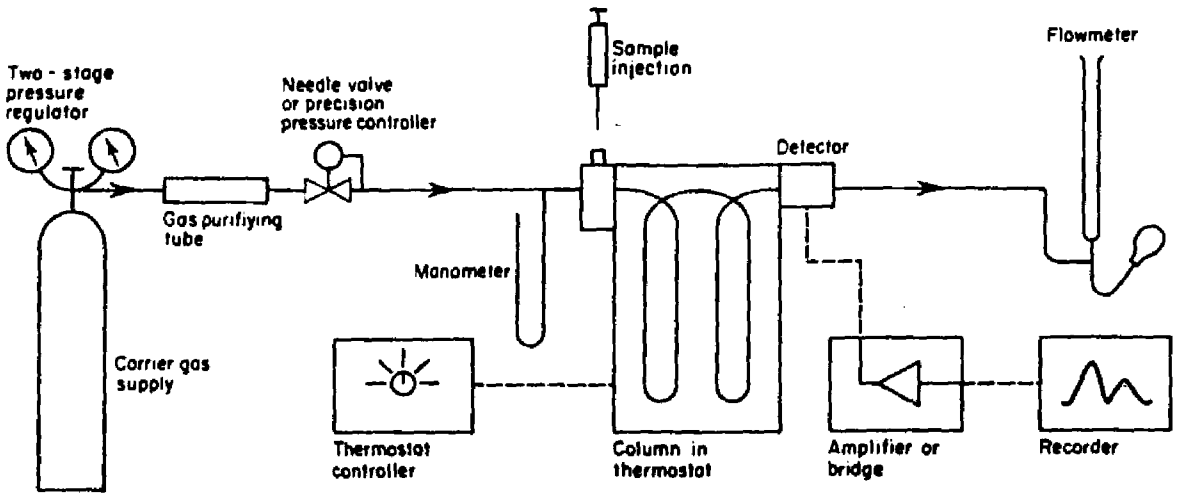

Figure III.3 Gas chromatograph for physiochemical measurements (124)

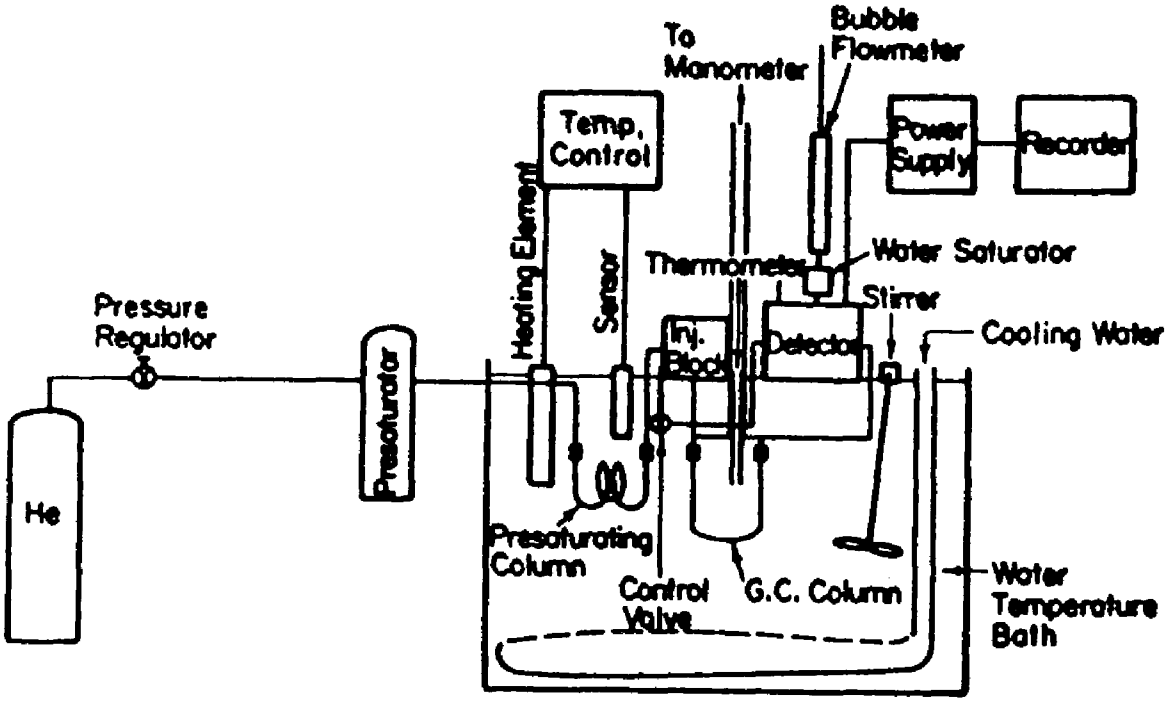

Figure III.4. Schematic diagram of modified gas chromatograph for measuring limiting activity coefficients in volatile solvents (3).

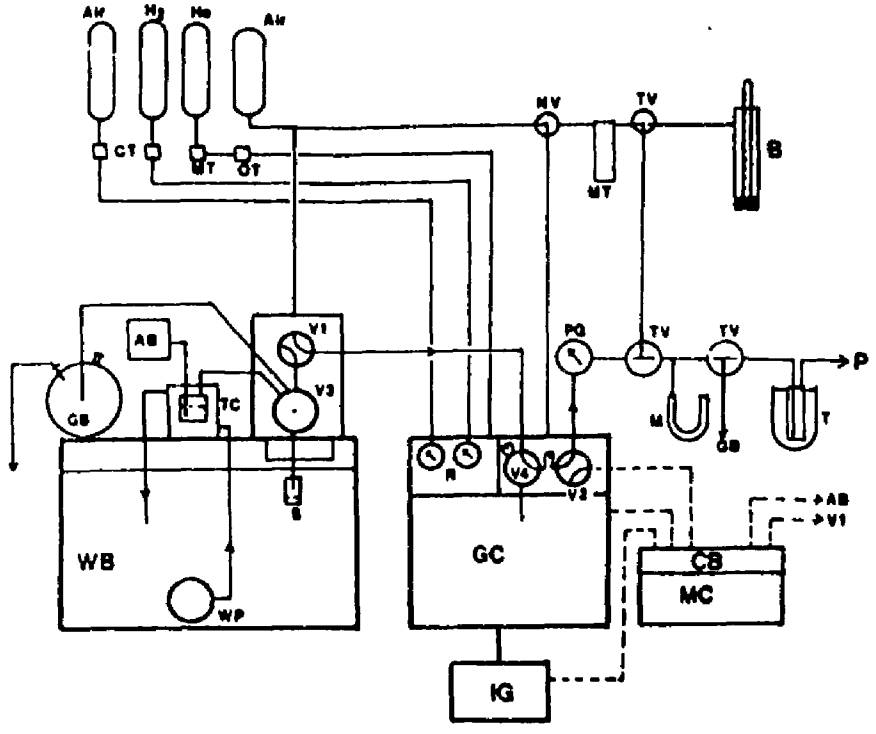

Figure III.5. Schematic diagram of HSGC setup: (WB) waterbath, (WP) thermostating water pump, (GB) glass sample bulb, (S) sample cell, (AB) precalibrated autoburet, (P) vacuum pump, (T) cold trap, (M) manometer, (PG) pressure gauge, (b) barometer, (V1,V2,V3,V4) valves, (MT) monostat, (NV) needle valves, (MT) moisture trap, (OT) oxygen trap, (IG) integrator, (MC) microcomputer, (GC) gas chromatograph, (CB) controller board, (tc) thermostated cell (81).

References

(1) Cori, L.; Delogu, P. "Measurement, Evaluation, and Prediction of Phase Equilibria," Kehiaian, H.V.; Renon, H., Eds., 1986, Elsevier Science Publishers, Amsterdam, p. 104.

(2) Gautreaux, M.F.; Coates, J. AIChE J. 1955, 1, 496.

(3) Eckert, C.A.; Newman, B.A.; Nicolaides, G.L.; Long, T.C. AIChE J. 1981, 27, 34.

(4) Swientoslawski, W.; Romer, W. Bull. Intern. Acad. Pol. Sci. Letters 1924, 59.

(5) Hala, E.; Pick, J.; Fried, V.; Vilim, O. "Vapor–Liquid Equilibrium," 1967, Pergamon Press, New York.

(6) Null, H.R. "Phase Equilibrium in Process Design," 1970, John Wiley & Sons, New York.

(7) Wong, K.F.; Eckert, C.A. Ind. Eng. Chem. Fundam. 1971, 10, 20.

(8) Thomas, E.R.; Newman, B.A.; Nicolaides, G.L.; Eckert, C.A. J. Chem. Eng. Data 1982, 27, 233.

(9) Hayden, J.G.; O'Connell, J.P. Ind. Eng. Chem. Process Des. Dev. 1975, 14, 209.

(10) Gibbs, J.W. "Collected Works," Vol. 1, 1928, Longmans, New York, p. 88.

(11)Duhem, P. "Le Potentiel Thermodynamique et ses Applications," 1886, Paris, p. 33.

(12) Wilson, G.M. J. Am. Chem. Soc. 1964, 86, 127.

(13) Van Laar, J.J. Z. Phys. Chem. 1910, 72, 723.

(14) Pividal, K.A.; Sandler, S.I. J. Chem. Eng. Data 1988, 33, 438.

(15) Dohnal, V.; Novotna, M. Collect. Czech. Chem. Commun. 1986, 51, 1393.

(16) Novotna, M.; Dohnal, V.; Holub, R. "Measurement, Evaluation and Prediction of Phase Equilibria," Kehiaian, H.V.; Renon, H., Eds., 1986, Elsevier Science Publishers, Amsterdam, p. 373.

(17) Margules, H. Sitzungber. Wien Akad. 1895, 104, 1243.

(18) Renon, H.; Prausnitz, J.M. AIChE J. 1968, 14, 135.

(19) Abrams, D.; Prausnitz, J.M. AIChE J. 1975, 21, 116.

(20) Tamir, A.; Wisniak, J. J. Chem. Eng. Data 1986, 31, 363.

(21) Wisniak, J.; Tamir, A. J. Chem. Eng. Data 1975, 20, 168.

(22) Boublikova, L.; Lu, B.C.Y. J. Appl. Chem. 1969, 19, 89.

(23) Herington, E.F.G. J. Inst. Petr. 1951, 37, 457.

(24) Redlich, O.; Kister, A. Ind. Eng. Chem. 1948, 40, 345.

(25) Young, C.L. Chromatogr. Rev. 1968, 10, 129.

(26) Prausnitz, J.M.; Lichtenthaler, R.N.; de Azevedo, E.G. "Molecular Thermodynamics of Fluid–Phase Equilibria," 2nd Edn., 1986, Prentice–Hall Inc., Englewood Cliffs, p. 545.

(27) Conder, J.R.; Young, C.L. "Physicochemical Measurement by Gas Chromatography," Wiley, Chichester, p. 10.

(28) Kenworthy, S.; Miller, J.; Martire, D.E. J. Chem. Educ. 1963, 40, 541.

(29) Conder, J.R.; Young, C.L. *ibid.*, p. 590.

(30) James, A.T.; Martin, A.J.P. Biochem. 1952, 50, 679.

(31) Dal Nogare, S.; Juvet, R.S. "Gas Liquid Chromatography," 1962, Interscience, New York, p. 73.

(32) Chromatographic Data J. Chromatogr. 1957, 2, D33.

(33) Conder, J.R.; Young, C.L. *ibid.*, p. 28.

(34) Conder, J.R.; Young, C.L. *ibid.*, p. 163.

(35) Locke, D.C. Adv. Chromatogr. (N.Y.) 1976, 14, 87.

(36) Laub, R.J.; Pecsok, R.L. "Physiochemical Applications of Gas Chromatography," 1978, Wiley, New York.

(37) Kwantes, A.; Rijnders, G.W.A. "Gas Chromatography, 1958," Desty, D.H., Ed., 1958, Butterworths, London, p. 125.

(38) Everett, D.H.; Stoddart, C.T.H. Trans. Faraday Soc. 1961, 57, 746.

(39) Desty, D.H.; Goldup, A.; Luckhurst, G.R.; Swanton, W.T. "Gas Chromatography, 1962," van Swaay, M., Ed., 1962, Butterworths, London, p. 67.

(40) Everett, D.H. Trans. Faraday Soc. 1965, 61, 1637.

(41) Cruickshank, A.J.B.; Windsor, M.L.; Young, C.L. Proc. Roy. Soc. A. 1966, 295, 259.

(42) Windsor, M.L.; Young, C.L. J. Chromatogr. 1967, 27, 355.

(43) Marin, A.J.P.; Synge, R.J.M. Biochem. 1941, 35, 358.

(44) Porter, P.E.; Deal, C.H.; Stross, F.H. J. Am. Chem. Soc. 1956, 78, 2999.

(45) Evered, S.; Pollard, F.H. J. Chromatogr. 1960, 4, 451.

(46) Ashworth, A.J.; Everett, D.H. Trans. Faraday Soc. 1960, 56, 1609.

(47) Littlewood, A.B. Anal. Chem. 1964, 36, 1441.

(48) Littlewood, A.B.; Willmott, F.W. Anal. Chem. 1966, 38, 1031.

(49) Parcher, J.F.; Weiner, P.H.; Hussey, C.L.; Westlake, T.N. J. Chem. Eng. Data 1975, 20, 145.

(50) Comanita, V.J.; Greenkorn, R.A.; Chao, K. J. Chem. Eng. Data 1976, 21, 491.

(51) Smiley, H.M. J. Chem. Eng. Data 1970, 15, 413.

(52) Vernier, P.; Raimbault, C.; Renon, H. J. Chim. Phys. Phys.–Chim. Biol. 1969, 66, 429.

(53) Harris, H.G.; Prausnitz, J.M. J. Chromatogr. Sci. 1969, 7, 685.

(54) Laub, R.J.; Martire, D.E.; Purnell, J.H. J. Chem. Soc. Faraday Trans. 2 1978, 74, 213.

(55) Everett, D.H.; Gainey, B.W.; Young, C.L. Trans. Faraday Soc. 1968, 64, 2667.

(56) Cruickshank, A.J.B.; Gainey, B.W.; Young, C.L. Trans. Faraday Soc. 1968, 64, 337.

(57) Desty, D.H.; Swanton, W.T. J. Phys. Chem. 1961, 65, 766.

(58) Yodovich, A.; Robinson, R.L.; Chao, K.C. AIChE J. 1971, 17, 1152.

(59) Turek, E.A.; Comanita, J.; Greenkorn, R.A.; Chao, K.C. J. Chem. Eng. Data 1976, 21, 209.

(60) Turek, E.A.; Arnold, D.W.; Greenkorn, R.A.; Chao, K.C. Ind. Eng. Chem. Fundam. 1979, 18, 426.

(61) Liu, Y.; Greenkorn, R.A.; Chao, K.C. J. Chem. Eng. Data 1981, 26, 386.

(62) Arnold, D.W. Ph.D. Dissertation, Purdue University, West Lafayette, IN, 1980; DA 1980, 41, 2257–B.

(63) Arnold, D.W.; Greenkorn, R.A.; Chao, K.C. J. Chem. Eng. Data 1982,

27, 123.

(64) Arnold, D.W.; Greenkorn, R.A.; Chao, K.C. J. Chem. Eng. Data 1987, 32, 103.

(65) Pecsar, R.E.; Martin, J.J. Anal. Chem. 1966, 38, 1661.

(66) Barker, P.E.; Hilmi, A.K. J. Gas Chromatogr. 1967, 5, 119.

(67) Leroi, J.C.; Masson, J.C.; Renon, H.; Fabries, J.F.; Sannier, H. Ind. Eng. Chem. Proc. Des. & Dev. 1977, 16, 139.

(68) Thomas, E.R.; Newman, B.A.; Long, T.C. Wood, D.A.; Eckert, C.A. J. Chem. Eng. Data 1982, 27, 399.

(69) Parcher, J.F.; Urone, P.J. J. Gas Chromatogr. 1964, 2, 184.

(70) Kruppa, R.F.; Henly, R.S.; Smead, D.L. Anal. Chem. 1967, 39, 851.

(71) Harris, H.G. Ph.D. Dissertation, University of California, Berkeley, CA, 1968; DA 1969, 30, 1101–B.

(72) Newman, B.A. Ph.D. Dissertation, University of Illinois, Urbana, IL, 1977; DA 1977, 38, 285–B.

(73) Berezkin, V.G. J. Chromatogr. 1978, 159, 359.

(74) Martin, R.L. Anal. Chem. 1961, 33, 347.

(75) Mathiasson, L.; Jonsson, J.A. J. Chromatogr. 1979, 179, 7.

(76) Terasawa, S.; Itsuki, H.; Yamaki, H. Anal. Chem. 1986, 58, 3021.

(77) Itsuki, H.; Terasawa, S.; Yamana, N.; Ohotaka, S. Anal. Chem. 1987, 59, 2918.

(78) Chen, S.S.; Zwolinski, B.J. J. Chem. Soc., Faraday Trans. 1974, 70, 1133.

(79) Wicarova, O.; Novak, J.; Janak, J. J. Chromatogr. 1970, 51, 3.

(80) Oweimreen, G.A.; Lin, G.C.; Martire, D.E. J. Phys. Chem. 1979, 83, 2111.

(81) Hussam, A.; Carr, P.W. Anal. Chem. 1985, 57, 793.

(82) Cruickshank, A.J.B.; Windsor, M.L.; Young, C.L. Proc. Roy. Soc. A. 1966, 295, 271.

(83) Dorzd, J.; Novak, J. J. Chromatogr. 1971, 165, 141.

(84) Hachenberg, H.; Schmidt A.P. "Gas Chromatography Headspace Analysis," 1977, Heyden and Son, London.

(85) Braithwaite, A.; Smith, F.J. "Chromatographic Methods," 4th Edn., 1985, Chapman and Hall, New York, p. 191.

(86) Mandl, B. Brauwissenschaft 1969, 22, 477.

(87) Mandl, B. Brauwissenschaft 1974, 27, 57.

(88) Jansen, V.J.; Horn, G.B. Am. Soc. Brew. Chem. 1965, 194.

(89) Rumani, R.J.; Ku, L. J. Food Sci. 1966, 31, 558.

(90) Basselle, R.; Ozeris, S.; Whitney, C.H. J. Food Sci. 1962, 28, 84.

(91) Hurst, R.E. Anal. Chem. 1975, 47, 1221.

(92) Jennings, W.; Shibamoto, T. "Qualitative Analysis of Flavours and Fragrances by Glass Capillary GC," 1980, Academic Press, London.

(93) Klimes, I.; Lamparsky, D. "Analysis of Foods and Beverages by Head Space Techniques," 1978, Academic Press, London, p. 95.

(94) Hachenberg, H. "Industrial GC Trace Analysis," 1973, Heyden and Son, London.

(95) Rohrschneider, L. Z. Anal. Chem. 1971, 255, 345.

(96) Crompton, T.R.; Myers, L. Plastics and Polymers 1968, 205.

(97) Jeffs, A.R. "Applied Headspace Analysis," Kolb, B., Ed., 1980, Heyden and Son, London, chapt. 12.

(98) Taylor, A.J. J. Med. Microbiol. 1978, 11, 9.

(99) Larson, L.; Mardh, P.A.; Odham, G. J. Clin. Microbiol. 1978, 7, 23.

(100) Renon, H.; Leroi, J.C.; Masson, J.C.; Fabries, J.F.; Sannier, H. Ind. Eng. Chem. Proc. Des. Dev. 1977, 16, 139.

(101) Prausnitz, J.M.; Lichtenthaler, R.N.; de Azevedo, E.G. *ibid.*, p. 213.

(102) Vogel, G.L.; Hamzavi–Abdel, M.A.; Martire, D.E. J. Chem. Thermodyn. 1983, 15, 739.

(103) Sagert, N.H.; Lau, D.W.P. J. Chem. Eng. Data 1986, 31, 475.

(104) Milanova, E.; Cave, G.C.B. Can. J. Chem. 1982, 60, 2697.

(105) Milanova, E. Ph.D. Dissertation, McGill University, Montreal, Quebec, 1975; DA 1976, 36, 4984–B.

(106) Afrashtehfar, S. Ph.D. Dissertation, McGill University, Montreal, Quebec, 1981; DA 1982, 42, 4076–B.

(107) Afrashtehfar, S.; Cave, G.C.B. Can. J. Chem. 1986, 64, 198.

(108) Acree, W.E.Jr. "Thermodynamic Properties of Nonelectrolyte Solutions," 1984, Academic Press, Orlando, pp. 30–57.

(109) Dymond, J.H.; Smith, E.B. "The Virial Coefficients of Gasas," 1969, Clarendon Press, Oxford.

(110) Smith, V.C.; Robinson, L.J. J. Chem. Eng. Data 1970, 15, 391.

(111) Yin, C.; Hassett, J.P. Environ. Sci. Technol. 1986, 20, 1213.

(112) Carter, C.W.; Suffet, I.H. "Fate of Chemicals in the Environment: Compartmental and Multimedia Models for Predictions," Swann, R.L.; Eschenroeder, A., Eds., 1983, American Chemical Society, Washington D.C., ACS Symp. Ser. No. 225, pp. 216–229.

(113) Carter, C.W.; Suffet, I.H. Environ. Sci. Technol. 1982, 16, 735.

(114) Landrum, P.F.; Nihart, S.R.; Eadie, B.J.; Gardner, W.S. Environ. Sci. Technol. 1984, 18, 187.

(115) Hassett, J.P.; Milicic, E. Environ. Sci. Technol. 1985, 19, 638.

(116) Klein, E.; Eichelberger, J.; Eyer, C.; Smith, J. Water Res. 1975, 9, 807.

(117) Locke, D.C.; Martire, D.E. Anal. Chem. 1967, 39, 921.

(118) Locke, D.C. J. Chromatogr. 1968, 35, 24.

(119) Alessi, P.; Kikic, I. Chromatographia 1974, 7, 299.

(120) Alessi, P.; Kikic, I. Gazz. Chim. Ital. 1974, 104, 1.

(121) Alessi, P.; Kikic, I. J. Chromatogr. 1974, 97, 15.

(122) Hammers, W.E.; Meurs, G.J.; De Ligny, C.L. J. Chromatogr. 1982, 246, 169.

(123) Locke, D.C. J. Chromatogr. Sci. 1974, 12, 433.

(124) Conder, J.R.; Young, C.L. *ibid.*, p. 98.

IV. Calculative Model Methods for Correlating and Estimating Activity Coefficients

The restrictions of the available experimental methods for the measurement of activity coefficients has limited the number of γ_i values that have been determined. Therefore, it would be advantageous to have methods for estimating these values from other thermodynamic parameters. "Classical thermodynamics has little to tell us about the activity coefficient; as always, classical thermodynamics does not give us the experimental quantity we desire but only relates it to another experimental quantity" (1). The Gibbs–Duhem equation (2,3) relates the partial molar quantities of one component in a mixture to those of another. At constant temperature and pressure

$$\sum_i x_i d\overline{m}_i = 0 \qquad (1)$$

where $\overline{m}_i$ is any partial molar property. Equation 1 holds for ideal as well as real solutions and can be rewritten in terms of excess partial molar properties as

$$\sum_i x_i d\overline{m}_i^e = 0 \qquad (2)$$

The Gibbs–Duhem relation is applicable to all excess partial properties. Since the partial molar excess Gibbs energy is directly related to the activity coefficient by

$$\overline{g}_i^{e,\infty} = \mu_i^{e,\infty} = RT \ln\gamma_i^\infty \qquad (3)$$

equation 2 can be written in terms of the activity coefficient as

$$\sum_i x_i \, d \ln\gamma_i^\infty = 0 \qquad (4)$$

which is a differential relation between the activity coefficients of all the components in the solution. This thermodynamic relation provides a useful tool for correlating and extending limited experimental data. In the case of a

binary solution for which isothermal data are available for one component and the pressure is sufficiently low to permit neglect of the effect of pressure on the liquid–phase activity coefficient (4), the Gibbs–Duhem equation may be written

$$x_1(\partial \ln\gamma_1/\partial x_1)_{T,P} = x_2(\partial \ln\gamma_2/\partial x_2)_{T,P} \qquad (5)$$

Equation 5 has three important applications (1): (i) given experimental data for γ_1 as a function of x_1, integration of equation 5 allows the calculation of γ_2 as a function of x_2; that is, in a binary system, activity coefficient data for one component can be used to predict γ_i for the other; (ii) given extensive experimental data for both γ_1 and γ_2 as a function of composition, the data can be tested for thermodynamic consistency by determining whether or not the data obey equation 5; and (iii) given limited data for γ_1 and γ_2, equation 5 can be integrated to obtain thermodynamically consistent equations which relate γ_1 and γ_2 to x. These equations contain a few adjustable parameters, which can be determined from the limited data. There is no unique integrated form of the Gibbs–Duhem equation; many forms are possible. To obtain a particular relation between γ_i and x, some model must be assumed which is consistent with the Gibbs–Duhem relation. A brief discussion of some of the models follows.

i. Margules Equation

In 1895, Margules (5) suggested that the data for γ_i can be represented by an empirical equation of the form

$$\ln\gamma_1 = \sum_k \alpha_k x_2^{\beta_k} \quad (\beta_k>1) \qquad (6)$$

where α_k and β_k are empirical constants to be determined from the data. The condition $\beta_k>1$ avoids singularities in $\ln\gamma_2$ when $x_2=0$ (4). Another form of

equation 5 is

$$d \ln(\gamma_1/\gamma_2)/dx_2 = 1/x_2 \, [d \ln\gamma_1/dx_2] \tag{7}$$

Substituting equation 6 into 7 yields

$$d \ln(\gamma_1/\gamma_2)/dx_2 = \sum_k \alpha_k\beta_k x_2^{\beta_k-2} \tag{8}$$

Integrating equation 8 gives

$$\ln\gamma_2 = \ln\gamma_1 - \sum_k [\alpha_k\beta_k/(\beta_k-1)]x_2^{\beta_k-1} - I \tag{9}$$

where I is a constant of integration. $\ln\gamma_1$ can be eliminated in equation 9 by substituting equation 6 to give

$$\ln\gamma_2 = \sum_k \alpha_k x_2^{\beta_k} - \sum_k [\alpha_k\beta_k/(\beta_k-1)]x_2^{\beta_k-1} - I \tag{10}$$

If component 2 exists as a pure liquid at the temperature of the solution, then it is common to use pure liquid 2 at that temperature as the standard state for γ_2 so that γ_2=1 when x_2=1. The constant of integration I then becomes

$$I = \sum_k \alpha_k - \sum_k [\alpha_k\beta_k/(\beta_k-1)] \tag{11}$$

and the expression for $\ln\gamma_2$ is

$$\ln\gamma_2 = \sum_k \alpha_k x_2^{\beta_k} - \sum_k [\alpha_k/(\beta_k-1)](\beta_k x_2^{\beta_k-1}-1) \tag{12}$$

If the data for γ_1 are adequately represented by equation 6 terminated after the fourth term (k=2,3,4) with β_k=k, then equation 6 becomes

$$\ln\gamma_1 = \alpha_2 x_2^2 + \alpha_3 x_2^3 + \alpha_4 x_2^4 \tag{13}$$

which is known as the four–suffix Margules equation (the *n*–suffix Margules equation gives $\ln\gamma_1$ as a polynomial in x_2 of degree *n*). The coefficients α_k must be found from the experimental data which give γ_1 as a function of the mole fraction. When this four–suffix Margules for $\ln\gamma_1$ is substituted into equation 12, the result for γ_2 is

$$\ln\gamma_2 = (\alpha_2 + 3\alpha_3/2 + 2\alpha_4)x_1^2 - (\alpha_3 + 8\alpha_4/3)x_1^3 + \alpha_4 x_1^4 \tag{14}$$

Equation 14 gives γ_2 in terms of constants which are determined exclusively from data for γ_1. The data can be partial pressures from isothermal

total–pressure studies (6–9), partial pressures from isobaric boiling–point data in an azeotropic system (10), and from dew point (T–y) data (11).

ii. Redlich–Kister Equation

Another way to develop the Margules equation is from excess functions in binary mixtures (12). Consider a binary mixture where the excess properties are taken with reference to an ideal solution where the standard state for each component is the pure liquid at the temperature and pressure of the mixture. Any expression for the molar Gibbs energy must obey the two boundary conditions: $g^e = 0$ when $x_1 = 0$ and $g^e = 0$ when $x_2 = 0$. A simple expression that obeys these boundary conditions is

$$g^e = Ax_1x_2 \tag{15}$$

where A is an empirical constant with units of energy, characteristic of components 1 and 2, which depends only on temperature, not on composition. Substituting into equation 3 yields

$$\bar{g}_i^e = (\partial n_T g^e/\partial n_i)_{T,P,n_j} = RT \ln\gamma_i \tag{16}$$

where n_i is the number of moles of i and n_T is the total number of moles. Since $x_1 = n_1/n_T$ and $x_2 = n_2/n_T$, this gives

$$\ln\gamma_1 = (A/RT)x_2^2 \tag{17}$$

$$\ln\gamma_2 = (A/RT)x_1^2 \tag{18}$$

which are called the two–suffix Margules equations. These represent simple liquid mixtures well, such as those of molecules of similar size, shape, and chemical nature, e.g. the benzene/cyclohexane system (13). Equations 17 and 18 are symmetric, if $\ln\gamma_1$ and $\ln\gamma_2$ are plotted against x_i, the two curves are mirror images. Both γ_i's are equal at infinite dilution:

$$\gamma_1^\infty = \lim_{x_1 \to 0} \gamma_1 = \exp(A/RT) \tag{19}$$

$$\gamma_2^{\infty} = \lim_{x_2 \to 0} \gamma_2 = \exp(A/RT) \qquad (20)$$

The coefficient A may be positive or negative, and it is often constant over small temperature ranges in simple systems (13,14).

Equation 16, and, hence, 17 and 18, are simple and only adequately describe simple solutions. In general, a more complicated relation is needed. The boundary conditions for equation 15 must be obeyed regardless of the complexity of the solution. Redlich and Kister (15) extended equation 15 by using a series expansion to get

$$g^e = x_1 x_2 [A + B(x_1 - x_2) + C(x_1 - x_2)^2 + D(x_1 - x_2)^3 + \ldots] \qquad (21)$$

where B, C, D,... are additional, temperature–dependent parameters, specific to the compound, which must be determined from experimental data. Equations 16 and 21 yield

$$RT \ln\gamma_1 = a^{(1)}x_2^2 + b^{(1)}x_2^3 + c^{(1)}x_2^4 + d^{(1)}x_2^5 + \ldots \qquad (22)$$

$$RT \ln\gamma_2 = a^{(2)}x_1^2 + b^{(2)}x_1^3 + c^{(2)}x_1^4 + d^{(2)}x_1^5 + \ldots \qquad (23)$$

where $a^{(1)}=A+3B+5C+7D$, $b^{(1)}=-4(B+4C+9D)$, $c^{(1)}=12(C+5D)$, $d^{(1)}=-32D$, $a^{(2)}=A-3B+5C-7D$, $b^{(2)}=4(B-4C+9D)$, $c^{(2)}=12(C-5D)$, $d^{(2)}=32D$. The number of parameters needed to represent the experimental data depends on the molecular complexity of the solution, the quality of the data, and the number of data points available. Most vapor–liquid equilibrium (VLE) data reported in the literature warrant no more than two or three constants (16). Redlich et al. (17) used 1, 2, and 4 constants for the systems n–hexane/toluene, benzene/isooctane, and ethanol/methylcyclohexane, respectively, due to the increase in complexity of these solutions (such as large differences in molecular size or higher degrees of hydrogen bonding). The Redlich–Kister equation is often used to test for thermodynamic consistency of experimental data (18,19).

iii. van Laar Equation

Wohl (20) proposed a general method for expressing excess Gibbs energies so that physical significance can be assigned to the constants in the equation. It is a power series in z_1 and z_2, the effective volume fractions of the two components, of the form

$$g^e/[RT(x_1q_1+x_2q_2)]=2a_{12}z_1z_2+3a_{112}z_1^2z_2+3a_{122}z_1z_2^2+ 4a_{1112}z_1^3z_2+4a_{1222}z_1z_2^3+6a_{1122}z_1^2z_2^2 \quad (24)$$

where $z_1 = x_1q_1/(x_1q_1+x_2q_2)$ and $z_2 = x_2q_2/(x_1q_1+x_2q_2)$. q_i is the effective volume, or cross section, of the molecule. It is a measure of the size and/or the sphere of influence of the molecule. a_i is an interaction parameter similar in significance to a virial coefficient.

For a system of two components which are somewhat similar chemically but have different molecular sizes, the Wohl expansion simplifies to the van Laar (21) equation

$$g^e/RT = (2a_{12}x_1x_2q_1q_2)/(x_1q_1+x_2q_2) \quad (25)$$

which when fit to equation 3 becomes

$$\ln\gamma_1 = A'/[1+(A'x_1/B'x_2)]^2 \quad (26)$$

$$\ln\gamma_2 = B'/[1+(B'x_2/A'x_1)]^2 \quad (27)$$

where $A' = 2q_1a_{12}$ and $B' = 2q_2a_{12}$. The van Laar equation works well for systems such as benzene/isooctane at 45°C (22) and n–propanol/water at 1.013 bar (temperature varied from 87.8 to 100°C) (23). At infinite dilution equations 26 and 27 simplify to

$$\ln\gamma_1^\infty = A/RT = A' \quad (28)$$

$$\ln\gamma_2^\infty = B/RT = B' \quad (29)$$

The Wohl–type expansion is also used in the three–suffix Margules equation for binary solutions such as those of acetone/chloroform, methanol/

chloroform, and acetone/methanol (24), and for the Scatchard–Hamer equation (25).

iv. Wilson Equation

Flory and Huggins (26–29) derived a simple expression for the activity coefficient for a mixture of molecules which are chemically similar but differ only in size, such as a polymer in a solvent:

$$\ln\gamma_1 = \ln[1-(1-1/r)\Phi_2^*]+(1-1/r)\Phi_2^* \qquad (30)$$

where r is the number of segments in a polymer molecule and Φ_2^* is the fraction of sites occupied by the polymer given by

$$\Phi_2^* = rN_2/(N_1+rN_2) \qquad (31)$$

where N_1 and N_2 are the number of molecules of solvent and polymer, respectively. Twenty years later, Wilson (30) considered the case where the components in a mixture differ not only in molecular size but also in intermolecular forces. On the basis of these molecular considerations, he derived the following equations for activity coefficients. They are based on an expression for the excess Gibbs energy defined with reference to an ideal Raoult's Law binary solution that obeys the boundary conditions that g^e vanishes as x_1 or x_2 go to zero:

$$\ln\gamma_1 = -\ln(x_1+\Lambda_{12}x_2)+$$
$$x_2[\Lambda_{12}/(x_1+\Lambda_{12}x_2)-\Lambda_{21}/(\Lambda_{21}x_1+x_2)] \qquad (32)$$

$$\ln\gamma_2 = -\ln(x_2+\Lambda_{21}x_1)+$$
$$x_1[\Lambda_{12}/(x_1+\Lambda_{12}x_2)-\Lambda_{21}/(\Lambda_{21}x_1+x_2)] \qquad (33)$$

The adjustable parameters Λ_{12} and Λ_{21} are given by

$$\Lambda_{12} = (v_2/v_1)\exp[-(\lambda_{12}-\lambda_{11})/RT] \qquad (34)$$

$$\Lambda_{21} = (v_1/v_2)\exp[-(\lambda_{12}-\lambda_{22})/RT] \qquad (35)$$

where the λ's are energies of interaction between the molecules designated by the subscripts.

Orye and Prausnitz (31) showed that for approximately 100 miscible binary systems of various chemical types, the Wilson equation represented the activity coefficients as well or better than the three–suffix Margules and the van Laar equation. Schreiber and Eckert (32) have come to a similar conclusion for systems at infinite dilution. Under those conditions, the Wilson equation simplifies to

$$\ln\gamma_1^{\infty} = -\ln\Lambda_{12}-\Lambda_{21}+1 \tag{36}$$

$$\ln\gamma_2^{\infty} = -\ln\Lambda_{21}-\Lambda_{12}+1 \tag{37}$$

This equation is limited to solutions of miscible liquids.

v. NRTL Equation

Following Wilson's derivation based on local composition, Renon and Prausnitz (33) developed the non–random, two liquid (NRTL) equation that is applicable to partially miscible as well as completely miscible systems. Activity coefficients are given by the relations

$$\ln\gamma_1 = x_2^2\{\tau_{21}[G_{21}/(x_1+x_2G_{21})]^2+ [\tau_{12}G_{12}/(x_2+x_1G_{12})^2]\} \tag{38}$$

$$\ln\gamma_2 = x_1^2\{\tau_{12}[G_{12}/(x_2+x_1G_{12})]^2+ [\tau_{21}G_{21}/(x_1+x_2G_{21})^2]\} \tag{39}$$

where $\tau_{12}=(g_{12}-g_{22})/RT$ and $\tau_{21}=(g_{21}-g_{11})/RT$, g_{ij} is an energy term characteristic of the i–j, interaction. $G_{12}=\exp(-\alpha_{12}\tau_{12})$, $G_{21}=\exp(-\alpha_{12}\tau_{21})$, and α_{12} is a measure of the randomness of the system. Renon and Prausnitz (33) obtained good results with their equation for the system nitroethane/isooctane, which has a miscibility gap below 30°C.

vi. UNIQUAC Equation

The NRTL equation (equations 38 and 39) requires three parameters. Experimental data for binary mixtures are usually not sufficiently plentiful or precise to yield that many meaningful binary parameters (34). Abrams and Prausnitz (35) derived a two–parameter equation which retains the Wilson equation (equation 34 and 35) advantage for nonrandom solutions containing molecules of different sizes but is not limited to completely miscible systems. They called it the universal quasi–chemical theory (UNIQUAC). The expression for g^e contains a combinatorial part which describes the dominant entropic contribution, and a residual part which reflects primarily the intermolecular forces responsible for the enthalpy of mixing. The combinatorial part is determined only by the size and shapes of the molecules and their composition; it requires only pure–component data. The residual part contains the two adjustable binary parameters to account for the intermolecular forces. The activity coefficients are given by

$$\ln\gamma_1 = \ln(\Phi_1^*/x_1)+(z/2)q_1\ln(\theta_1/\Phi_1^*)+\Phi_2^*(l_1-r_1l_2/r_2)-q_1'\ln(\theta_1'+\theta_2'\tau_{21})+ \theta_2'q_1'[\tau_{21}/(\theta_1'+\theta_2'\tau_{21})-\tau_{12}/(\theta_2'+\theta_1'\tau_{12})] \quad (40)$$

$$\ln\gamma_2 = \ln(\Phi_2^*/x_2)+(z/2)q_2\ln(\theta_2/\Phi_2^*)+\Phi_1^*(l_2-r_2l_1/r_1)-q_2'\ln(\theta_2'+\theta_1'\tau_{12})+ \theta_1'q_2'[\tau_{12}/(\theta_2'+\theta_1'\tau_{12})-\tau_{21}/(\theta_1'+\theta_2'\tau_{21})] \quad (41)$$

Parameters r, q, and q' are pure–component molecular–structure constants depending on molecular size and external areas, z is the coordination number set equal to 10, $l_1=(z/2)(r_1-q_1)-(r_1-1)$ and $l_2=(z/2)(r_2-q_2)-(r_2-1)$, Φ_i^* is the segment fraction given by $\Phi_1^*=x_1r_1/(x_1r_1+x_2r_2)$ and $\Phi_2^*=x_2r_2/(x_1r_1+x_2r_2)$, θ_i and θ_i' are area fractions given by $\theta_1=x_1q_1/(x_1q_1+x_2q_2)$, $\theta_2=x_2q_2/(x_1q_1+x_2q_2)$, $\theta_1'=x_1q_1'/(x_1q_1'+x_2q_2')$, and $\theta_2'=x_2q_2'/(x_1q_1'+x_2q_2')$. τ_{12} and τ_{21} are the adjustable parameters given in terms of characteristic energies

Δu_{12} and Δu_{21} by

$$\tau_{12} = \exp(-\Delta u_{12}/RT) = \exp(-a_{12}/T) \quad (42)$$

$$\tau_{21} = \exp(-\Delta u_{21}/RT) = \exp(-a_{21}/T) \quad (43)$$

Originally, q was identical to q', but it was found (36) that to obtain an optimum fit for systems containing alcohol and water these must differ since the surface of interaction q' is smaller than the geometric external surface q (because of hydrogen bonding). For all other systems, $q=q'$. There are good data sources of the structural constants and the binary parameters for the UNIQUAC equation (36–39).

UNIQUAC has a wide range of applicability. The acetonitrile/benzene (40) and the n–hexane/nitroethane systems (41) exhibit positive deviations from Raoult's Law, whereas the acetone/chloroform (24) and the methanol/diethylamine systems (42) exhibit negative deviations from Raoult's Law. All these data were fit accurately by the UNIQUAC equation.

vii. ASOG Method

In 1925, Langmuir (43) suggested the estimation of the thermodynamic properties of mixtures by considering the interactions between the different functional groups of which the individual molecules were composed. This suggestion only recently became practical because large data bases and accessible computers are required for the successful operation of any useful scheme.

The analytical solution of groups (ASOG) method, developed by Deal, Derr, and Wilson (44,45), and further elaborated by Kojima and Tochigi (46) is a semi–empirical group–contribution scheme based on earlier work by Redlich, Derr, Pierotti, and Papadopoulous (47,48).

The activity coefficient is divided arbitrarily into two parts, a combinatorial term due to differences in the sizes of the component molecules, and a residual term due to differences in intermolecular forces:

$$\ln\gamma_i = \ln\gamma_i^{comb} + \ln\gamma_i^{res} \tag{44}$$

Each molecule is divided into its component functional groups; $-CH_3$, $-CH_2-$, –OH, –CHO, etc. Each pair of groups is assigned a value of the group interaction parameter. These are computed from experimental VLE data on a large number of carefully selected 'key' binary mixtures. Each group is also assigned a volume. $\ln\gamma_i^{comb}$ depends only on the number of size groups in the various molecules that constitute the mixture. From the athermal Flory–Huggins equation (equation 30) the value for γ_i^{comb} is computed by

$$\ln\gamma_i^{comb} = 1 - R_i + \ln R_i \tag{45}$$

where

$$R_i = s_i / \sum_j s_j x_j \tag{46}$$

where x_j is the mole fraction of component j in the mixture and s_j is the number of size groups in molecule j. Parameter s_j is independent of temperature, hence, so is γ_i^{comb}. The summation extends over all components, including component i.

The expression for $\ln\gamma_i^{res}$ is based on the Wilson equation (equations 32 and 33). To calculate γ_i^{res} all the group mole fractions X_k must be known. The subscript k stands for a particular group in molecule j. This is given by

$$X_k = \sum_j x_j v_{kj} / \left[\sum_j x_j \sum_k v_{kj}\right] \tag{47}$$

where v_{kj} is the number interaction groups k in molecule j. The γ_i^{res} is then given by

$$\ln\gamma_i^{res} = \sum_k v_{ki} \ln\Gamma_k - \sum_k v_{ki} \ln\Gamma_k^* \tag{48}$$

where Γ_k is the activity coefficient of group k in the mixture and Γ_k^* is the

activity coefficient of group k in the standard state. Activity coefficient Γ_k is given by

$$\ln\Gamma_k = -\ln\sum_l X_l A_{kl} + [1 - \sum_l (X_l A_{lk} / \sum_m x_m A_{lm})] \qquad (49)$$

where A_{kl} and A_{lk} ($A_{kl} \neq A_{lk}$) are group–interaction parameters which depend on temperature. These parameters are obtained from reduction of VLE data, and a substantial number have been reported (44). The summations extend over all groups present in the mixture.

Group parameters obtained from available experimental data for some mixtures can be used to predict activity coefficients in other mixtures that contain the same groups, but not necessarily the same molecules.

viii. UNIFAC Method

A similar but more widely used and convenient method to ASOG was developed by Fredenslund and Jones (49,50). The method, called universal functional activity coefficient (UNIFAC), is described in detail in a monograph by the developers (51). It, too, is a solution–of–groups method whose idea is to utilize existing phase–equilibrium data for predicting phase equilibria of systems for which no experimental data are available. UNIFAC has two essential features: (i) suitable reduction of experimentally–obtained activity coefficient data to yield parameters characterizing interactions between pairs of structural groups in nonelectrolyte systems; and (ii) use of these parameters to predict activity coefficients for other systems which have not yet been studied experimentally but which contain the same functional groups.

The activity coefficient is split into a combinatorial part and a residual part (equation 44), just as in ASOG. However, the method is based on the

UNIQUAC equation (equations 40 and 41).

The combinatorial part uses the UNIQUAC equation directly to describe both group size and surface area and is given by

$$\ln \gamma_i^{comb} = \ln(\Phi^*_i/x_i)+(z/2)q_i\ln(\theta_i/\Phi^*_i)+l_i- (\Phi^*_i/x_i)\sum x_i l_i \quad (50)$$

r_i (found in the expression for l_i after equation 41) and q_i are calculated as the sum of the group volume and area parameters R_k and Q_k by

$$r_i = \sum \nu_k^{(i)} R_k \quad (51)$$

$$q_i = \sum \nu_k^{(i)} Q_k \quad (52)$$

where $\nu_k^{(i)}$, always an integer, is the number of groups of type k in molecule i. Group parameters R_k and Q_k are obtained from the van der Waals group volume V_{wk} and surface areas A_{wk} given by Bondi (52)

$$R_k = V_{wk}/15.17 \quad (53)$$

$$Q_k = A_{wk}/2.5\times10^9 \quad (54)$$

The normalization factors 15.17 and 2.5×10^9 are determined by the volume and external surface area of a CH_2 unit in polyethylene. R_k and Q_k values have been tabulated (cf. ref. 53).

The residual part of the activity coefficient uses the solution–of–groups concept:

$$\ln\gamma_i^{res} = \sum_k \nu_k^{(i)}(\ln \Gamma_k - \ln \Gamma_k^{(i)}) \quad (55)$$

where Γ_k is the group residual activity coefficient and $\Gamma_k^{(i)}$ is the residual activity coefficient of group k in a reference solution containing only molecules of type i (similar to ASOG's Γ^* in equation 48). $\Gamma_k^{(i)}$ is necessary to normalize γ_i to unity as $x_i \to 1$.

The group activity coefficient is found from the relation

$$\ln \Gamma_k = Q_k[1-\ln(\sum_m \theta_m \Psi_{mk})-\sum_m (\theta_m \Psi_{km}/\sum_n \theta_m \Psi_{nm})] \quad (56)$$

where θ_m is the area fraction of group m given by

$$\theta_m = Q_m X_m / \sum_n Q_n X_n \qquad (57)$$

where X_m is the mole fraction of group m in the mixture. Ψ_{mn}, the group interaction parameter, is given by

$$\Psi_{mn} = \exp[-(U_{mn}-U_{nn})/RT = \exp(-a_{mn}/T) \qquad (58)$$

where U_{mn} is a measure of the energy of interaction between groups m and n. The group interaction parameters a_{mn} must be evaluated from experimental VLE data. Values of this constant have been tabulated (cf. ref. 54).

Zarkarian et al. (55) found that UNIFAC will generally not give good predictions of liquid phase activity coefficients over the whole concentration range if the group interaction parameters are estimated from limiting activity coefficients alone, even if the data base came from a large set of systems (e.g., 15 systems). However, starting with GLC–determined γ_2^∞ values, and applying the Flory–Huggins theory (equation 31), they correlated values at finite dilution for solute mole fractions below 0.4.

Kikic et al. (56) augmented the combinatorial term in the UNIFAC expression (equation 50) by

$$\ln \gamma_i^{comb} = [\ln(\Psi_i/x_i)+1-\Psi_i/x_i]- (1/2)zq_i[\ln(\Phi_i^*/\theta_i)+1-\Phi_i^*/\theta_i] \qquad (59)$$

where $\Psi_i = r_i^{2/3}x_i/\sum_j r_j^{2/3}x_j$. They later found this to give good results for alkane/ketone mixtures (57). Weidlich, Gmehling, and Berg (18,19) used γ_i^∞ values determined by headspace GC to extend the UNIFAC parameter data base. More recently, they (58) used a modified UNIFAC model similar to Kikic et al. (56,57) to predict limiting activity coefficients. Bastos et al. (59) used the modified UNIFAC method to correlate 11,500 data points. They achieved an average relative error of 20% for about 70% of the data points,

which include 190 pairs of parameters of 40 different groups. Banerjee and Howard (60) used the modified UNIFAC method to estimate solubilities and partition coefficients from derived activity coefficients.

vii. MOSCED Mothed

Thomas and Eckert (61) developed a modified separation of cohesive energy density (MOSCED) model, based on the regular solution–of–groups theory (62,63), to predict limiting activity coefficients for polar and associating systems. Starting from the relation for the excess Gibbs energy

$$g^e = \phi_1\phi_2(x_1v_1+x_2v_2)[c_{11}+c_{22}-2(c_{11}c_{22})^{1/2}] \qquad (60)$$

where c is the cohesive energy density given by

$$c_{11} = \lambda_1^2+\tau_1^2+\sigma_1\tau_1+\alpha_1\beta_1 \qquad (61)$$

$$c_{22} = \lambda_2^2+\tau_2^2+\sigma_2\tau_2+\alpha_2\beta_2 \qquad (62)$$

$$c_{12} = \lambda_1\lambda_2+\tau_1\tau_2+(1/2)(\sigma_1\tau_2+\sigma_2\tau_1+\alpha_1\beta_2+\alpha_2\beta_1) \qquad (63)$$

where the $\lambda_i\lambda_j$, $\tau_i\tau_j$, $\sigma_i\tau_j$ and $\alpha_i\beta_j$ terms represent the dispersion, orientation, induction, and hydrogen bonding forces, respectively. λ is a measure of the polarizability of a molecule, τ represents its polarity, σ reflects the ability of the nonpolar part of a molecule to interact with a dipole, and α and β are acidity and basicity parameters, respectively. The difference in molecular size between the solute 2 and the solvent 1 is accounted for by the Flory–Huggins (26–29) term

$$d_{12} = \ln(v_2/v_1)+1-v_2/v_1 \qquad (64)$$

to give an expression for the limiting activity coefficient

$$\ln\gamma_2^\infty = (v_2/RT)[(\lambda_1-\lambda_2)^2+(\tau_1-\tau_2)^2+(\sigma_1-\sigma_2)(\tau_1-\tau_2)+ (\alpha_1-\alpha_2)(\beta_1-\beta_2)]+\ln(v_2/v_1)+1-(v_2/v_1) \qquad (65)$$

Rewriting equation 65 in a form similar to Weimer and Prausnitz (64) and

adding solvent–dependent asymmetry correction parameters Ψ_1 and ξ_1, which increase with increasing polarity and extent of association of the solvents yields

$$\ln\gamma_2^{\infty} = (v_2/RT)[(\lambda_1-\lambda_2)^2+q_1q_2(\tau_1-\tau_2)^2/\Psi_1+ (\alpha_1-\alpha_2)(\beta_1-\beta_2)/\xi_1]+d_{12} \quad (66)$$

Thomas and Eckert (61) compared the MOSCED method to UNIFAC and found, for 3357 γ_2^{∞}'s, an average error of 9.1% with good comparisons to literature values. The UNIFAC method, however, had an average error of 20.5%. Park and Carr (65) examined 77 γ_2^{∞} values by the MOSCED and UNIFAC methods and arrived at average errors of 17.6% and 21.0%, respectively.

References

(1) Reid, R.C.; Prausnitz, J.M.; Sherwood, T.K. "The Properties of Gases and Liquids," 3rd Edn., 1977, McGraw–Hill Book Co., New York, p. 296.

(2) Gibbs, J.W. "Collected Works," Vol. 1, 1928, Longmans, New York, p. 88.

(3) Duhem, P. "Le Potentiel Thermodynamique et ses Applications," 1886, Paris, p. 33.

(4) Prausnitz, J.M.; Lichtenthaler, R.N.; de Azevedo, E.G. "Molecular Thermodynamics of Fluid–Phase Equilibria," 2nd Edn., 1986, Prentice–Hall, Inc., Englewood Cliffs, p. 210.

(5) Margules, H. Sitzungber. Wien Akad. 1895, 104, 1243.

(6) Hermsen, R.W.; Prausnitz, J.M. Chem. Eng. Sci. 1963, 18, 485.

(7) Orye, R.V.; Prausnitz, J.M. Trans. Faraday Soc. 1965, 61, 1338.

(8) Byre, S.M.; Gibbs, R.E.; Van Ness, H.C. AIChE J. 1973, 19, 238.

(9) Abbott, M.M.; Van Ness, H.C. AIChE J. 1975, 21, 62.

(10) Miller, H.C.; Bliss, H. Ind. Eng. Chem. 1940, 32, 123.

(11) Bellemans, A. Bull. Soc. Chim. Belg. 1959, 68, 355.

(12) Prausnitz, J.M.; Lichtenthaler, R.N.; de Azevedo, E.G. *ibid.*, p. 203.

(13) Scatchard, G.; Wood, S.E.; Mochel, J.M. J. Phys. Chem. 1939, 43, 119.

(14) Pool, R.A.H.; Saville, G.; Herrington, T.M.; Shields, B.D.C.; Staveley, L.A.K. Trans. Faraday Soc. 1962, 58, 1692.

(15) Redlich, O.; Kister, A.T. Ind. Eng. Chem. 1948, 40, 341.

(16) Prausnitz, J.M.; Lichtenthaler, R.N.; de Azevedo, E.G. *ibid.*, p. 205.

(17) Redlich, O.; Kister, A.T.; Turnquist, C.E. Chem. Eng. Prog. Symp. Ser. 1952, 48, 49.

(18) Weidlich, U.; Gmehling, J. J. Chem. Eng. Data 1985, 30, 95.

(19) Weidlich, U. Berg, J.; Gmehling, J. J. Chem. Eng. Data, 1986, 31, 313.

(20) Wohl, K. Trans. AIChE 1946, 42, 215

(21) Van Laar, J.J. Z. Phys. Chem. 1910, 72, 723.

(22) Weissman, S.; Wood, S.E. J. Chem. Phys. 1960, 32, 1153.

(23) Carlson, H.C.; Colburn, A.P. Ind. Eng. Chem. 1942, 34, 581.

(24) Severns, W.H.; Sesonske, A.; Perry, R.H.; Pigford, R.L. AIChE J. 1955, 1, 401.

(25) Scatchard, G.; Hamer, W.J. J. Am. Chem. Soc. 1935, 57, 1805.

(26) Flory, P.J. J. Chem. Phys. 1941, 9, 660.

(27) Flory, P.J. J. Chem. Phys. 1942, 10, 51.

(28) Huggins, M.L. J. Phys. Chem. 1941, 9, 440.

(29) Huggins, M.L. Ann. N.Y. Acad. Sci. 1942, 43, 1.

(30) Wilson, G.M. J. Am. Chem. Soc. 1964, 86, 127.

(31) Orye, R.V.; Prausnitz, J.M. Ind. Eng. Chem. 1965, 57, 19.

(32) Schreiber, L.B.; Eckert, C.A. Ind. Eng. Chem. Proc. Des. Dev. 1971, 10, 572.

(33) Renon, H.; Prausnitz, J.M. AIChE J. 1968, 14, 135.

(34) Prausnitz, J.M.; Lichtenthaler, R.N.; de Azevedo, E.G. *ibid.*, p. 238.

(35) Abrams, D.; Prausnitz, J.M. AIChE J. 1975, 21, 116.

(36) Anderson, T.F.; Prausnitz, J.M. Ind. Eng. Chem. Proc. Des. Dev. 1978, 17, 552.

(37) Anderson, T.F.; Prausnitz, J.M. Ind. Eng. Chem. Proc. Des. Dev. 1978, 17, 561.

(38) Gmehling, J; Onen, U.; Arlt, W.; Weidlich, U.; Grenzheuser, P.; Kolbe, B. Vapor–Liquid Equilibrium Data Collection; DECHEMA Chemistry Series; DECHEMA 1977–1984, Frankfurt, Vol. I, 13 parts.

(39) Prausnitz, J.M.; Grens, E.A.; Anderson, T.F.; Eckert, C.A.; Hseih, R.; O'Connel, J.P. "Computer Calculations for Multicomponent Vapor–Liquid and Liquid–Liquid Equilibria," 1980, Prentice–Hall, Inc., Englewood Cliffs.

(40) Brown, I.; Smith, F. Aust. J. Chem. 1955, 8, 62.

(41) Edwards, J.B. Ph.D. Dissertation, Georgia Institute of Technology, Atlanta, GA, 1962.

(42) Nakanishi, K.; Shirai, H.; Minamiyama, T. J. Chem. Eng. Data 1967, 12, 591.

(43) Langmuir, I. "The Distribution and Orientation of Molecules, 3rd Colloid Symp. Monogr.," 1925, Chemical Catalog Co., New York.

(44) Derr, E.L.; Deal, C.H. Inst. Chem. Eng. Symp. Ser. Lond. 1969, 3, 40.

(45) Wilson, G.M.; Deal, C.H. Ind. Eng. Chem. Fundam. 1962, 1, 20.

(46) Kojima, K.; Tochigi, K. "Prediction of Vapor–Liquid Equilibria by the ASOG Method," 1979, Elsevier, Amsterdam.

(47) Redlich, O.; Derr, E.L.; Pierotti, G. J. Am. Chem. Soc. 1959, 81, 2283.

(48) Derr, E.L.; Papadopoulous M. J. Am. Chem. Soc. 1959, 81, 2285.

(49) Fredenslund, A.; Jones, R.L.; Prausnitz, J.M. AIChE J. 1975, 21, 1086.

(50) Fredenslund, A.; Gmehling, J.; Michelsen, M.L.; Rasmussen, P.; Prausnitz, J.M. Ind. Eng. Chem. Proc. Des. Dev. 1977, 16, 450.

(51) Fredenslund, A.; Gmehling, J.; Rasmussen, P. "Vapor–Liquid Equilibria Using UNIFAC," 1977, Elsevier, Amsterdam.

(52) Bondi, A. "Physical Properties of Molecular Liquids, Crystals, and Glasses," 1968, Wiley, New York.

(53) Reid, R.C.; Prausnitz, J.M.; Sherwood, T.K. *ibid.*, p. 348.

(54) Reid, R.C.; Prausnitz, J.M.; Sherwood, T.K. *ibid.*, p. 352.

(55) Zarkarian J.A.; Anderson, F.E.; Boyd, J.A.; Prausnitz, J.M. Ind. Eng. Chem. Proc. Des. Dev. 1979, 18, 657.

(56) Kikic, I.; Alessi, P.; Rasmussen, P.; Fredenslund, A. Can. J. Chem. Eng. 1980, 58, 253.

(57) Alessi, P.; Kikic, I.; Fredenslund, A.; Rasmussen, P. Can. J. Chem. Eng. 1982, 60, 300.

(58) Weidlich, U.; Gmehling, J. Ind. Eng. Chem. Res. 1987, 26, 1372.

(59) Bastos, J.C.; Soares, M.E.; Medina, A.G. Ind. Eng. Chem. Res. 1988, 27, 1269.

(60) Banerjee, S.; Howard, P.H. Environ. Sci. Technol. 1988, 22, 839.

(61) Thomas, E.R.; Eckert, C.A. Ind. Eng. Chem Proc. Des. Dev. 1984, 23, 194.

(62) Scatchard, G. Chem. Rev. 1931, 8, 321.

(63) Hildebrand, J.H.; Wood, S.E. J. Chem. Phys. 1933, 1, 817.

(64) Weimer, R.F.; Prausnitz, .M. Hydrocarbon Process. Petrol. Refiner. 1965, 44, 237.

(65) Park, J.H.; Carr, P.W. Anal. Chem. 1987, 59, 2596.

V. Nonsteady State Gas Chromatography

i. Description and Theory

NSGC was first described by Belfer (1) in the Russian journal Neftekhimia. He presented a theory similar to the derivation below, and applied the method, which he called Nonsteady State GC, to the determination of γ_2^∞ of pentane and hexane in octane, nonane, and decane solvents, and ethanol in hexadecanol. The technique has also given reliable limiting activity coefficients in acetonitrile and octane solvents (2).

In NSGC, the GC solvent is almost as volatile as the solutes at the temperature of operation, and is, therefore, not a stationary phase. The solvent is itself being eluted from the column during the chromatography of the solutes, but at a rate slower than the elution rates of solutes injected into the column. The solvent is introduced by syringe as a slug into the hot GC injection port, condenses in the column which is packed only with solid support, and after rapidly equilibrating with the helium carrier gas and saturating the packing, slowly evaporates out of the column. This is depicted in Figure V.1. The constant rate of solvent elution produces a steady baseline which can be adjusted to a low–scale value. Solutes are injected repetitively during solvent elution, and because the total volume of solvent decreases with time, the solute retention time decreases between successive injections over the lifetime of the column, as depicted in Figure V.2.

The simple relationship between the change in net retention volume, ΔV_N, and γ_2^∞ is obtained as follows. In normal GC, V_N, the solute retention volume less that of air, corrected for the column pressure drop, is related to the limiting activity coefficient by

$$V_N = KV_1 = RTw_1/p_2^oM_1\gamma_2^\infty = RTn_1/p_2^o\gamma_2^\infty \quad (1)$$

where V_1, w_1, M_1, and n_1 are respectively the volume, weight, molecular weight, and number of moles of solvent in the column and p_2^o is the solute vapor pressure. K is the distribution coefficient. This equation is derived assuming the vapor phase is ideal and the solutions are sufficiently dilute to be in the Henry's Law region.

In NSGC, the net retention volume will decrease at a rate proportional to the loss of solvent phase. Expressed as a differential change,

$$dV_N = KdV_1 = (RT/p_2^o\gamma_2^\infty)dn_1 \quad (2)$$

Since loss of solvent at constant flow rate F and constant column temperature T is directly proportional to time, it is convenient to define a NSGC parameter ϕ, characteristic of a given solute and solvent, in terms of the change in net retention volume over successive injection times, $d\theta$, by

$$\phi = -(1/F)(dV_N/d\theta) \quad (3)$$

Thus, because of the linear loss of solvent with time, an aliquot of solute injected at time t_1 will have a net retention volume V_{N_1}, and, at a later time t_2, will have V_{N_2},

$$\phi = (-1/F)[(V_{N_1}-V_{N_2})/(t_2-t_1)] \quad (4)$$

The loss of solvent over the same time interval, at constant F and T, is

$$-(dn_1/d\theta) = n_vF \quad (5)$$

where n_v is the number of moles of volatilized solvent per unit volume of gas phase, related to its vapor pressure p_1^o at the column temperature, by

$$n_v = p_1^o/RT \quad (6)$$

Thus, combining equations 2–6 yields

$$(dV_N/d\theta) = (RT/p_2^o\gamma_2^\infty)(dn_1/d\theta) = (RT/p_2^o\gamma_2^\infty)(p_1^oF/RT) = F\phi \quad (7)$$

so that

$$\gamma_2^{\infty} = (p_1^0/p_2^0)/\phi = \pi/\phi \qquad (8)$$

where π is the ratio of solvent to solute vapor pressures. Therefore, all one needs to determine γ_2^{∞} are the vapor pressures and the experimental change in solute retention volume between successive injections.

ii. Experimental

Activity coefficients of several solutes in various solvents were obtained using a lab–assembled GC at 25°C. The instrument, built from components, is a dual column, dual thermal conductivity detector (TCD) GC fitted with identical 4 ft. × 1/8 in. od or 6 ft. × 1/8 in. od stainless steel (s.s.) columns packed with 80/100 mesh Supelcoport, or with s.s. columns of the same dimensions packed with DMCS–treated glass beads of 80/100 mesh. A Lauda Refrigerating Circulator model RMS–20 with a control accuracy of ±0.01°C was used as a thermostated oven. The TCD was a Gow–Mac dual hotwire cell with a Gow–Mac Power Supply Bridge Control Unit model 40–200.

Because of the presence of organic solvent vapors in the GC effluent, the only practical detector to use is a TCD. As discussed by Eckert et al. (3), there are problems of reduced sensitivity with organic vapor–saturated carrier gases, but the TCD sensitivity is still adequate. To facilitate balancing the detector bridge, a dual–column GC is used. The two columns are packed only with solid support. Good long–term control of temperature and pressure is essential.

From 0.05 to 4.00 ml of solvent is injected into the hot injection ports of the two columns, depending on which solvent and which packing are used. Equilibration of the solvent with the support and with the mobile phase occurs

in a few minutes, as evidenced by the stabilization of the baseline. The recorder pen is adjusted downscale using an attenuation between 16× and 128× depending on the solute and temperature. Less than a microliter of solute gives about half–scale peaks at these attenuations, despite the presence of the solvent vapors. In our experiments, 0.1 μl of solute is injected and, in most cases, peaks from which retention time measurements could be made resulted at an attenuation of 32×. Solutes are injected repetitively over the lifetime of the column. Again, the slope of the plot of retention time vs. injection time is the parameter ϕ. This plus literature vapor pressures yield γ_2^∞.

Though, mathematically, ϕ can be simplified to just $\Delta t_R/\Delta t$, as was done originally (1,15), the flow rate must be considered. V_R is simply the product of the retention time, t_R, multiplied by the flow rate, F. (Since the air peak retention time is related to the weight of solvent in the column, and since the solute retention time is decreasing with the elution of solvent, the air peak retention volume does not have to be subtracted from the retention volume. Therefore, V_R can be used instead of V_N.) Recall that

$$\phi = (-1/F)[(V_{N_1}-V_{N_2})/(t_2-t_1)] \qquad (4)$$

Mathematically, the flow rates should cancel out. But one must remember that because the inlet pressure is constant, since the solvent is eluting with time, the viscosity decreases, and the flow rate increases with time. This must be accounted for. Therefore, t_R is multiplied by the average flow rate between the time of solute injection and its corresponding elution, and the whole equation is divided by the average flow rate over the complete experimental run. The flow rates are measured using a standard soap bubble meter and are corrected to column conditions to give the true flow rate by the usual equation

$$F_{corr} = F_{fm}(T_{col}/T_{fm})(P_{fm}/P_o) \qquad (9)$$

where the subscript fm refers to flow meter conditions, T_{col} is the column temperature, P_{fm} is the carrier gas pressure in the flow meter which is equal to the difference between atmospheric pressure and the vapor pressure of water P_w at that temperature (P_{atm}–P_w), and P_o is the carrier gas pressure at the outlet of the column, which is equal to P_{atm}. The retention volume is further corrected for the pressure drop across the column by the equation

$$V_R^o = V_R J_2^3 \tag{10}$$

where the pressure–gradient correction factor J_2^3 is given by

$$J_2^3 = (3/2)\{[(P_i/P_o)^2-1]/[(P_i/P_o)^3-1]\} \tag{11}$$

where P_i is the column inlet pressure. Therefore, the equation for γ_2^∞ which is used in practice is

$$\gamma_2^\infty = (p_1^o/p_2^o)/[-1/\bar{F}(\Delta V_R^o/\Delta t)] \tag{12}$$

where $\bar{F}$ is the average flow rate over a complete experimental run.

The effects of column length and volume of solvent loading have been investigated and are discussed in section iv. Investigation of how the solvent packs and moves through the column is discussed in sections vii and viii. Applications of γ_2^∞, such as the solubility of a solute , Henry's Law constant, and octanol/water partition coefficient, are discussed at the end of the next section.

iii. Water Solvent

Since water pollution is a primary concern and, therefore, there is a relatively large amount of data on water, it was the first solvent chosen for this study. C_1 to C_4 primary and secondary alcohols and C_3 to C_5 ketones were the solutes of interest because of their higher volatility than water. The experiment was initially carried out at 50°, 40°, and 20°C. Literature values

were found for 25^0C, so the results at that temperature were from interpolation of the experimentally determined values (Table V.1).

The measurements were done on 4 ft. × 1/8 in. od stainless steel columns packed with 1.30 g of 80/100 mesh Supelcoport. The flow rate was set to 20 ml/min. on the dry (solid support only) columns, and 0.3 ml of glass–distilled H_2O was injected into each column. Within a few minutes (less than two minutes at the higher temperatures) after the solvent was injected, the recorder pen began jumping wildly off–scale to both the up– and down–scale sides. After allowing the system to equilibrate (20 min. at 50^0C and 60 min. at 20^0C) (Figure V.3), the recorder pen was adjusted down–scale using an attenuation of anywhere from 16× for the more soluble compounds to 128× for the less soluble ones (since the more soluble the longer the t_R, and the longer the t_R the shorter and broader the peaks, requiring smaller attenuations to quantify them). Repetitively, 0.1 μl of solute was injected into one of the columns, the working column, over varying time intervals (Figure V.4). The second column served as a reference column to balance the Wheatstone bridge in the TCD. Thus, a relatively stable baseline was achieved even though the stationary phase was constantly eluting out of the column.

As cited earlier, the flow rate must be included in the γ_2^∞ to account for the viscosity changes in the column. The column conditions are constantly changing and this affects the experimental results. However, in these initial experiments, the retention time vs. time data was fit by a simple linear least squares analysis to give the denominator of equation 8,

$$\phi = \Delta t_R/\Delta t \qquad (13)$$

and the corrections leading to equation 12 had not yet been implemented, i.e. the assumption that the flow rates should cancel was accepted. The results of

these experiments are listed in Table V.1. The reproducibility was good, 7% standard deviations at 50°C, as were the least squares correlations of the plots used for the interpolations, better than 0.95.

Though the results did come close to some of the literature values cited by Mash and Pemberton (6), the data on a whole (except 1– and 2–propanol) were considerably lower than the values in Table V.2. Subsequently it was realized that the flow rate increases significantly, up to 20%, with time. Therefore, the corrections leading up to equation 12 must be implemented. The experiment was repeated, this time at the desired temperature of 25°C and with solvent loadings of 0.50 ml. This was found to be the maximum size solvent injection in which the most soluble solutes, such as methanol and ethanol, would still give peaks that could be triangulated so that retention time measurements could be made within the first few hours of the column lifetime. All other conditions were the same as in the first experiment. Table V.2 lists the results. The reproducibility was not as good as in the first experiment (8%–14% standard deviation) but the agreement with literature data improved. However, it should be noted that Mash and Pemberton (6) cite differences in literature values of up to 40% for some compounds and up to at least 20% for most others.

Eckert, et al. (3,16) and Mash and Pemberton (6) used a GLC method which requires presaturation of the carrier gas with the solvent and weighing the column before and after the experiment. This is a tedious and error–prone process. In NSGC, the solvent is introduced into the carrier gas stream via the injection port, and, after a given amount of time the solvent completely elutes out of the column. No weighings ever need be done. Also, many determinations can be done during the column lifetime. A 0.50 ml injection of

water solvent, under the conditions of the measurements, takes 9 hours to elute completely. Depending on the solubility of the solute in this solvent, at a dry column flow rate of about 20 ml/min., a single experimental run takes between 1 and 2 hours. Therefore, between 4 and 6 determinations can be done with one solvent injection.

The determinations were carried out in the order in which they are listed in Table V.2. That is, after the columns equilibrated, 7 injections of methanol were made at 10 minute intervals, then 7 of ethanol, etc., etc., until the column emptied out of all its solvent. (This will be referred to below as the column having died.) It turns out, then, that sometimes a solute was studied during the beginning of the column lifetime, at times during the middle, and at the end. It was found that regardless of when the experiment was done, the results were the same, within the expected error range. Sometimes the earlier runs yielded lower γ_2^∞ values and sometimes higher ones. There was random error only of the data, no systematic dependence on when the sample was studied relative to the life of the column. This supports the model depicted in Figures V.1 and V.2. When the columns equilibrate, a plateau is reached after which the rate of elution remains the same. Even though the amount of solvent in the column is constantly decreasing, the rate of decrease is constant. More experimental data supporting this model are presented in later sections of this chapter.

The same systems (alcohols and ketones in water) were then studied using 4 ft. × 1/8 in. stainless steel columns packed with 6.74 g of DMCS treated glass beads. Because this is a nonporous packing, much less solvent is needed than with Supelcoport. The maximum loading was found to be 0.05 ml for the alcohols and 0.20 ml for the ketones. Ketones are much less soluble in

water than the alcohols are so they will yield sharper peaks with shorter retention times. Even with injections of 0.05 ml of water, solvent bubbled out of the column end after the loading. The experiment was not at all reproducible, with percent standard deviations (%s) of as high as 150% for 1–butanol and between 30 and 50% for most of the rest of the solutes. Only 1–propanol had a %s of 15.5, but it gave an average γ_2^∞ (of the experimental runs) of 84.3, between 6 and 7 times higher than it should be. The chromatograms from these experiments showed very rough baselines. A solvent elution plateau was not observed.

a. Solubility

Water solubility is one of the most important parameters affecting the fate and transport of organic substances in the environment. Chemicals that have high water solubilities tend to have relatively low adsorption coefficients for soils and sediments and relatively low bioconcentration factors in aquatic life. These compounds also tend to be more readily biodegradable by microorganisms in soil, surface water, and sewage treatment plants. Specialized transport pathways, such as volatilization from solution and washout from the atmosphere by rain, are also affected by the extent of water solubility (27). Water solubilities can be calculated from γ_2^∞ by (28)

$$C_s = 5.56\times10^4/\gamma_2^\infty \ (\mathrm{mol/m^3}) \qquad (17)$$

Lyman (29) states that a reasonable estimate of C_s may be obtained, assuming the chemical does not dissociate (or associate with itself) to any significant extent in very dilute solutions, from equation 17 if $\gamma_2^\infty > 1000$. None of the solutes studied met this condition. Furthermore, substances such as methanol and ethanol are completely miscible in water, so a calculated value of C_s

would be meaningless.

b. Henry's Law Constant

The Henry's Law constant (H) relates the concentration of a compound in the gas phase to its concentration in the liquid phase (see Chapter II.iii). Since volatilization of gases and hydrophobic organic pollutants from water bodies to the atmosphere is a significant environmental pathway, knowledge of the Henry's Law constant is essential in calculating the direction and rate of mass transfer (17). For example, when crude oils are spilled on land or water, evaporation is often a significant process of mass loss from the spill. The evaporation of these liquid mixtures is dependent on H. The Henry's Law constant is a function of the liquid composition, temperature, and the fraction of liquid which has evaporated (18). H is related to the solute's limiting activity coefficients by (17)

$$H = 18\times10^{-6} p_2^o \gamma_2^\infty \ (m^3 atm/gmol) \qquad (14)$$

Table V.3 lists H–values for the solutes studied in water. The results are generally within 10% of the literature values, with acetone and 2–pentanone at 2%. There is a need for experimentally–derived H–values. Mackay (19) writes, "... considerable discrepancies exist in the literature even for common compounds. It is believed that bringing together vapor pressure, solubility, and H data for homologous series will promote the establishment of more accurate values for all three properties." He reviewed Henry's Law constants for 167 chemicals, of which only 40 values came from direct measurement. The rest were calculated from solubility and vapor pressure data.

Nirmalakhandan and Speece (20) list H–values for 180 chemicals derived by the quantitative structure–activity relationship (QSAR) model.

Our NSGC results for alcohols are two orders of magnitude higher than the calculative model–derived values. The calculative model method apparently did not account for some significant factors, leading to erroneously low values.

A direct application of the Henry's Law constant is the calculation of the half–life of a pollutant in a body of water. Assuming the substance is uniformly distributed, the half–life can be expressed as (21)

$$\tau_{1/2} = 0.69Z/K_L \qquad (15)$$

where Z is the mean depth of the water body (cm) and (22)

$$K_L = 1/k_l + 1/(Hk_g/RT) \qquad (16)$$

where k_l and k_g are the liquid– and gas–phase exchange coefficients (cm/sec), respectively. Values for these coefficients have been tabulated (17,22–25). These values lend understanding to the controlling rate processes of the volatilization of pollutants from water. Thomas (26) summarizes Mackay's findings in the following categories: (i) if $H < 3\times10^{-7}$ atm m^3/mol, the substance is less volatile than water; (ii) for $10^{-7} < H < 10^{-5}$ atm m^3/mol, the substance volatilizes slowly; (iii) for $H > 10^{-5}$ atm m^3/mol, the substance is more volatile than water. If the substance is less volatile in water than the water is, it will have a half–life on the order of years, assuming it does not degrade by some mechanism, e.g. biological, hydrolytic, photochemical, etc. However, since NSGC can not be used to measure the limiting activity coefficients of a solute in a solvent if it is less volatile in the solvent than the solvent is (it will only elute once all the solvent has come out), determination of H for category (i) solutes by NSGC is impossible.

c. Octanol/Water Partition Coefficient

The octanol/water partition coefficient (K_{ow}) is defined, for a

two–phase octanol/water system, as the ratio of a concentration of a compound in the octanol phase to its concentration in the aqueous phase. It can be related to the limiting activity coefficient by (30)

$$K_{ow} = 0.151\gamma_2^{\infty,w}/\gamma_2^{\infty,o} \qquad (18)$$

where the superscripts w and o refer to water and octanol solvents, respectively. In recent years, K_{ow} has become a required property in studies of the environmental fate of organic chemicals. K_{ow} is used to predict the ability of compounds to bioaccumulate (31) and to sorb on soils and sediments (32). $\gamma_2^{\infty,w}$ can readily be determined by NSGC. Octanol, however, is relatively non–volatile and will yield too long a column lifetime for a NSGC determination to be practical. If a value for $\gamma_2^{\infty,o}$ can be obtained (e.g. from the original GLC experiment, see Chapt. III.B.i) then K_{ow} can easily be calculated.

iv. Ethanol and Methanol Solvents

Limiting activity coefficients for six solutes in ethanol solvent are listed in Table V.4. Results for both the Supelcoport and glass bead columns are compared. As long as the column is completely saturated at the beginning of the run, the experiment is reproducible, regardless of the packing. The amount of solvent to be injected was determined by the level at which adding more would not decrease γ_2^{∞} and would not increase the column lifetime. For example (see Table V.5), for the system benzene in ethanol solvent studied on the 4 ft. Supelcoport columns, a 0.50 ml solvent loading yields a γ_2^{∞} value of 6.93, 1.00 ml yields 6.22, 1.50 ml yields 5.49, and 1.75 ml yields 5.45. Also, a 0.50 ml loaded column lasts for 3 hours, while both a 1.50 ml and a 1.75 ml loaded column last for about 7 hours. The non–porous glass bead columns

were fully saturated with 0.5 ml of ethanol and gave results close to the data determined on Supelcoport. The reproducibility of both these experiments is good, with 2 %s for some of the glass bead results to 5 %s for the Supelcoport data.

To determine the correct solvent loading to use on the Supelcoport columns, 4 ft. and 6 ft. columns were compared (see Table V.5). Both were packed with the same mesh–size Supelcoport and both were 1/8 in. od. The only difference was the amount of packing which is proportional to the length. As cited earlier, the 4 ft. columns contained 1.30 g of solid support, while the 6 ft. columns contained 1.86 g. When the same amount of solvent was tried in each column, the 6 ft. one gave higher apparent values of γ_2^∞. For a solvent loading of 0.75 ml, the 4 ft. column gave for benzene in ethanol a γ_2^∞ of 7.02 while the 6 ft. column yielded 7.86. Comparing solvent loadings of 0.50 ml to 0.75 ml on the 6 ft. column yields a γ_2^∞ of 8.10 as compared to 7.86. Similar effects are observed for all solutes. The longer the column, the more solvent must be injected to yield an accurate limiting activity coefficient. This, too, demonstrates that the column must be completely saturated to be able to reach the solvent elution rate plateau necessary for NSGC to give accurate results.

Table V.6 lists γ_2^∞ data for various solutes in methanol. Here, too, Supelcoport and glass bead columns of the same mesh–size are compared. On Supelcoport, 2.50 ml solvent loadings were used and 1.50 ml loadings on the glass beads. These volumes were determined the same way as with ethanol. The experiments on both solid supports are reproducible.

The effect of varying the inlet pressure on the column was studied. If the inlet pressure is too high it yields high γ_2^∞ values. For example, for acetone

in methanol on Supelcoport with a 2.50 ml solvent loading, at 30 psi_g γ_2^∞ = 3.46, at 25 psi_g γ_2^∞ = 2.85, at 20 psi_g γ_2^∞ = 2.40, and at 15 psi_g γ_2^∞ = 2.25. Lower inlet pressures would cause very slow flow rates, making the determinations difficult and impractical. However, the results at 15 psi_g are accurate with respect to the glass beads experiment. This, too, implies the elution rate plateau model. If the inlet pressure is too high and the solvent forced to elute at too high a rate, a stable plateau would not be maintained. The solvent leaves the column too quickly for determinations in an "active" column, as will become evident in later sections. The results would, therefore, not be accurate.

v. Chloroform Solvent

It was not experimentally feasible to study CH_2Cl_2, CCl_4, or $CHCl_3$ solvents on the glass bead columns at ambient or even sub–ambient temperatures. Even as much as a 3.00 ml solvent loading with an inlet pressure (P_i) of 10 psi_g (F = 15.5 ml/min) lasted only 50 min. and never stabilized. The baseline noise was too large to differentiate peaks. Lowering the column temperature to 10°C, though it gave a column lifetime of 90 min., did not give a more stable baseline. No constant elution rate plateau was ever reached.

Changing to the 4 ft. Supelcoport columns and setting the experimental conditions back to 25°C and the P_i to 12 psi_g yielded a 105 min. column lifetime for a 4.00 ml solvent loading. The baseline stabilized after 60 min., leaving enough time for 5 solute injections. Table V.7 lists the solutes studied in chloroform and their NSGC–determined γ_2^∞ values. The reproducibility is good and the data seem reasonable. One would expect dichloromethane to

have a γ_2^∞ slightly in excess of 1 because of its higher polarity than chloroform. CH_2Cl_2 has a dipole moment (μ_p, debyes) of 1.8 as compared to 1.1 for chloroform (35). Carbon tetrachloride is less volatile in $CHCl_3$ than $CHCl_3$ is and therefore did not elute until the column died. Ethanol, benzene, and acetone also share this property. Even 1–chloropropane (B.P. = 46°C, p_2^o = 340 mmHg (12)) is not volatile enough. Chloroform is a good solvent, but its high volatility limits the solutes which can be studied.

Dichloromethane was too volatile a solvent under the experimental conditions used for chloroform. A 4.00 ml solvent loading at a P_i of 11.8 psi_g yielded a 45 min. column. Although the baseline stabilized after 30 min., at t = 32 min., a baseline shift occurred that resembled an eluting peak. The same happened when P_i was lowered to 10 psi_g. There was never a constant elution rate plateau and, therefore, never a workable NSGC system. An attempt to study CCl_4 was initiated but the detector broke down while trying to determine the optimum conditions. It seemed that the same conditions used for $CHCl_3$ would have worked for CCl_4 but progress on this series of solvents was stopped when, though there was a fair rate of air exchange in the lab, the investigator found himself always tired and nauseous. Some form of venting of the solvents that would allow for flow rate measurements but not affect F is necessary. Possibly, a 3–way valve to an appropriate trap would work. In addition, it is probable that the chlorocarbons destroyed the filaments in the detector.

vi. n–Hexane and n–Heptane Solvents

Injections of 4.00 ml of n–pentane at T_{col} = 25°C and P_i = 12 psi_g on Supelcoport gave a 20 min. column lifetime; 5.00 ml gave the same results.

Injections of 4.00 ml of n–hexane, however, resulted in a 70 min. column lifetime which required 45 min. to stabilize after the solvent loading. This left 25 min. for the determinations, just enough time for three solute injections. The results are listed in Table V.8. As expected, γ_2^∞ for n–pentane is close to one, being nonpolar and of similar structure to the solvent. Methanol has a high γ_2^∞, being polar compared to the solvent. There is a high %s for methanol and a large room for error. Methanol is only slightly soluble in n–hexane and elutes quickly. Its retention time was 0.92 min. at the beginning of the column lifetime and 0.53 min., approximately the same as the t_R of air, at the end. There is, therefore, a large margin of error in measuring its t_R.

In Table V.9, γ_2^∞ values for acetone, n–pentane, and methanol in n–heptane solvent are listed. The results are close to those in n–hexane, as expected considering the similarity of the two solvents. The experimental conditions, however, were not the same. n–Heptane is much less volatile. It has a p_2^o of 47.718 mmHg (33) as compared to 149.44 mmHg (33) for n–hexane. Therefore, a smaller solvent loading volume would have a longer residence time in the column and still maintain a stable elution rate plateau. So, raising the P_i to 20 psi_g would only affect the residence time of the solvent and the retention time of the solutes. A higher P_i would have upset the elution plateau just as a low P_i would to a highly volatile solvent. Under these conditions, 3.00 ml saturated the columns and gave a column lifetime of greater than two hours. Equilibration and stabilization time, however, was still 60 min. The retention times for methanol were shorter than in n–hexane, 0.69 min. at the beginning of the column lifetime and 0.39 min. at the end. The data, however, had a much lower %s than in n–hexane.

No comparison was done with the glass bead columns using these two

solvents. Operational conditions were not found for n–hexane but were found for h–heptane. A 3.20 ml solvent loading at 25°C and P_i = 10 psi_g gave an 85 min. column lifetime with a stabilization and equilibration time of 60 min. It is probable that there would have been enough time to do 3 solute injections. Results comparable to those from the Supelcoport columns are expected.

vii. n–Octane Solvent

n–Octane, being less volatile than water (p_2^0 = 13.976 mmHg (33) as compared to p_2^0 = 23.756 mmHg for water (34)), offered the opportunity once again to study variations in γ_2^∞ data obtained during different fractions of the column lifetime. Since n–octane is less viscous than water (at 25°C, η_L = 0.509 centipoises for n–octane as compared to η_L = 0.764 centipoises for water (35)) and has a lower surface tension (at 20°C , 21.80 dynes/cm for n–octane as compared to 72.75 dynes/cm for water (44)) the flow dynamics (as will be explained later) may differ. It may behave more like a volatile solvent and the column may desaturate more quickly. If the flow dynamics are different, the stable elution rate plateau may change and/or disappear. This would cause data from later in the lifetime to be different than values determined nearer the beginning, as with highly volatile solvents. If the columns were not completely saturated by the solvent, the γ_2^∞ results would be too high (see section V.iv), probably due to solute–solute interactions.

The three solutes studied in n–hexane and n–heptane were studied here. Since n–octane is a homolog of those two solvents, the γ_2^∞ values for the solutes should be approximately the same. The column lifetime was split into four equal fractions of about 50 min. each and five experimental runs for each solute were done in each fraction. The average of the five runs should be taken

as the limiting activity coefficient determined in that fraction of the column lifetime. The optimum experimental conditions at 25°C were found to be 2.00 ml solvent loadings at $P_i = 25$ psi_g on Supelcoport (yielding flow rates from 55 to 65 ml/min, depending when in the column lifetime the run was done), with a 60 min. equilibration and stabilization time after the solvent injection. This gave a 4.5 hour column lifetime. The solute runs were done in series, 5 solute injections of acetone, then 5 of n–pentane, 5 of methanol, and 5 of acetone again. After the fourth run the columns died, another 2.00 ml of n–octane were injected, 60 min. were given for equilibration and stabilization, and the series was continued (n–pentane, methanol, etc.). In a given solvent loading the same solute was run at the beginning and the end of the column lifetime.

Table V.10 lists γ_2^∞ values for the first five experimental runs done for each solute. This is an indiscriminate drawing of values since there is no set fraction comparison being taken into account. The average for n–pentane for the five runs is made up of one data value from the first fraction, two from the second, one from the third, and one from the fourth. Acetone has three from the first fraction, none from the second, one from the third, and one from the fourth. Methanol has one from the first, one from the second, two from the third, and one from the fourth. Table V.11 lists the average value of all 20 experimental runs done for each solute throughout the column lifetime. Every fraction of the column lifetime is equally represented for each fraction. Table V.12 lists the values for the first fraction, Table V.13 the second, Table V.14 the third, and Table V.15 the last fraction before the columns died.

It is evident from Tables V.14 and V.15 that nearer the end of the column lifetime, the columns were not sufficiently saturated to give the constant elution rate plateau necessary for infinite dilution measurements.

Except for methanol, the results were apparently too high! This significantly raises the overall average of all the runs. It explains why in Table V.10, acetone with 3 first–fraction values but no second–fraction data, had a γ_2^∞ close to the overall average, while methanol with 2 third–fraction values was so high. The comparison of interest, though, is between Tables V.12 and V.13, the first two fractions after solvent loading. The reproducibility of the experiment was much better in the second fraction than in the first (lower %s). The γ_2^∞ for n–pentane was closer to its value in n–heptane and n–hexane solvents in the second fraction than it was in the first. So, too, for methanol, except that its third fraction value was even more precise. The γ_2^∞ for acetone, however, was closer in the first fraction than in the second. In addition, the value for n–pentane should be nearly unity, and this was more true for the first fraction than for the second.

To resolve this issue, the solutes were run on the glass bead columns. The experimental conditions for complete saturation so as to attain a stable elution rate plateau were 1.50 ml solvent loadings at $P_i = 15$ psi_g. This gave a column lifetime of 2 hours, of which 60 min. was the equilibration time, and a flow rate of from 18 to 24 ml/min during the run. Table V.16 lists the results for these determinations. Every run was done over a complete column lifetime. The results follow the same pattern that the Supelcoport ones did. The acetone data are more precise with respect to the first fraction and n–pentane with respect to the second. Methanol, however, has an even lower γ_2^∞ value on the glass bead column than in the first Supelcoport fraction, and a much lower value than in the other two solvents.

It must be once again noted that methanol has a very short retention time, always less than a minute, even at the lower flow rates on the glass bead

columns. This reduces the precision of these measurements (%s = 34.9). For the other two solutes, the results of the first two fractions and the glass bead columns determinations are all within the experimental error defined by the %s of their respective runs and within a 95% confidence level of a standard t–test. So, all the results are essentially equal and, hence, there is some form of a constant rate elution plateau that is reached after stabilization and is maintained as long as there is enough solvent in the column to support it.

A possible mechanism explaining why n–octane requires a larger solvent loading than water (2.00 ml as compared to 0.50 ml for water) at the same temperature and inlet pressure, and has a shorter column lifetime (4.5 hrs. as compared to 9 hrs. for water) on the 4 ft. Supelcoport column involves viscosity and surface tension. Rejection of the possibility that the same amount of solvent is left in the column after stabilization and equilibration is necessary for this model. Therefore, the weight of solvent w_1 at the beginning of the usable column lifetime was calculated using equation 1. The column retains 0.38 ml of water and approximately all the n–octane. The effect of the viscosity and surface tension of a solvent on its rate of elution can be explained in the following way. Viscosity is a measure of the internal fluid friction which tends to oppose any dynamic change in the fluid motion (45). Surface tension is explained in the following way. At low gas densities, the surface molecules are attracted sidewise and toward the bulk liquid by forces acting upon the molecules of a surface layer, but experience less attraction in the direction of the bulk gas. Thus, the surface layer is in tension and tends to contract to the smallest area compatible with the mass of material, container restraints, and external forces (46). The higher the viscosity and surface tension, the higher the force necessary for flow. When a large volume of solvent is injected into

the column, a plug will be formed in the path of helium flow. Helium will blow out of the column just enough solvent for the gas to be able to flow through it; the helium will break the plug. This appears as a bubbling out of the end of the column shortly after a solvent loading greater than the capacity of the column is injected into it. Since water has a higher surface tension than n–octane, it will require more force to break through the water plug. Therefore, if P_i is held constant, the water plug would have to be smaller than the n–octane plug for equilibration to take place on the same time scale. Viscosity is also a factor in the volume of the solvent loading. True, water is more dense than n–octane so that a smaller volume still contains more mass. However, the reason why 0.50 ml of water will saturate the column while it takes 2.00 ml of n–octane to accomplish this is there is more of an opposing force by the water than by n–octane. For the solvent to flow requires a force from behind. There is an opposing force (pressure drop) by the solid support. High viscosity compliments the pressure drop effect.

Once an open pathway for the helium is formed, the elution of solvent occurs only by liquid–vapor partitioning. However, the solvent is in bulk here (as will be demonstrated in the next section). This means that when the helium flows over the bulk solvent it increases its rate of evaporation (the VLE will demand that more n–octane enter the vapor phase to maintain saturation). Since the P_i is held constant throughout an experimental run, volatility effects being ignored, the higher the surface tension, the slower the bulk solvent will move in the direction of bulk gas; hence, the longer the column lifetime will be. Because helium has a maximum dew point for the various solvents, as long as there is enough solvent in the column to saturate the vapor phase, there will be a constant elution rate of that amount of solvent

into the vapor. The viscosity and surface tension will, therefore, also determine the rate of change in flow rate. The higher the viscosity and surface tension, the less a change in F will occur over a given time interval.

Testimony to the effect of the pressure drop is given by the results of an experiment carried out on glass columns. A liquid solvent front was visible at a certain point along the column. No matter how much solvent was injected, the front apparently never moved beyond that point. The excess was seen bubbling out of the end of the column. There was a maximum injection volume reached, however, after which the pressure on the syringe was too great to depress the plunger. Recall there is the pressure of the carrier entering the injection port stopping the solvent from moving in that direction. Therefore, other factors to be considered when doing an NSGC experiment are the viscosity and surface tensions of the solvent.

The other determining factor is the adsorptivity and/or wetting of the packing by the solvent (glass beads only wet). Though the packing is inert and does not affect the measurement, how well it adsorbs or is wet by the solvent affects the ability to make the measurement. Supelcoport adsorbs n–octane and glass beads are wet by it, therefore, constant elution rate plateaus are reached and γ_2^∞ measurements can be accurately made on both. Water, however, does not wet DMCS–treated glass beads, so determinations could not be made on that solid support.

viii. Column Dynamics

To get a picture of what is going on inside the column, to see how the solvent saturates the packing, whether it is actually in bulk, and whether the solute sees effectively the same amount of solvent to warrant the claim of

infinite dilution, the following analysis was done. The ratio of the film thicknesses of a solvent in two different columns, and at different times during the column lifetime, is a physical measure of whether a constant elution rate plateau has been reached. If the ratio of the film thickness of a column that has achieved the plateau to that of another column is unity, then both columns contain enough bulk solvent for a limiting activity coefficient determination to be made. If the film thickness of a column near the beginning of its lifetime is the same as that of another column at a later time, it would imply that the coating on the packing, or, otherwise put, the saturation by solvent is equivalent. Of course the solvent is eluting with time and, therefore, there would be less total solvent in the column at a later time than at an earlier one. However, the film thickness is what the solute sees in the column with a constant elution rate plateau. As will shortly be developed, the film thickness ratio determinations are made via plate height calculations which come from solute peak data. If the film thickness ratios for different times in the column life are unity, it must be that the solute sees an equivalent saturation of solvent throughout the "active" lifetime of the column. Since both the solute and the solvent move through the column by liquid–vapor phase partitioning, the solute peak (used to calculate the plate height) can be thought of as a measure of what the solute sees in the vapor phase. If the solvent concentration in the vapor phase is constant, as measured by comparable film thickness ratios, the solvent must have a constant rate of elution, *ergo*, the constant elution rate plateau model, q.e.d.

Martin and Synge (37) defined the height equivalent to a theoretical plate (H) as 'a unit of column length sufficient to bring the gas issuing from it into equilibrium with the solute in the immobile phase throughout the unit.' It

is a measure of the efficiency of the column. From the term of the van Deemter equation that describes the solute profile in a column limited by stationary phase mass transfer, the plate height is given by (38)

$$H = (2/3)[kd_f^2 \bar{u}/(1+k)^2 D_g] \quad (19)$$

where k is the mass distribution ratio of solute between phases given by (39)

$$k = (t_R/t_o)-1 \quad (20)$$

d_f is the thickness of the equivalent liquid film, D_g is the diffusivity of the solute in the solvent, and $\bar{u}$ is the average velocity of the mobile phase. Since the desired expression is the ratio of film thicknesses, dividing H_2 for one column by H_1 for another gives

$$H_2/H_1 = [k_2 d_{f_2}^2 (1+k_1)^2/k_1 d_{f_1}^2 (1+k_2)^2] \quad (21)$$

and solving for the film thickness ratio (since $\bar{u} \propto F$) gives

$$d_{f_2}/d_{f_1} = [H_2 k_1 F_1 (1+k_2)^2/H_1 k_2 F_2 (1+k_1)^2] \quad (22)$$

H can be determined from a solute peak by the expression (39)

$$H = (L/16)(t_w/t_R)^2 \quad (23)$$

where L is the column length (cm) and t_w is the base width of the peak at the baseline between the tangents extrapolated from the points of inflection of the peak (in time units).

Six ft. (183 cm) by 1/8 in. od ss columns packed with 80/100 mesh DMCS treated glass beads were prepared and determinations were done on them at different solvent loadings and inlet pressures. Acetone in n–octane solvent was the system used. The results were compared with determinations done on the 4 ft. (122 cm) glass bead columns. Table V.17 lists the conditions of the various experimental runs done. Table V.18 lists some of the parameters calculated from the data, and Table V.19 lists some of the determined ratios. The peak number is a measure of how late into the column lifetime the

measurement was made. Solute injections were done every 10 minutes. Acetone has a short retention time in n–octane under the experimental conditions.

A 6 ft. column requires more than a 1.50 ml solvent loading to achieve saturation. This can clearly be seen by the data in Table V.17. Comparison of peak # 2 of set 697 with its corresponding peak in set # 701 gives a ratio of 0.757, far from unity. If two columns that have not been saturated are compared (sets # 695 and 696 and sets # 697 and 698) the ratios do approach unity. This is expected since the the solute sees the same amount of solvent in both cases (t_R data are similar) even though the plateau does not exist. Sets 701 and 702 definitely have attained plateaus. One and one–half ml of n–octane on a 4 ft. column achieves saturation (see section V.vii). Therefore, the ratio of 0.972 is expected.

Another experiment was also carried out to verify this model. A second GC, Perkin Elmer Vapor Fractometer model 154, was hooked up to the exhaust of the working GC and vapor phase sampling of the eluent was done to determine how much n–octane is in the vapor phase. A heated line was connected from the working GC column to the 1.4 ml gas sampling valve on the Perkin Elmer and samples were taken every 10 minutes during the column lifetime. The peaks were integrated by a Shimadzu Chromatopac C–R36A integrating recorder. From a calibration curve made by direct solvent injection it was determined that for example, for sets 701 and 702, there was approximately 4 μl ($\pm$0.5 μl) of n–octane in a 1.4 ml gas sample during the active lifetime of the column, yielding a constant vapor phase mole fraction of $y = 0.28$. This proves that during the usable part of the column lifetime, the same amount of solvent was constantly in the vapor phase. A plateau was

reached at which the solvent eluted.

ix. Vapor Phase Interactions

Vapor liquid equilibrium will be affected by vapor phase interactions. If the measurements for liquid phase nonideality are made when there is the vapor phase present, the interactions in the vapor phase will interfere with the measurement. Gas phase nonideality is accounted for via the fugacity coefficient. This is the gas phase counterpart of the activity coefficient. As discussed in section III.A and III.B.i, Eckert et al. (3,16) accounted for gas phase nonideality in their expressions for the activity coefficient but found it to be insignificant and, therefore, ignored it. This work has also reached the same results.

The fugacity coefficient can be calculated from the second virial coefficient B by the following method (43). B is calculated by the method of Tsonopoulos (40–42) from the equation for nonpolar systems

$$B = (f^{(0)} + \omega f^{(1)})RT_c/P_c \qquad (24)$$

where T_c and P_c are the critical temperatures and pressures, respectively, ω is the acentric factor, and $f^{(0)}$ and $f^{(1)}$ are given by

$$f^{(0)} = 0.1445 - 0.330/T_r - 0.1385/T_r^2 - 0.0121/T_r^3 - 0.0000607/T_r^8 \qquad (25)$$

$$f^{(1)} = 0.0637 + 0.331/T_r^2 - 0.423/T_r^3 - 0.008/T_r^8 \qquad (26)$$

where T_r is the reduced temperature equal to T/T_c. For polar systems, the term $f^{(2)}$ is added to equation 24 given by

$$f^{(2)} = a/T_r^6 - b/T_r^8 \qquad (27)$$

where a and b are constants specific to the system, values of which are given in reference 43. Also in reference 43is a discussion of the calculation of B

values for the mixtures, such as were encountered in the γ_2^∞ measurements done here.

The fugacity coefficient for a binary system with a carrier gas is given by

$$\ln\phi_2 = [2(y_1B_{12}+y_2B_{22}+y_3B_{32})-B_m]P/RT \qquad (28)$$

where subscript 1 is the solvent, 2 the solute, and 3 the carrier gas, y_i is the mole fraction in the vapor phase, B_{ij} is the interaction virial coefficient for species i and j, and B_m is the mixture virial coefficient (see reference 43).

Table V.20 lists the virial coefficients necessary to calculate the fugacity coefficients of some sample cases, and Table V.21 list the fugacity coefficient of those systems. The results are near unity and, hence, the effect of vapor phase nonideality on the measured γ_2^∞ is small and will always be well within the experimental error, which is estimated to be of the order of 10% from the overall reproducibility of the method and from the limits of measurement of the short retention times and fast flow rates. These fugacity corrections can therefore be ignored.

Table V.1

Limiting Activity Coefficients in Water[a]

Compound	γ_2^∞ 50°C	40°C	20°C	25°C[b]	p_2^o(mmHg)[c]
Methanol	1.54	1.47	1.29	1.36	125.4
Ethanol	3.82	3.24	2.55	2.86	59.8
1–Propanol	12.5	11.7	9.98	10.7	20.9
2–Propanol	7.71	6.86	5.19	5.87	45.2
1–Butanol	45.5	44.6	38.6	40.8	6.18
2–Butanol	21.7	20.8	17.6	18.9	18.3
Acetone	6.88	6.21	4.61	5.24	231.0
2–Butanone	23.5	24.6	17.2	20.2	90.60
2–Pentanone	83.3	79.8	61.2	67.8	35.40
3–Pentanone	85.1	92.4	72.3	78.2	35.43

[a] The flow rate correction was not included in these data.

[b] The values at 25°C are from interpolation from data at 50, 40, and 20°C.

[c] Vapor pressures for the alcohols are from reference (4) and for the ketones from reference (5) at 25°C.

Table V.2

Limiting Activity Coefficient in Water at 25°C

Compound	γ_2^∞ exptl.	γ_2^∞ lit.	p_2^o(mmHg)[a]	s[b]
Methanol	1.74	1.63[c]	125.4	±0.17
Ethanol	4.03	3.74[d]	59.8	±0.52
1–Propanol	15.0	11.7[e]	20.9	±1.3
2–Propanol	7.75	6.54[e]	45.2	±0.69
1–Butanol	53.7	53.5[f]	6.18	±7.1
2–Butanol	22.4	24.7[e]	18.3	±2.1
Acetone	7.31	7.17[g]	231.0	±0.79
2–Butanone	27.6	26.2[e]	90.60	±3.5
2–Pentanone	102	104.0[e]	35.40	±15
3–Pentanone	113	104[e]	35.43	±16

[a] Vapor Pressures for the alcohols are from reference (4) and for the ketones from reference (5) at 25°C.

[b] s refers to the standard deviation of the five experimental runs done for each compound. The reported experimental value is the average of these five determinations.

[c] reference (6); [d] reference (7); [e] reference (8); [f] reference (9); [g] reference (10)

Table V.3

Henry's Law Constants in Water at 25°C

Compound	H (m^3 atm $gmol^{-1}$) exptl.	lit.[a]
Methanol	5.17×10^{-6}	4.84×10^{-6} [c]
Ethanol	5.71×10^{-6}	5.30×10^{-6} [d]
1–Propanol	7.43×10^{-6}	5.79×10^{-6} [e]
2–Propanol	8.30×10^{-6}	7.00×10^{-6} [e]
1–Butanol	7.86×10^{-6}	7.83×10^{-6} [f]
2–Butanol	9.72×10^{-6}	1.07×10^{-5} [e]
Acetone	4.00×10^{-5}	3.92×10^{-5} [g]
2–Butanone	5.91×10^{-5}	5.61×10^{-5} [e]
2–Pentanone	8.56×10^{-5}	8.72×10^{-5} [e]
3–Pentanone	9.48×10^{-5}	8.72×10^{-5} [e]

[a] Literature values were calculated from activity coefficients in the cited references.

[c] reference (6); [d] reference (7); [e] reference (8); [f] reference (9); [g] reference (10).

Table V.4

Limiting Activity Coefficients in Ethanol at 25°C on Supelcoport and DMCS–Treated Glass Beads

	γ_2^∞			
Compound	exptl.^{sp}/(s)[a]	exptl.^{g}/(s)	lit.	p_2^o(mmHg)
Benzene	5.45/(±0.63)	5.21/(±0.14)	6.0[b]	94.39[c]
n–Pentane	7.68/(±0.45)	9.49/(±0.26)	9.0[d]	508.47[c]
Ethyl Acetate	3.62/(±0.20)	3.61/(±0.08)		94.191[e]
CH_2Cl_2		2.50/(±0.14)		434.74[f]
$CHCl_3$	1.62/(±0.08)	1.71/(±0.05)		199.1[c]
CCl_4		5.14/(±0.09)		114.5[c]

[sp] sp refers to experimental runs done on Supelcoport solid support.

[g] g refers to experimental runs done on DMCS treated glass beads as a solid support.

[a] s refers to the standard deviation of the five experimental runs done for each compound. The reported experimental value is the average of these five determinations.

[b] reference (11); [c] reference (12); [d] reference (3); [e] reference (13); [f] reference (14)

Table V.5

Solvent Loading Determinations for Ethanol Solvent on Supelcoport from γ_2^∞ Data of Bezene as the Solute

L(ft.)[a]	sl(ml)[b]	clt(hrs)[c]	γ_2^∞
4	0.50	3	6.93
4	0.75	4.5	7.02
4	1.00	6	6.22
4	1.50	7	5.49
4	1.75	7	5.45
6	0.50	3	8.10
6	0.75	4.5	7.86

[a] L is the column length.

[b] sl is the solvent loading volume of the run.

[c] clt is the column lifetime.

Table V.6

Limiting Activity Coefficients in Methanol at 25°C on Supelcoport and DMCS–Treated Glass Beads

	γ_2^∞			
Compound	exptl.^{sp}/(s)[a]	exptl.^{g}/(s)	%Δ[b]	p_2^o(mmHg)
Benzene	7.52/(±0.33)	7.17/(±0.16)	4.65	94.39[c]
n–Pentane	17.3/(±0.2)	19.5/(±1.0)	11.2	508.47[c]
Acetone	2.25/(±0.07)	2.16/(±0.07)	4.00	231.0[d]
CH_2Cl_2	2.60/(±0.10)	2.81/(±0.06)	7.47	434.74[e]
$CHCl_3$	2.32/(±0.23)	2.34/(±0.05)	0.855	199.1[c]
CCl_4	7.53/(±0.25)	7.58/(±0.19)	0.660	114.5[c]

[sp] sp refers to experimental runs done on Supelcoport solid support.

[g] g refers to experimental runs done on DMCS treated glass beads as a solid support.

[a] s refers to the standard deviation of the five experimental runs done for each compound. The reported experimental value is the average of these five determinations.

[b] %Δ refers to the percent difference between the values determined on Supelcoport and on glass beads.

[c] reference (11); [d] reference (5); [e] reference (14).

Table V.7

Limiting Activity Coefficients in Chloroform at 25°C

on Supelcoport

Compound	γ_2^∞	s[a]
n–Pentane	2.13	±0.06
CH_2Cl_2	1.26	±0.02
Methanol	9.55	±0.62

[a] s refers to the standard deviation of the five experimental runs done for each compound. The reported experimental value is the average of these five determinations.

Table V.8

Limiting Activity Coefficients in n–Hexane at 25°C on Supelcoport

Compound	γ_2^∞	s[a]
n–Pentane	1.15	±0.02
Acetone	7.40	±0.23
Methanol	91.0	±17.1

[a] s refers to the standard deviation of the five experimental runs done for each compound. The reported experimental value is the average of these five determinations.

Table V.9

Limiting Activity Coefficients in n–Heptane at 25°C on Supelcoport

Compound	γ_2^∞	s[a]
n–Pentane	1.13	±0.05
Acetone	7.80	±0.08
Methanol	90.3	±6.6

[a] s refers to the standard deviation of the five experimental runs done for each compound. The reported experimental value is the average of these five determinations.

Table V.10

Limiting Activity Coefficients in n–Octane at 25°C

on Supelcoport

(first 5 experimental runs done)

Compound	γ_2^∞	s[a]
n–Pentane	1.19	±0.19
Acetone	7.63	±0.85
Methanol	102	±14

[a] s refers to the standard deviation of the five experimental runs done for each compound. The reported experimental value is the average of these five determinations.

Table V.11

Limiting Activity Coefficients in n–Octane at 25°C on Supelcoport (all experimental runs)

Compound	γ_2^∞	s[a]
n–Pentane	1.15	±0.17
Acetone	7.70	±1.01
Methanol	88.8	±20.0

[a] s refers to the standard deviation of the five experimental runs done for each compound. The reported experimental value is the average of these five determinations.

Table V.12

Limiting Activity Coefficients in n–Octane at 25°C

on Supelcoport

(solute is first experimental run after solvent loading)

Compound	γ_2^∞	s[a]
n–Pentane	0.994	±0.087
Acetone	7.06	±0.55
Methanol	75.6	±19.2

[a] s refers to the standard deviation of the five experimental runs done for each compound. The reported experimental value is the average of these five determinations.

Table V.13

Limiting Activity Coefficients in n–Octane at 25°C

on Supelcoport

(solute is second experimental run after solvent loading)

Compound	γ_2^∞	s[a]
n–Pentane	1.06	±0.05
Acetone	6.77	±0.20
Methanol	92.0	±22.0

[a] s refers to the standard deviation of the five experimental runs done for each compound. The reported experimental value is the average of these five determinations.

Table V.14

Limiting Activity Coefficients in n–Octane at 25°C

on Supelcoport

(solute is third experimental run after solvent loading)

Compound	γ_2^∞	s[a]
n–Pentane	1.17	±0.09
Acetone	8.02	±0.45
Methanol	89.3	±24.1

[a] s refers to the standard deviation of the five experimental runs done for each compound. The reported experimental value is the average of these five determinations.

Table V.15

Limiting Activity Coefficients in n–Octane at 25°C

on Supelcoport

(solute is last experimental run after solvent loading)

Compound	γ_2^∞	s[a]
n–Pentane	1.40	±0.06
Acetone	8.95	±0.82
Methanol	98.1	±11.2

[a] s refers to the standard deviation of the five experimental runs done for each compound. The reported experimental value is the average of these five determinations.

Table V.16

Limiting Activity Coefficients in n–Octane at 25°C

on DMCS–Treated Glass Beads

Compound	γ_2^∞	s[a]
n–Pentane	1.08	±0.07
Acetone	6.93	±0.82
Methanol	65.5	±22.8

[a] s refers to the standard deviation of the five experimental runs done for each compound. The reported experimental value is the average of these five determinations.

Table V.17

Description of Sets Used for Film Thickness Ratio Study

Set #	#p[a]	P_i(psig)	sl(ml)[b]	L(cm)[c]	clt(min)[d]
695	7	27.3	0.50	183	97
696	7	27.0	1.00	183	117
697	10	27.0	1.50	183	133
698	8	31.9	1.50	183	111
699	3	20.7	0.50	122	56
700	5	20.5	1.00	122	79
701	7	20.4	1.50	122	83
702	5	24.4	1.50	122	67

[a] #p is the number of solute injections in the run.

[b] sl is the solvent loading volume of the run.

[c] L is the column length.

[d] clt is the column lifetime.

Table V.18

Data from Selected Peaks of Film Thickness Ratio Study

Set #	p#[a]	H(cm)	k	F(ml/min)	t_R(min)
695	1	1.15	5.58	31.4	1.61
695	2	1.24	5.22	32.0	1.49
696	1	1.10	5.47	30.7	1.61
697	2	0.904	6.96	27.8	2.17
697	8	1.16	2.37	37.1	0.69
698	2	0.687	7.37	34.9	2.00
698	8	1.80	2.07	47.9	0.53
699	1	2.49	3.67	32.4	0.91
700	1	0.847	4.79	30.3	1.20
701	2	0.598	5.45	26.9	1.50
702	2	0.817	5.10	37.2	1.13

[a] p# is the number of the solute peak in the run.

[b] sl is the solvent loading volume of the run.

[c] L is the column length.

[d] clt is the column lifetime.

Table V.19

Film Thickness Ratios for Different Columns

Set #'s	Peak #'s	d_{f_2}/d_{f_1}
695/696	1/1	0.982
695/697	2/2	1.02
695/699	1/1	1.27
696/700	1/1	0.845
697/701	2/2	0.757
697/698	8/8	1.07
698/702	2/2	0.925
701/702	2/2	0.972

Table V.20

Virial Coefficients for Selected Systems

System	Type of B	Value(ml/mol)
Methanol	B_{22}	–1816.223
n–Pentane	B_{22}	–1224.209
n–Octane/n–Pentane	B_{12}	–2302.147
Water/Methanol	B_{12}	–994.1984
Methanol/Helium	B_{23}	28.60094
n–Pentane/Helium	B_{23}	42.68534
$nC_8/nC_5/He$	B_m	–220.2486
H_2O/MeOH/He	B_m	–8.948027

Table V.21

Solute Fugacity Coefficients for Selected Systems

System	ϕ_2
$nC_8/nC_5/He$	0.95
$H_2O/MeOH/He$	0.98

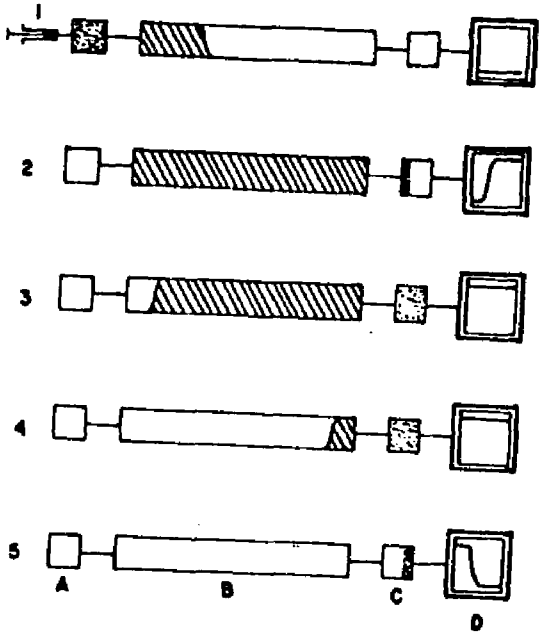

Figure V.1. Schematic Representation of NSGC. A, injection port; B, column packed with solid support; C, TCD; D, recorder. Hatched lines represent liquid solvent and dots solvent vapor. 1, liquid solvent is injected, evaporates and condenses on solid support as carrier gas moves vapors through the column; recorder pen reads carrier baseline. 2, solvent fills column, begins to elute into hot TCD; recorder shows solvent breakthrough front. 3 and 4, carrier gas continues to elute solvent, and solvent shows high baseline because of solvent vapors. 5, solvent completely eluted from column; recorder shows return of baseline down solvent tail to carrier gas reading as solvent vapor tail moves through detector.

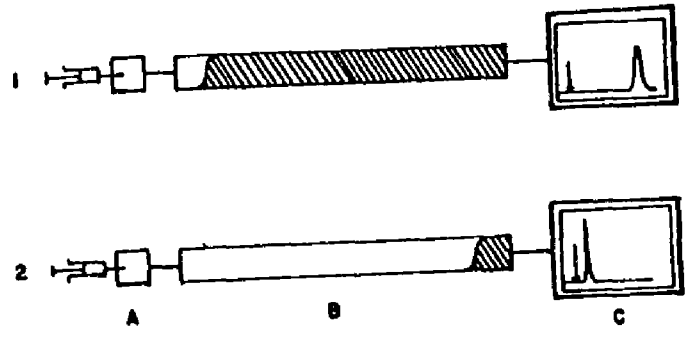

Figure V.2. Schematic Representation of Nonsteady State Chromatograms. A, injection port; B, column in early and late stages of lifetime; C, TCD and recorder. 1, solute injected at an early time in column life; recorder baseline adjusted downscale from Figure V.1–3. 2, solute injected at later stage of column life. Difference in t_R is exaggerated.

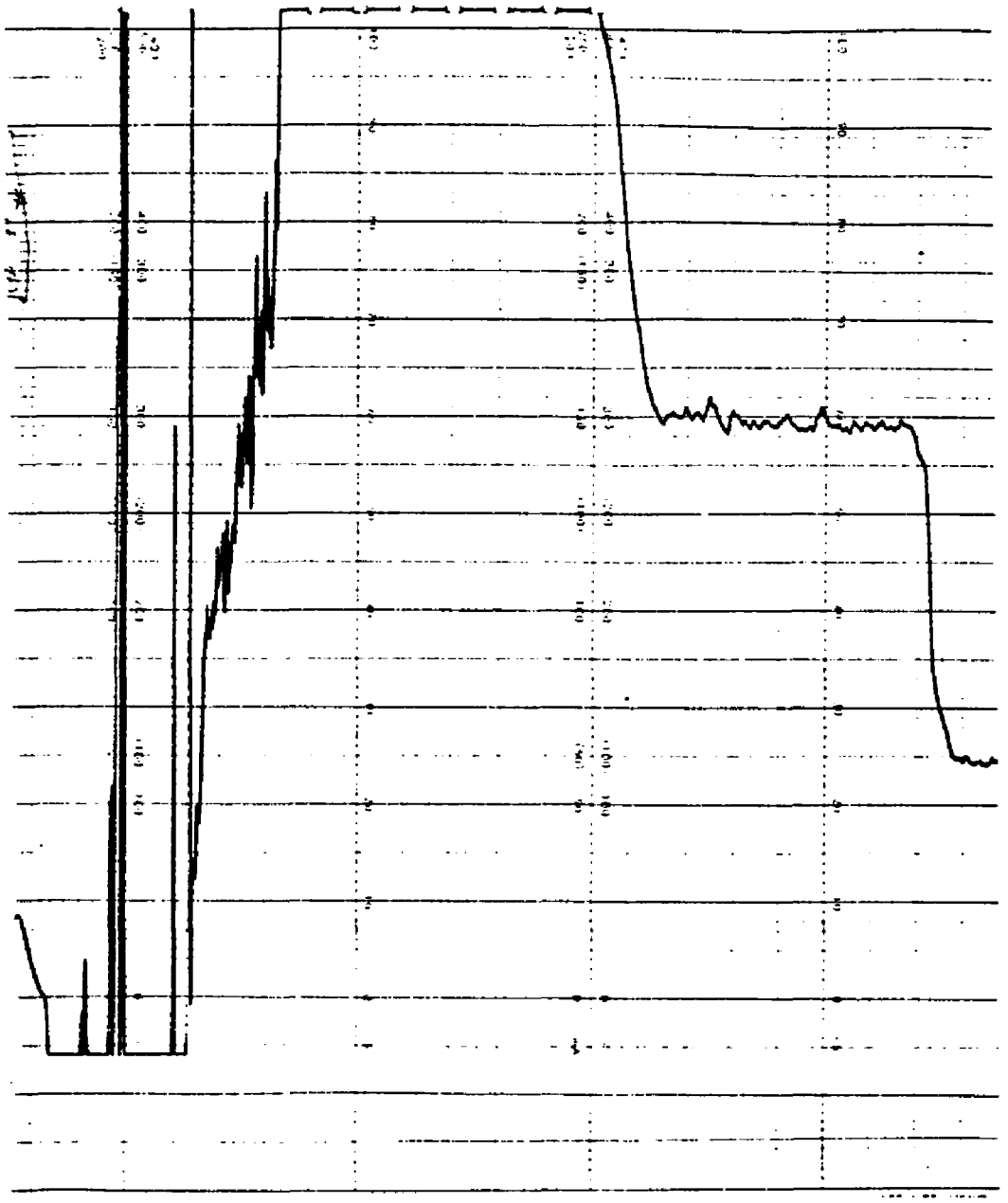

Figure V.3. Sample NSGC chromatogram of stabilization and equilibration. The two spikes on the left correspond to moment of solvent injection. The interval between chart paper lines is 20 min. The sharp descent of the recorder pen on the right corresponds to manually adjusting the baseline.

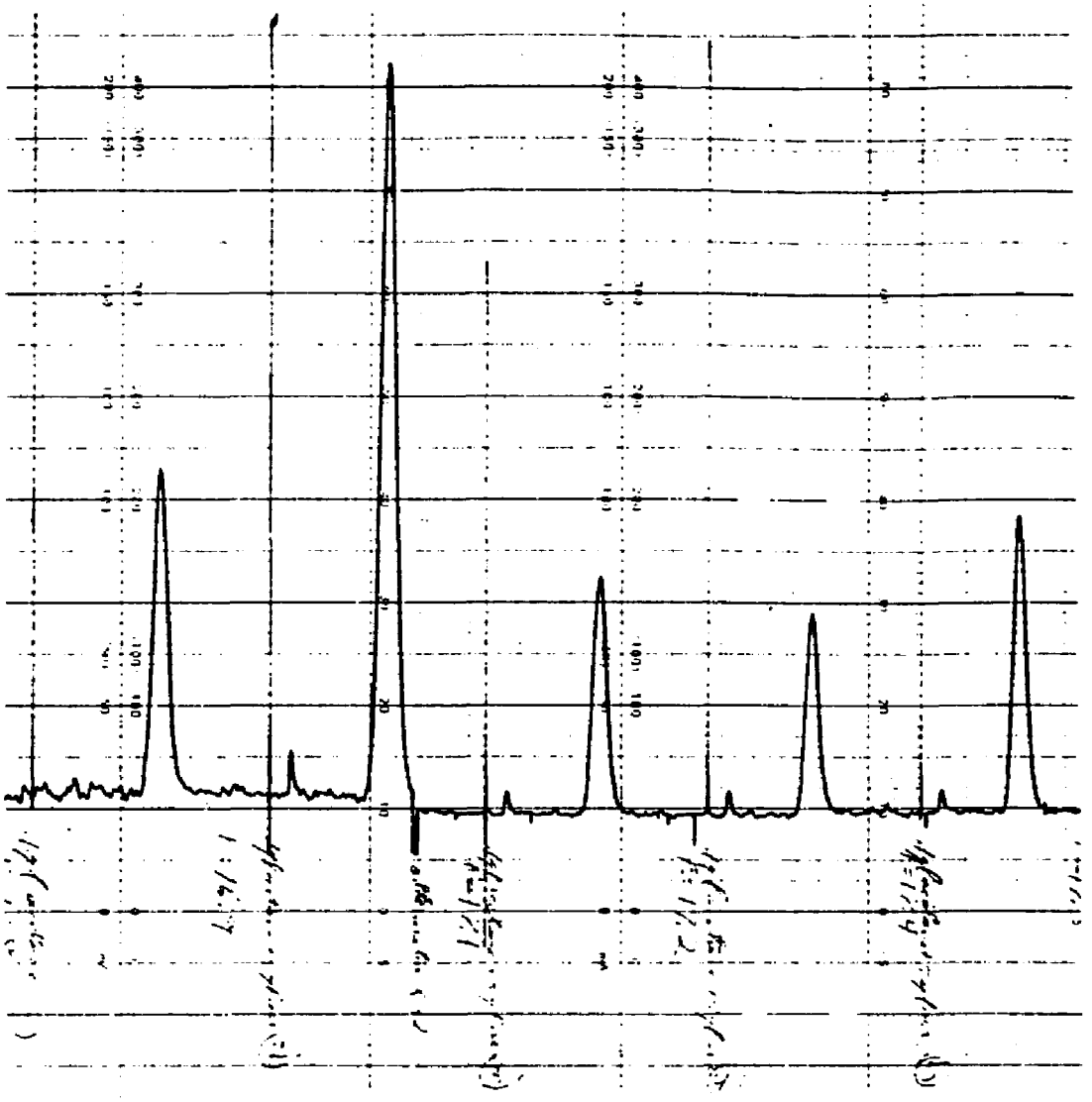

Figure V.4. Sample NSGC chromatogram of experimetal run. The spikes correspond to solute injections, and the peaks to solute elutions. The interval between the spikes and the corresponding peaks (to the right of a spike) is constantly decreasing.

References

(1) Belfer, A.J. Neftekhim. 1972, 12, 435; CA 1973, 78, 20591.

(2) Belfer, A.J.; Locke, D.C. Anal. Chem. 1985, 56, 2485.

(3) Thomas, E.R.; Newman, B.A.; Long, C.; Wood, D.A.; Eckert, C.A. J. Chem. Eng. Data 1982, 27, 399.

(4) Wilhoit, R.C.; Zivolnski, B.J. J. Phys. and Ref. Data 1973, 2, suppl. #1.

(5) Ambrose, D.; Ellender, J.H.; Lees, E.B.; Sprake, C.H.S.; Townsend, R. J. Chem. Thermodyn. 1975, 7, 453.

(6) Mash, C.J.; Pemberton, R.C. NPL Report Chem. 111 July 1980, National Physical Laboratory, Teddington, UK.

(7) Hanson, S.R.; Miller, F.A. J. Phys. Chem. 1954, 58, 193.

(8) Pierotti, G.J.; Deal, C.H.; Derr, E.L. Ind. Eng. Chem. 1959, 51, 95.

(9) Butler, J.A.V.; Ramchandani, C.N.; Thomson, J. J. Chem. Soc. 1935, 280.

(10) Buttery, R.G.; Ling, L.C.; Guadagni, D.G. J. Agr. Food Chem. 1969, 17, 385.

(11) Deal, C.H.; Derr, E.L. Ind. Eng. Chem. Proc. Des. Dev. 1964, 3, 394.

(12) National Academy of Sciences "International Critical Tables," Vol. 3, McGraw–Hill, New York, pp.216–219.

(13) Rossini, F.D. "Selected Values of Physical and Thermodynamic Properties of Hydrocarbons and Related Compounds," 1953, American Petroleum Institute, Pittsburgh.

(14) Philippe, A. J. Chem. Thermodyn. 1973, 5, 431.

(15) Landau, I.; Locke, D.C.; Belfer, A.J. paper presented at Eastern Analytical Symposium, Oct. 1986, New York.

(16) Eckert, C.A.; Newman, B.A.; Nicolaides,G.L.; Long, T.C. AIChE J. 1981, 27, 33.

(17) Mackay, D.; Shiu, W.Y.; Sutherland, R.P. Environ. Sci. Technol. 1979, 13, 333.

(18) Stiver, W.; Mackay, D. Environ. Sci. Technol. 1984, 18, 834.

(19) Mackay, D.; Shiu, W.Y. J. Phys. Chem. Ref. Data 1981, 10, 1175.

(20) Nirmalakhandan, N.N.; Speece, R.E. Environ. Sci. Technol. 1988, 22, 1349.

(21) Thomas, R.G. "Handbook of Chemical Property Estimation Methods," Lyman, W.J.; Reehl, W.; Rosenblatt, D.H., Eds., 1982, McGraw–Hill, New York, p. 15–13.

(22) Mackay, D.; Leinonen, P.J. Environ. Sci. Technol. 1975, 9, 1178.

(23) Mackay, D.; Wolkoff, A.W. Environ. Sci. Technol. 1973, 7, 611.

(24) Thomas, R.G. *ibid.*, p. 15–24.

(25) Verschueren, K. "Handbook of Environmental Data on Organic Chemicals," 1977, Van–Nostrand Reinhold, New York.

(26) Thomas, R.G. *ibid.*, p. 15–15.

(27) Lyman, W.J. "Handbook of Chemical Property Estimation Methods," Lyman, W.J.; Reehl, W.; Rosenblatt, D.H., Eds., 1982, McGraw–Hill, New York, p. 2–1.

(28) Arbuckle, W.B. Environ. Sci. Technol. 1983, 17, 537.

(29) Lyman, W.J. *ibid.*, p. 3–8.

(30) Lyman, W.J. *ibid.*, p. 1–49.

(31) Neely, W.B.; Branson, D.R.; Blau, G.E. Environ. Sci. Technol. 1974, 8, 1113.

(32) Karickhoff, S.W.; Brown, D.S.; Scott, T.A. Water Res. 1979, 13, 241.

(33) "Selected Values of Properties of Hydrocarbons and Related Compounds," Research Project #44, 1954, American Petroleum Institute, Pittsburgh.

(34) "International Critical Tables," *ibid.*, p. 212.

(35) Reid, R.C.; Prausnitz, J.M.; Sherwood, T.K. "The Properties of Gases and Liquids," 3rd Edn., 1977, McGraw–Hill, New York, Appendix A.

(36) Reid, R.C.; Prausnitz, J.M.; Sherwood, T.K. *ibid.*, p. 391.

(37) Martin, A.J.P.; Synge, R.L.M. Biochem. J. 1941, 35, 1358.

(38) Conder, J.R.; Young, C.L. "Physicochemical Measurement by Gas Chromatography," 1979, Wiley, Chichester, p. 52.

(39) Braithwaite, A.; Smith, F.J. "Chromatographic Methods," 4th Edn., 1985, Chapman and Hall, London, p. 16.

(40) Tsonopoulos, C. AIChE J. 1974, 20, 263.

(41) Tsonopoulos, C. AIChE J. 1975, 21, 827.

(42) Tsonopoulos, C. AIChE J. 1978, 22, 1112.

(43) Reid, R.C.; Prausnitz, J.M.; Sherwood, T.K. *ibid.*, chapts. 3,4,5.

(44) Weast, R.C., Ed. "Handbook of Chemistry and Physics," 56th Edn., 1975–1976, CRC Press, Cleveland, p. F–46.

(45) Reid, R.C.; Prausnitz, J.M.; Sherwood, T.K. *ibid.*, p. 391.

(46) Reid, R.C.; Prausnitz, J.M.; Sherwood, T.K. *ibid.*, p. 602.